HEI HEALTH EFFECTS INSTITUTE

Noninvasive Determination of Respiratory Ozone Absorption: The Bolus-Response Method

James S. Ultman, Abdellaziz Ben-Jebria, and Shu-Chieh Hu
Department of Chemical Engineering Pennsylvania State University, University Park, PA

Includes the Commentary of the Institute's Health Review Committee

Research Report Number 69
August 1994

HEI HEALTH EFFECTS INSTITUTE

The Health Effects Institute, established in 1980, is an independent and unbiased source of information on the health effects of motor vehicle emissions. HEI studies all major pollutants, including regulated pollutants (such as carbon monoxide, ozone, nitrogen dioxide, and particulate materials), and unregulated pollutants (such as diesel engine exhaust, methanol, and aldehydes). To date, HEI has supported more than 120 projects at institutions in North America and Europe.

HEI receives half its funds from the U.S. Environmental Protection Agency and half from 28 manufacturers and marketers of motor vehicles and engines in the U.S. However, the Institute exercises complete autonomy in setting its research priorities and in disbursing its funds. An independent Board of Directors governs the Institute. The Research Committee and the Review Committee serve complementary scientific purposes and draw distinguished scientists as members. The results of HEI-funded studies are made available as Research Reports, which contain both the Investigator's Report and the Review Committee's evaluation of the work's scientific and regulatory relevance.

HEI Statement

Synopsis of Research Report Number 69

Noninvasive Determination of Respiratory Ozone Absorption: The Bolus-Response Method

BACKGROUND

Ozone is a ubiquitous irritant air pollutant that is a major constituent of photochemical smog. When inhaled, it can react with cellular biomolecules. Human and animal studies show that exposure to sufficiently high concentrations of ozone causes decreases in lung function and increases in markers of airway inflammation. The U.S. Environmental Protection Agency (EPA) has classified ozone as a criteria pollutant, and established a National Ambient Air Quality Standard of 0.12 parts per million (ppm) as an hourly average. This Standard is currently being reevaluated by the EPA.

For regulators to establish appropriate standards for ozone, they need to know the relations among the ambient concentration of the gas (exposure), the amount of gas absorbed in the respiratory tract and its tissues (dose), and the subsequent health effects (responses). For ozone, the relation between exposure and response is well established. However, few data are available that link exposure to dose, and dose to response because of the technical difficulties of making such measurements. This study, sponsored by the Health Effects Institute, sought to develop methods to quantify ozone dose and the efficiency of ozoneabsorption in different regions of the respiratory tract.

APPROACH

Dr. James Ultman and colleagues used a fast-responding ozone measurement system, which they had developed with previous HEI support, to noninvasively measure the absorption of inhaled ozone in different regions of the respiratory tract of healthy adult men. While the subject was breathing through the measuremrnt apparatus, a narrow 10-mL bolus of ozone was introduced into the inhaled air at a predetermined point. This caused the bolus of ozone to be inhaled to a desired volumetric depth in the lungs. By comparing the amounts of ozone inhaled and exhaled, they calculated the cumulative efficiency of ozone absorption (called the bolus-response analysis method). By delivering the bolus to other depths and then relating these depths to anatomical regions of the respiratory tract, they quantified the absorption efficiency of ozone in the upper and lower airways, and in the gas-exchange region of the lungs. To mimic different exposure scenarios, they measured ozone absorption while the subjects breathed through the mouth or nose. Ozone concentrations from 0.5 to 4 ppm were used. These data were used in a theoretical model of ozone absorption to estimate the ozone dose rate to different regions of the respiratory tract.

RESULTS AND IMPLICATIONS

The investigators made substantial improvements in the technology to measure ozone absorption in the respiratory tract of human subjects by developing a fast-responding ozone analyzer and incorporating this instrument into a computer-controlled bolus inhalation system. When they measured the distribution of ozone in different regions of the respiratory tract, they found that with quiet mouth breathing, 50% of the ozone was absorbed in the mouth and oropharynx, and the remainder was absorbed within the conducting airways. When breathing nasally, about 80% of the ozone was absorbed in the upper airways, showing that the nose protects the lungs from ozone exposure. With increasing flow rates, more ozone reached and was absorbed by the lower airways and gas-exchange tissues in the lungs. During exercise, which entails both oral breathing and high flow rates, the dose rate of ozone to the lower airways and gas-exchange tissues would be more than three times the dose rate than when at rest. These investigators have provided a valuable research tool for studies that measure doses of ozone and other gases, and their results have advanced our understanding of how this pollutant is absorbed by the respiratory tract.

This Statement, prepared by the Health Effects Institute (HEI) and approved by its Board of Directors, is a summary of a research project sponsored by HEI from 1990 to 1992. This study was conducted by Dr. James Ultman of Pennsylvania State University. The following Research Report contains both the detailed Investigators' Report and a Commentary on the study prepared by the Institute's Health Review Committee.

Library of Congress Catalog No. for the HEI Research Report Series: WA 754 R432.

The paper in this publication meets the minimum standard requirements of the ANSI Standard Z39.48-1984 (Permanence of Paper) effective with Report Number 21, December 1988, and with Report Numbers 25, 26, 32, and 51 excepted. Reports 1 through 20, 25, 26, 32, and 51 are printed on acid-free coated paper.

TABLE OF CONTENTS

Research Report Number 69

Noninvasive Determination of Respiratory Ozone Absorption: The Bolus-Response Method

James S. Ultman, Abdellaziz Ben-Jebria, and Shu-Chieh Hu

Noninvasive Determination of Respiratory Ozone Absorption: The Bolus-Response Method

James S. Ultman, Abdellaziz Ben-Jebria, and Shu-Chieh Hu

ABSTRACT

Morphometric studies in animals exposed to ozone (O_3)*, and mathematical simulations of O_3 transport in human lungs indicate that O_3 toxicity is focal in nature, causing tissue damage that is more pronounced in the proximal alveolar region (the proximal end of the respiratory airspaces in our compartment models) than in other airways. These findings suggest that the internal distribution of O_3 uptake must be known in order to assess health risk reliably. In previous work (Ultman and Ben-Jebria 1990), we developed a fast-responding chemiluminescent O_3 analyzer and a small-scale O_3 generator, both of which are suitable for respiratory measurements. The objective of the current research was to integrate these instruments into a bolus inhalation system capable of noninvasively measuring the longitudinal distribution of O_3 absorption in intact human lungs. With this system we aimed to carry out baseline experiments in healthy men during quiet oral breathing at a respiratory flow rate of 250 mL/sec, determine the effect of alternative respiratory flow rates between 150 and 1,000 mL/sec, compare the absorption distribution during quiet oral breathing with that during quiet nasal breathing, and ascertain the influence of a peak inspired concentration between 0.3 and 4.0 parts per million (ppm).

Ozone uptake (Λ) was expressed as the amount of O_3 absorbed during a single breath relative to the amount in the inhaled bolus. Measurements of Λ were correlated with the penetration volume (V_P) of the bolus into the respiratory tract. Values of V_P less than 70 mL were considered to be associated with the upper airways, values between 70 and 180 mL were associated with the lower conducting airways, and values greater than 180 mL were associated with the respiratory airspaces. During quiet oral breathing, Λ increased smoothly with V_P, with 50% of the inhaled O_3 absorbed in the upper airways and the balance absorbed within the lower conducting airways. This compares favorably with the results of direct-sampling methods, which have indicated that 40.4% of continuously inhaled O_3 is removed by the extrathoracic airways (Gerrity et al. 1988). The effect of increasing the respiratory flow, which occurs when people exercise, was to shift the Λ-V_P distribution distally so that significantly less O_3 was absorbed in the upper airways and more reached the respiratory airspaces. Compared with oral breathing, nasal breathing caused a proximal shift in the Λ-V_P distribution to the extent that absorption in the upper airways increased from 50% to 80%. This trend, previously documented in dogs (Yokoyama and Frank 1972) but not in humans, is probably the result of the large surface: volume ratio, intense flow patterns, and ample supply of mucus substrates in the nose. Therefore, as exercise load increases, the lower conducting airways and respiratory airspaces become more susceptible to O_3 damage because of normal changes in breathing from nasal to oral and increases in respiratory flow. The peak O_3 concentration of an inhaled bolus did not have a significant effect on the Λ-V_P distribution. This implies that the diffusion and chemical reaction processes dictating O_3 absorption are linear.

INTRODUCTION

Ozone resulting from the photochemical reaction of automobile emissions is an urban air pollutant that can have adverse effects on human health, particularly in the lung. In many previous laboratory studies, individuals were exposed for one to four hours to controlled levels of O_3 as high as 1 ppm, and decrements in their lung function were documented with routine spirometric tests of parameters such as forced expired volume (FEV) and specific airway resistance (Colucci 1983). From the more recent of these studies, it appears that changes in both the mechanical and biochemical status of the lungs are possible even during acute exposures of two hours at concentrations as low as

* A list of abbreviations appears at the end of the Investigators' Report.

This Investigators' Report is one part of Health Effects Institute Research Report Number 69, which also includes a Commentary by the Health Review Committee, and an HEI Statement about the research project. Correspondence concerning the Investigators' Report may be addressed to Dr. James S. Ultman, Department of Chemical Engineering, The Pennsylvania State University, 106 Fenske Laboratory, University Park, PA 16802-4400.

Although this document was produced with partial funding by the United States Environmental Protection Agency under Assistance Agreement 816285 to the Health Effects Institute, it has not been subjected to the Agency's peer and administrative review and therefore may not necessarily reflect the views of the Agency, and no official endorsement should be inferred. The contents of this document also have not been reviewed by private party institutions including those that support the Health Effects Institute; therefore, it may not reflect the views or policies of these parties, and no endorsement by them should be inferred.

0.12 ppm (McDonnell et al. 1983; Koren et al. 1989). The responses of different subjects to the same ambient O_3 concentration show considerable variation (McDonnell et al. 1985). Undoubtedly, some of this variation is due to the use of ambient O_3 concentration as a surrogate for the O_3 dose delivered to those tissues responsible for changes in lung function.

Mathematical simulations indicate that O_3 is not uniformly distributed to all lung tissue and that the proximal alveolar region (the proximal end of the respiratory airspaces in our compartment models) receives a far greater dose than other lung regions (McJilton et al. 1972; Miller et al. 1978). Morphometric studies of the lungs of animals exposed subchronically for one to six weeks to O_3 concentrations as low as 0.12 ppm confirm that the proximal alveolar region incurs the most cell injury (Mellick et al. 1977; Barry et al. 1985). From these results it is clear that the distribution of O_3 dose among different regions in the lung must be known if unique dose-response relations are to be established. It is not sufficient to characterize O_3 exposure in terms of ambient concentration.

We previously developed a bolus-response method for noninvasively assessing the regional distribution of inert insoluble indicator gases (Ultman et al. 1978; Ben-Jebria et al. 1981). The primary purpose of the research reported here was to extend the method to O_3. In particular, a small volume of O_3 is rapidly introduced into an inhaled airstream, and the O_3 concentration is continually monitored at the airway opening throughout the remainder of the inspiration and the following expiration. The absorption of O_3 during this single breath is then computed as the difference between the integrals of inspired and expired O_3 concentration data. Moreover, O_3 absorption can be mapped as a function of V_P (the airway volume to which a bolus would penetrate if there were no absorption) by using data from a series of test breaths in which bolus injection occurs at a different time during each inhalation.

Using a respiratory O_3 analyzer and a small-scale O_3 generator developed in previous Health Effects Institute–sponsored research (Ultman and Ben-Jebria 1990), we assembled an automated bolus inhalation apparatus for testing human subjects. In the first series of experiments with this apparatus, we measured the longitudinal distribution of O_3 absorption in the lungs of healthy male subjects during quiet oral breathing (baseline experiments). In addition to providing useful dosimetry data, this study helped to define the resolution and limitations of the apparatus.

An important concern regarding O_3 dose is the influence of the high respiration rates concomitant with exercise. Theoretically, when the flow of gas through a tube increases, the concentration boundary layer near the wall of the conduit becomes thinner, and resistance to radial diffusion diminishes (Treybal 1980). Simultaneously, a higher flow rate reduces the time that is available for diffusion to occur. Because the enhancement of diffusion by boundary layer thinning is roughly proportional to $(\text{Flow})^{0.5}$, and the attenuation of diffusion by decreased residence time is proportional to $(\text{Flow})^{1.0}$, these opposing effects should result in a decrease in absorption efficiency. If this logic applies in lung airways, then an increase in respiratory flow would diminish the fraction of O_3 absorbed into the upper airways, and a greater portion of inhaled O_3 would penetrate to the lower airways.

Studies in intact upper airways of dogs (Yokoyama and Frank 1972) indicate, in support of the theoretical prediction, that a 10-fold increase in airflow reduces O_3 absorption efficiency by 50% to 70%. However, recent data indicate that this effect is much smaller in human subjects. In a group of 18 male subjects, a doubling of the respiratory frequency from 12 to 24 beats per minute at a fixed tidal volume reduced absorption efficiency by only 6% in extrathoracic airways (upper airways and trachea) (Gerrity et al. 1988). This limited flow sensitivity is possible if the aqueous solubility of O_3 is so low that it is much less resistant to diffusion in the gas phase than it is in mucous and epithelial cell layers. On the other hand, the results of Gerrity and associates (1988) are questionable because their slow-responding gas analyzer undoubtedly underestimated O_3 concentration, particularly at the breathing frequency of 24 beats per minute.

In the second series of experiments, we further explored the effects of respiratory flow in the human lung (flow experiments). The bolus-response method was used to measure the distribution of O_3 absorption in healthy men during oral breathing at a variety of respiratory flow rates.

Another important issue regarding O_3 dose is the relative ability of the nasopharyngeal and oropharyngeal pathways to remove O_3 from inhaled air before it reaches the lower airways. During inspiration, the point of air entry normally switches from the nose to the mouth as minute ventilation increases above 30 L/min (Niinimaa et al. 1980). Therefore, a difference in the absorption efficiency of these two upper airway paths could contribute to a change in lower airway dose when there is an exercise-induced elevation of respiratory flow.

Data obtained in the upper airways of dogs demonstrate that the nose has twice the absorption efficiency of the mouth (Yokoyama and Frank 1972). This is consistent with the conventional wisdom that the nose, with its large surface:volume ratio and richly perfused mucosa, is well designed for gas uptake (Brain 1970). It is surprising that in human subject studies, the mouth had a slightly higher absorption efficiency than the nose (Gerrity et al. 1988).

In the third series of experiments, we applied the bolus-response method to study the relative absorption efficiencies of the nose and mouth (oral-nasal experiments). The influence of nasal breathing versus oral breathing on the distribution of ozone absorption in the lower airways was also evaluated. Gerrity and associates (1988) had to use a pharyngeal sampling tube to monitor O_3 concentration between the upper and lower conducting airways. Condensation and mucous accumulation in the tube, although corrected for, may have distorted their data. Because the bolus-response method differentiates between absorption in various lung regions without the use of intraairway sampling tubes, we believe that our data are more reliable.

A third important consideration regarding O_3 dose is the effect of exposure concentration on absorption efficiency. In a linear absorption process, diffusion follows Fick's law, solubilities can be described by Henry's law, and all chemical reactions have first-order kinetics with respect to O_3 concentration. As a result, O_3 uptake is proportional to inhaled O_3 concentration, and absorption efficiency is independent of it. On the other hand, in situations in which solubility, diffusion, and reaction are described by nonlinear formulas, absorption efficiency will depend on the inhaled O_3 concentration.

In studies of acute O_3 exposure in isolated dog airways, absorption efficiency was inversely related to the inhaled concentration in the range of 0.1 to 20 ppm (Vaughan et al. 1969; Yokoyama and Frank 1972), indicating that mucus and tissue may become saturated with O_3. However, later experiments in guinea pigs and rabbits over an exposure range of 0.1 to 2 ppm (Miller et al. 1979), as well as in humans over an exposure range of 0.1 to 0.4 ppm (Gerrity et al. 1988), demonstrated that exposure concentration had no effect on absorption efficiency. Possibly this discrepancy is due to differences in the ranges of inhaled concentrations that were explored or, alternatively, to differences in lung anatomy between the dog, which has a disproportionately long trachea, and the other animals.

In the fourth series of experiments, we studied the effect of O_3 concentration on O_3 dosimetry (concentration experiments). In particular, we measured the absorption distributions resulting from the injections of boluses with different peak O_3 concentrations.

SPECIFIC AIMS

The general objective of our research is to measure noninvasively the distribution of O_3 absorption in intact human lungs under a variety of exposure and respiratory conditions. In previous research, a respiratory O_3 analyzer and a small-scale O_3 generator were developed. The aims of the current research were as follows:

1. Incorporate this O_3 analyzer and bolus generator into a computer-controlled bolus inhalation apparatus.
2. Measure the longitudinal distribution of O_3 during quiet oral breathing at a flow rate of 250 mL/sec (baseline experiments).
3. Evaluate the effect on O_3 absorption of changes in respiratory flow rates from 150 to 1,000 mL/sec (flow experiments).
4. Study the effect on O_3 absorption of nasal versus oral breathing (oral-nasal experiments).
5. Determine the O_3 absorption distribution at peak inspired bolus concentrations of 0.5, 1, 2, and 4 ppm (concentration experiments).

These aims have been slightly modified from those enumerated in the original research proposal. The respiratory flow rate characteristic of quiet breathing in aims 2, 4, and 5 was reduced from 300 to 250 mL/sec because at the lower flow the subjects found it easier to produce a triangular respired volume waveform free of an end-expiratory pause. The range of flow rates in aim 3 was reduced from 200–2,000 to 150–1,000 mL/sec because the dynamic response of the O_3 analyzer was not sufficiently rapid to produce reliable data above 1,000 mL/sec. Also in aim 3, we originally planned to characterize the sensitivity of O_3 absorption to separate changes in inspiratory and expiratory flow. We later decided to simulate the influence of physical activity on O_3 absorption, in which case it is more realistic to maintain inspiratory flow equal to expiratory flow. In aim 5, the addition of measurements at a peak inhaled O_3 level of 4 ppm extended the range over which concentration effects were evaluated. This should have improved the likelihood of observing such effects, if they actually exist.

THEORETICAL CONSIDERATIONS

OZONE ABSORPTION THEORY

The transport of a solute from a carrier gas to a liquid phase is traditionally characterized by an overall mass transfer coefficient, K, representing the absorption rate normalized by the concentration driving force and the interfacial surface area (Treybal 1980). When this area is not known, the surface:volume ratio, a, is introduced as a second parameter such that Ka is the absorption rate normalized by the concentration driving force and the volume of the gas-filled conduit. To formulate a simplified mathematical model for interpreting absorption data, we solved the diffusion equation, Equation A.1, found in Appendix A, for

the case of steady flow through a straight tube (Ben-Jebria et al. 1991). This analysis predicts that the fraction of entering O_3 that penetrates to the tube exit is given by

$$1 - \Lambda = \exp(-Ka\Delta V/\dot{V}), \quad (1)$$

where Λ is the amount of absorbed O_3 relative to the amount in an entering bolus, $\dot{V}$ is the volumetric gas flow, and ΔV is the tube volume. This equation is valid for any shape of the entering bolus. However, in the derivation of Equation 1, it was assumed that Ka is constant, the backpressure of solute from the tube wall is negligible, and axial convection in the gas phase is much greater than axial dispersion.

In modeling O_3 absorption in the respiratory system, the airways are visualized as a series of compartments, each of which behaves as a separate tube (Figure 1). Longitudinal position within this compartment model is specified by a volume coordinate, V_P, corresponding to the penetration of a bolus beyond the O_3 sampling point at $V_P = 0$ during inhalation. Compartment 1 is bounded at its proximal end by $V_{P,0}$, the position of the airway opening relative to the O_3 sampling point; it is bounded at its distal end by $V_{P,1}$. The volume of this compartment is, therefore, $(V_{P,1} - V_{P,0})$. Because a bolus traverses this volume twice during each breath, the appropriate ΔV for compartment 1 is $2(V_{P,1} - V_{P,0})$. Moreover, O_3 is not absorbed in the mouthpiece assembly, which is proximal to $V_{P,0}$; therefore, all of the O_3 detected at the sampling point enters compartment 1. According to Equation 1, the fraction of inhaled O_3 that penetrates through compartment 1 is then

$$(1 - \Lambda_1) = \exp[-2(Ka)_1(V_{P,1} - V_{P,0})/\dot{V}], \quad (2)$$

where Ka, the value of the mass transfer parameter, has been assumed to be constant within compartment 1 ($[Ka]_1$).

Compartment 2 is bounded at its proximal end by $V_{P,1}$ and at its distal end by $V_{P,2}$. As $(1 - \Lambda_2)$ is the amount of O_3 that reaches the distal boundary relative to the amount of inhaled O_3, and $(1 - \Lambda_1)$ is the O_3 that enters at the proximal boundary relative to the amount inhaled, $(1 - \Lambda_2)/(1 - \Lambda_1)$ is the amount of O_3 that penetrates compartment 2 relative to the amount that enters the compartment. Using this nomenclature, Equation 1 becomes

$$(1 - \Lambda_2)/(1 - \Lambda_1) = \exp[-2(Ka)_2(V_{P,2} - V_{P,1})/\dot{V}]. \quad (3)$$

This equation can be generalized for an arbitrary compartment i with a proximal boundary $V_{P,i-1}$, a distal boundary $V_{P,i}$, and a mass transfer parameter, $(Ka)_i$.

$$(1 - \Lambda_i) = (1 - \Lambda_{i-1})\exp[-2(Ka)_i(V_{P,i} - V_{P,i-1})/\dot{V}] \quad (4)$$

In correlating the absorbed fraction data collected in bolus-response experiments, we require an equation for Λ as a continuous function of V_P. Making use of the assumption that $(Ka)_i$ is constant in compartment i, Equation 4 can be rewritten to relate Λ to any V_P between $V_{P,i-1}$ and $V_{P,i}$.

$$(1 - \Lambda) = (1 - \Lambda_{i-1})\exp[-2(Ka)_i(V_P - V_{P,i-1})/\dot{V}] \quad (5)$$

Taking the natural logarithm of both sides of Equation 5 results in the formula

$$-\log_e(1 - \Lambda) = [2(Ka)_i/\dot{V}]V_P - [\log_e(1 - \Lambda_{i-1}) + 2(Ka)_i V_{P,i-1}/\dot{V}]. \quad (6)$$

Therefore, a regression of $-\log_e(1 - \Lambda)$ versus V_P in the range $V_{P,i-1}$ to $V_{P,i}$ will have a slope $2(Ka)_i/\dot{V}$ from which Ka can be determined.

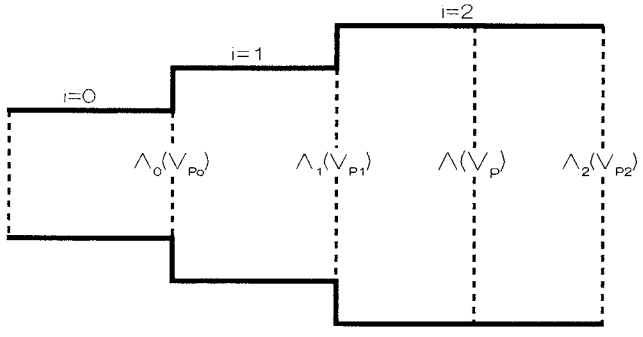

Figure 1. The compartmental absorption model. In this diagram of three compartments of the diffusion model, Λ_i is the fractional absorption at a penetration volume, V_{Pi}, representing the distal end of compartment i; and Λ is the fractional absorption at an arbitrary penetration volume, V_P, within the $i = 2$ compartment.

DECOMPOSITION OF THE OVERALL MASS TRANSFER COEFFICIENT

The O_3 absorption process can be better understood by considering the individual factors that contribute to K. Situated in the path of O_3 molecules absorbing into an airway wall is a series of diffusional resistance layers: the boundary layer of the flowing respiratory gas, the liquid-lining layer (i.e., mucus in lower airways and surfactant in respiratory airspaces), the epithelial cell layer, the subepithelial tissue, and the bronchial circulation. Because O_3 reacts so rapidly with the epithelial membrane (Pryor 1992), the surface of these cells is maintained at a very low O_3 concentration, and the gas boundary layer and the liquid-lining layer are the major impediments to O_3 absorption. Therefore, the overall mass transfer resistance, $1/K$, can be equated to the sum of the diffusion resistances through the gas boundary layer, $1/k_g$, and the liquid-lining layer, λ/k_ℓ (Ultman 1988):

$$1/K = 1/k_g + \lambda/k_\ell, \quad (7)$$

where k_g and k_ℓ are the individual mass transfer coefficients in the gas and liquid-lining layers, respectively, and λ is an equilibrium partition coefficient defined as the molar concentration of O_3 in air relative to that in mucus or surfactant.

Whereas k_ℓ depends on the diffusion and reaction dynamics within the liquid-lining layer but is independent of the external gas flow, the value of k_g is directly affected by $\dot{V}$. In general, k_g can be related to $\dot{V}$ by a power-law equation of the form

$$k_g = m\dot{V}^n, \quad (8)$$

where m and n are parameters whose values depend on the geometry of the gas-liquid surface and the nature of the flow (e.g., laminar or turbulent). After substitution of Equation 8 and division by a, Equation 7 becomes

$$Ka = 1/[\lambda/k_\ell a + 1/(ma\dot{V}^n)]. \quad (9)$$

By regressing Ka values measured at several different flows to Equation 9, it is possible to determine the constants: $k_\ell a$, ma, and n. However, separate values for k_ℓ and m can be obtained only if an estimate of a is available from anatomic data.

METHODS AND STUDY DESIGN

SUBJECT CHARACTERISTICS

Only healthy male subjects were used in this study. After being given an explanation of the study, each subject was asked to complete an informed-consent form, a medical questionnaire, and a standard spirometric test to determine his forced vital capacity (FVC), forced expired volume in one second (FEV_1), and forced expiratory flow from 25% to 75% of the vital capacity (FEF_{25-75}). The subjects' characteristics and the experiments in which they participated are summarized in Table 1. Nine subjects were included in the baseline and in the flow and the oral-nasal experiments. Six subjects completed the concentration experiments.

A subject was included in this study if his responses to the medical questionnaire indicated that he had not smoked within the past three years; had no history of hay fever, asthma, allergic rhinitis, chronic respiratory disease, or cardiac diseases; had not used medication within one week of the study; and did not have an activity pattern that predisposed him to air pollutant exposure. Moreover, a sub-

Table 1. Characteristics of Subjects[a]

Subject	Study[b]	Age (years)	Height (cm)	Weight (kg)	FVC (L)	FEV_1 (L)	FEV_1/FVC (%)	FEF_{25-75} (L/sec)	V_D (mL)
1	1,2	40	163	61	4.3 [108]	3.4 [106]	79 [94]	3.9 [103]	155
2	1	21	183	75	6.2 [106]	5.6 [118]	90 [106]	6.7 [129]	186
3	4	28	180	61	4.1 [75]	3.6 [81]	87 [103]	4.4 [82]	220
4	1,2	29	174	69	5.4 [108]	3.8 [94]	70 [83]	2.8 [60]	170
5	3	28	175	69	5.2 [102]	4.6 [110]	88 [104]	6.0 [117]	155
6	1,2	29	176	57	4.4 [86]	3.1 [74]	71 [84]	5.2 [116]	189
7	1,2	31	185	85	6.0 [106]	4.8 [105]	80 [96]	4.7 [87]	130
8	3,4	29	178	71	5.8 [110]	5.0 [117]	87 [103]	5.8 [110]	180
9	1	26	175	70	4.9 [95]	4.4 [105]	90 [106]	4.1 [79]	161
10	3	22	173	63	4.9 [96]	4.6 [110]	93 [109]	7.4 [141]	189
11	2,3	27	178	86	6.0 [113]	4.8 [110]	79 [94]	4.8 [90]	159
12	3,4	26	193	91	7.6 [119]	6.1 [118]	81 [97]	6.3 [105]	244
13	3	29	183	75	7.0 [125]	5.3 [118]	76 [91]	4.6 [84]	176
14	2	28	191	91	6.9 [112]	5.5 [111]	80 [96]	5.5 [93]	169
15	1,2	47	173	68	5.5 [124]	3.7 [105]	67 [82]	2.0 [46]	175
16	4	28	170	66	5.4 [113]	3.9 [101]	73 [85]	3.0 [61]	202
17	1,2	31	178	80	5.5 [106]	4.4 [104]	80 [95]	4.0 [87]	145
18	2	30	175	86	5.2 [103]	4.3 [105]	83 [98]	4.1 [90]	162
19	3,4	28	201	98	7.0 [103]	5.6 [102]	80 [97]	5.2 [83]	200
20	3	27	185	75	7.0 [121]	4.6 [97]	65 [77]	3.1 [55]	135
21	4	29	183	80	6.0 [108]	4.5 [100]	75 [90]	3.6 [66]	—
22	3	21	168	68	5.1 [106]	4.2 [106]	82 [95]	4.3 [85]	180
23	1	30	176	73	4.3 [84]	3.4 [82]	79 [94]	2.6 [55]	152

[a] FVC = forced vital capacity, FEV_1 = forced expired volume in one second, FEF_{25-75} = forced expiratory flow from 25% to 75% of the vital capacity, V_D = volume of carbon dioxide dead space. Values in brackets are the forced expired parameters expressed as percentages of the predicted values (Knudsen et al. 1976).

[b] Study 1 = baseline experiments; study 2 = flow experiments; study 3 = oral-nasal experiments; study 4 = concentration experiments.

ject was included in this study only if the spirometry test indicated that his FEV_1:FVC ratio was 75% or more of the predicted value. At the beginning and the end of each experimental session, the subject completed a second questionnaire to document the appearance of symptoms commonly associated with O_3 irritation: shortness of breath, cough or urge to cough, chest burning or discomfort, or difficulty in taking a deep breath. None of the subjects perceived any of these symptoms.

These screening procedures as well as the bolus-response protocol described below were approved by the Pennsylvania State University's Institutional Review Board.

APPARATUS

The inhalation system was made possible by a small-scale O_3 bolus generator and a fast-responding chemiluminescent O_3 analyzer that we previously developed (Ultman and Ben-Jebria 1990). The O_3 generator consisted of a miniature ultraviolet source that continuously passed a stream of an O_3-air mixture through a 20-mL hold-up tube vented to a fume hood. When an O_3 bolus was required, a pair of three-way solenoid valves at the inlet and outlet of the hold-up tube were simultaneously energized, allowing a pressurized stream of clean air to enter the hold-up tube and propel its contents into the subject's mouthpiece assembly. This device reproducibly produced boluses with a nominal volume of 10 mL, a peak concentration of 3 ppm, and an O_3 content of up to 0.4 μg. The O_3 analyzer used a photomultiplier tube to detect the chemiluminescence produced by the gas-phase reaction of O_3 with 2-methyl-2-butene under a moderate vacuum. At the required inlet sample flow rate of 400 mL/min, this instrument had a minimum detectable limit of 0.018 ppm and a 10% to 90% step-response time of 110 msec. (The step-response time is the time required for the O_3 analyzer output to increase from 10% to 90% of its ultimately steady level in response to a step increase in O_3 concentration.) The static calibration of analyzer output voltage versus known O_3 concentration was linear with a negative voltage intercept for O_3 concentrations of 0.03 to 10 ppm, and was curvilinear with a decreasing slope for O_3 concentrations below 0.03 ppm. The analyzer output was also sensitive to the presence of carbon dioxide (CO_2): for every 1% substitution of oxygen (O_2) in air with 1% CO_2, there was a 3.8% increase in the output voltage.

The inhalation system (Figure 2) originated with a stainless steel mouthpiece assembly, containing a proximal injection port connected to the bolus generator, and two distal sampling ports connected to the O_3 chemiluminescent analyzer and to a CO_2 monitor. A rubber mouthpiece through which the subject breathed was located at the distal end

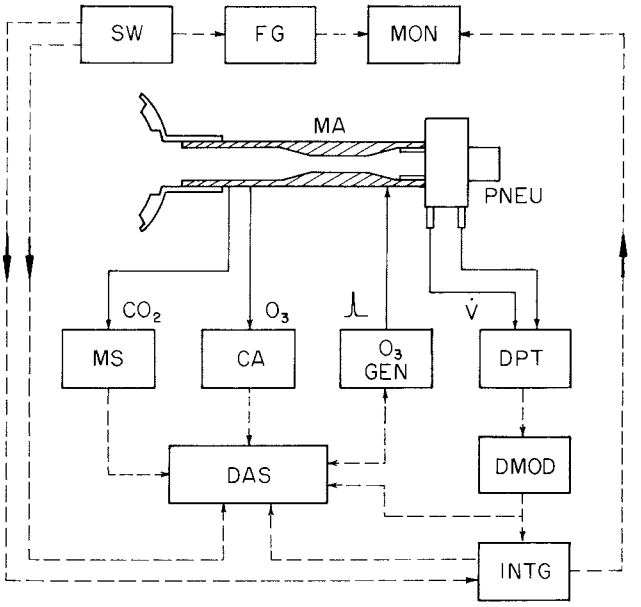

Figure 2. Diagram of the experimental inhalation system. Solid lines represent pneumatic interconnections, and dashed lines represent electrical interconnections. CA = chemiluminescent analyzer, which monitors O_3 concentration; DAS = data acquisition system (570 Keithley, Cleveland, OH, driven by a 386 Zenith workstation), which records flow and concentration signals and triggers bolus injection at the appropriate inspired volume; DMOD = carrier demodulator (CD19, Validyne, Northridge, CA), which provides flow signal to the DAS and respiratory flow integrator; DPT = differential pressure transducer (MP45, Validyne); FG = function generator (HP3310B, Hewlett-Packard), which provides time base to the monitor; INTG = respiratory flow integrator (FV156, Validyne), which provides the respired volume signal to the monitor and to the DAS; MON = monitor (603 storage monitor, Tektronix, Beverton, OR), which displays the respiratory volume pattern for the subject; MA = mouthpiece assembly (see Figures 3 and 4); MS = respiratory mass spectrometer (RMS-6, McGaw Respiratory Therapy), and in-line capnometer (4210A, Hewlett-Packard), which monitor the CO_2 concentration in the mouthpiece assemblies of Figures 2 and 3, respectively; O_3 GEN = O_3 generator, which releases the bolus when triggered from DAS; PNEU = pneumotachograph, which transduces flow into pressure differential (No. 1 or No. 2, Fleisch, Richmond, VA); SW = subject switchbox, which sends the initiation pulse to the FG and DAS and also restarts the INTG.

of the assembly, and a pneumotachograph used to monitor respiratory flow was mounted to the proximal end of the assembly. Figure 3 shows the detailed design of the mouthpiece assemblies used in the baseline and the flow experiments. In that case, CO_2 was monitored by a mass spectrometer (RMS6, McGaw Respiratory Therapy, Waltham, MA), and good radial mixing of the O_3 bolus with inspired air was ensured by funneling the flow through a venturi-type constriction in the central portion of the assembly. The breathing fixture used in the oral-nasal experiments was somewhat different (Figure 4). A more reliable CO_2 analyzer (47210A Infrared Capnometer, Hewlett-Packard, Waltham, MA) was substituted for the mass spectrometer. The in-line optical cell used as the sensing element in the capnometer was integrated into the mouthpiece assembly in place of the venturi constriction. Also, for nasal measurements, the rubber mouthpiece was replaced by a modified

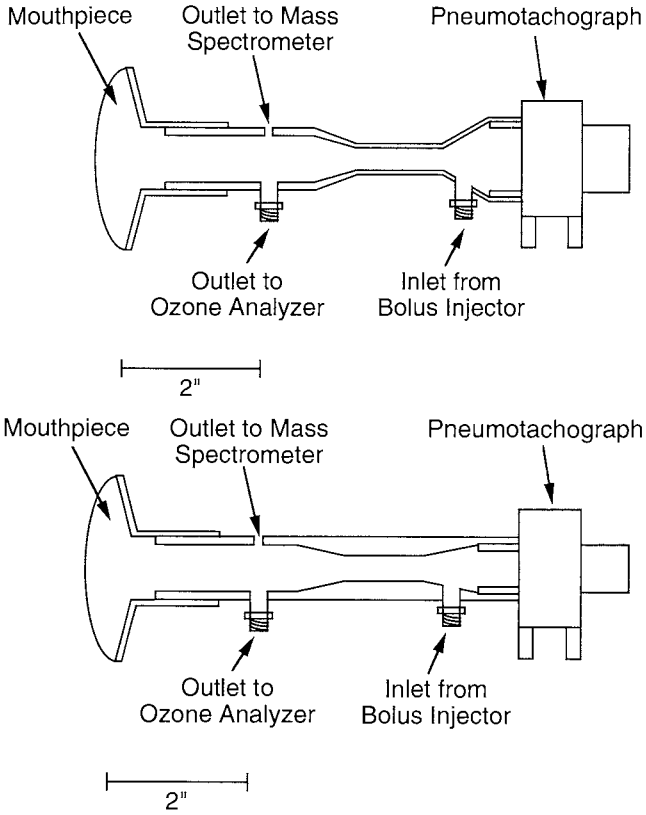

Figure 3. Mouthpiece assemblies for baseline experiments (bottom) and flow experiments (top). The principal difference between these designs is the distal coupling to the pneumotachograph. A Fleisch No. 1 pneumotachograph was used in the baseline experiments, and a larger Fleisch No. 2 pneumotachograph was used in the flow experiments. This diagram is approximately to scale.

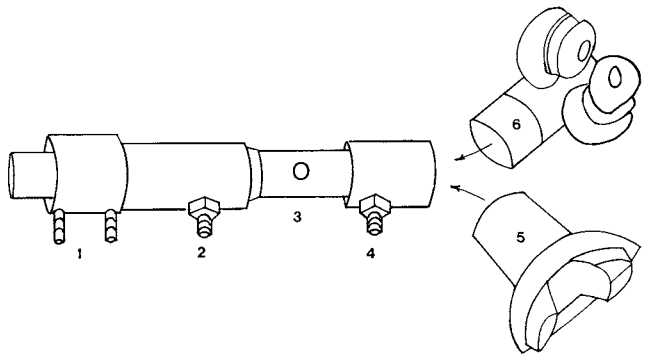

Figure 4. Breathing fixture for oral-nasal and concentration experiments. The fixture consists of (1) a Fleisch No. 1 pneumotachograph, (2) a proximal interconnection tube containing the bolus injection port, (3) an in-line optical capnometer cell, and (4) a distal interconnection tube containing the O_3 sampling port. Depending on the desired mode of breathing, either (5) a rubber mouthpiece or (6) a plastic nasal cannula was positioned at the end of the interconnecting tube.

continuous positive-applied-pressure cannula (231700, Puritan-Bennett, Lenexa, KS) that utilized a pair of soft rubber "pillows" to ensure a comfortable but tight fit with each nostril.

In all experiments, the differential pressure from the pneumotachograph was converted to a flow signal by a transducer and carrier demodulator. The flow signal was then processed by an analog integrator to obtain a respired volume signal that was displayed on the vertical axis of an analog storage monitor and was simultaneously transmitted to a computer-driven data acquisition and control system. To initiate a test breath, the subject depressed a switch that served the following three functions: it activated the function generator that supplied a ramp function to the horizontal (i.e., time) axis of the storage monitor; it restarted the analog flow integrator; and it prompted the data acquisition system to begin recording concentration and flow data. All data acquisition, signal processing, and data analysis tasks were implemented using ASYST2.0 software (Macmillan Software Co., Rochester, NY) in a digital host computer (Z386 Workstation, Zenith Corp., Springfield, MO).

CALIBRATIONS

Before each experimental session, the flow signal from the demodulator was calibrated with a rotameter (No. 12, Gilmont Instruments, Great Neck, NJ) previously standardized with a wet test meter. The horizontal gain of the storage monitor was calibrated with a standard timing signal provided by the clock of the host computer. The analog integrator output was then adjusted to provide a desired slope on the storage monitor when airflow through the pneumotachograph was 250 mL/sec. The O_3 analyzer was calibrated using multiple O_3 concentrations in air produced by a photometric standard (49PS, Thermoenvironmental Instruments, Franklin, MA). The sensitivity of the O_3 analyzer to CO_2 was checked by using a certified gas mixture containing 6% CO_2, 15% O_2, and 79% nitrogen (N_2). The CO_2 channel of the mass spectrometer was calibrated by using the same 6% CO_2 mixture, and the infrared capnometer was calibrated with its own internal standard.

The step-response time of the O_3 analyzer was determined by using a low dead-volume solenoid valve (three-way Teflon series 1, General Valve Corp., Fairfield, NJ), which rapidly switched between an air source and a 0.5 ppm O_3 source. The response time of the CO_2 channel of the mass spectrometer was found by manually withdrawing its sampling capillary into room air from a tube containing the 6% CO_2 gas mixture. The response time of the infrared capnometer was specified by the manufacturer. The 10% to 90% step-response times of the three gas analyzers were

similar: 110 msec for the O_3 analyzer, 70 msec for the mass spectrometer, and 200 msec for the infrared capnometer.

The delay times of the O_3 analyzer, mass spectrometer, capnometer, and pneumotachograph signals were measured under conditions approximating bolus inhalation. While a steady airflow of 150 to 1,000 mL/sec was directed distally through a mouthpiece assembly, a bolus of 6% CO_2 in ozonated air was released by triggering the bolus injection valve with a signal from the data acquisition system. The data acquisition system then determined the difference between the time that the valve was energized and the times that a pulse disturbance was first detected in the signals. Finding that the delay times for the O_3 analyzer signal (235 msec), the mass spectrometer signal (140 msec), and the capnometer signal (150 msec) were all independent of airflow, we concluded that the influence of the mouthpiece assembly was negligible when compared with that of the gas analyzers. The delay time of the pneumotachograph was only 15 msec.

PROTOCOL

In each experimental session, the subject was seated comfortably on a stool. During oral breathing, the subject wore noseclips. To carry out a test breath, the subject donned the rubber mouthpiece or nasal cannula, activated the inhalation apparatus by depressing a switch, and took a single breath from functional residual capacity (FRC) while viewing the electron beam trace on the storage monitor. Throughout this breath, the subject attempted to match the beam trace to a triangular respired volume pattern that was predrawn on the monitor screen. At a predetermined set point during inhalation, the data acquisition system automatically triggered the injection of an O_3 bolus. The volume of air that the subject inspired between the O_3 injection and the apex of the triangular breathing pattern determined the penetration of the bolus into the lungs. A subject completed an entire set of measurements (either baseline, flow, oral-nasal, or concentration) within a single session of two to four hours. In a typical set of measurements, bolus injection was targeted at 19 penetration volumes of 20 to 200 mL in increments of 10 mL; when it was possible to discern an expired bolus at penetration volumes of more than 200 mL, additional measurements were made. To avoid possible systematic errors associated with O_3 preexposure, half the subjects progressed from low to high penetration volumes and the other half progressed from high to low penetration volumes.

In the baseline, oral-nasal, and concentration experiments, the function generator was always set at 0.125 Hz, and the predrawn breathing pattern corresponded to a single 500-mL breath with inhaled and exhaled flow rates targeted at 250 mL/sec. In the flow experiments, the frequency setting on the function generator was changed so that alternative respiratory flow rates of 150, 250, 500, 750, and 1,000 mL/sec were targeted at a fixed tidal volume of 500 mL. In these sessions, the subjects found it easiest to progress from low to high flow rates, completing all 19 penetration volume increments at a given flow rate before going on to the next highest flow rate.

In the oral-nasal experiments, half the subjects completed the oral measurements before beginning the nasal measurements, and for the remaining subjects, the order of experimentation was reversed. Similarly, in the concentration experiments, half the subjects progressed from low to high concentrations, and for the remaining subjects, the order of concentration changes was reversed. In all experiments, a breath was deemed acceptable if the subject could maintain his average respiratory flow within ±15% of the targeted value. Measurements were replicated at least three times at each penetration volume increment during the baseline and oral-nasal experiments, and at least once during the flow and concentration experiments.

DATA ANALYSIS AND STATISTICAL METHODS

DIGITAL SIGNAL CONDITIONING

The flow, O_3, and CO_2 analyzer signals obtained in a test breath were each digitized at 200 Hz and recorded for a six-second interval by the data acquisition system. The time at which the breath was initiated and the time at which the O_3 bolus was triggered were also recorded. The first step in the data analysis was to apply calibrations to the analyzer output signals to convert them into corresponding O_3 volume fractions (F_{O_3}) and CO_2 volume fractions (F_{CO_2}). Taking into account differences in delay times, the F_{O_3} and F_{CO_2} data sets were translated along their time axes to properly align them with the flow data. Then, F_{O_3} at each time point was multiplied by a standard factor, $(1 - 3.8\ F_{CO_2})$, to account for the influence of CO_2 on the chemiluminescent analyzer. Figure 5 shows data from a typical test breath that was processed in this manner.

To compensate for the distortion in the O_3 analyzer signal caused by an imperfect dynamic response, a first-order correction was applied to the F_{O_3} data according to the equation

$$(F_{O_3})_{corr} = F_{O_3} + \tau\, dF_{O_3}/dt, \qquad (10)$$

where τ (50 msec) is the exponential time constant computed from the 10% to 90% step-response time (110 msec) of the O_3 analyzer, and dF_{O_3}/dt is the time derivative of the

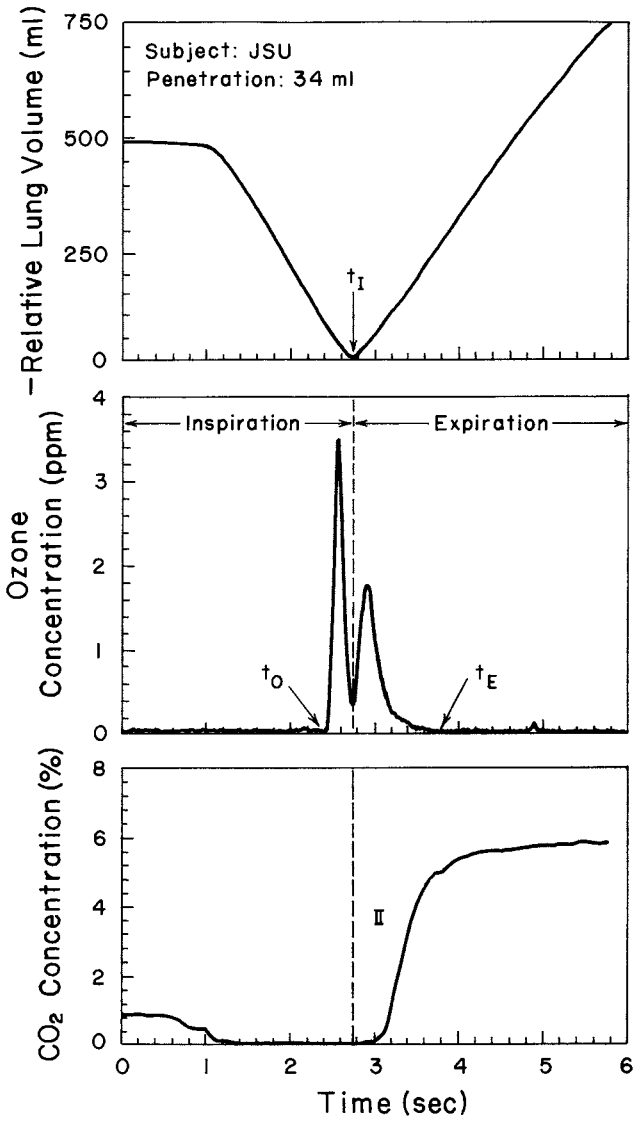

Figure 5. Representative data from a single test breath. Voltage signals were converted to physical variables using the instrument calibrations, and time axes were translated to correct for delay times of the mass spectrometer and the O_3 analyzer. The origin corresponds to the initiation of the test breath, t_I is the end of inspiration, t_O is the time when the first nonzero O_3 concentration is detected, and t_E is the time when the last nonzero O_3 concentration is detected. "II" represents the phase-II transition in expired CO_2 concentration from the pure dead space gas to the alveolar gas.

uncorrected O_3 fraction. As dF_{O_3}/dt was found by numerical differentiation, it was necessary to preprocess the F_{O_3} data with a 20-Hz low-pass time-domain digital filter to avoid undue amplification of noise. This resulted in a signal:noise ratio varying from 9:1 at 0.1 ppm O_3 to 40:1 at 1 ppm O_3.

Values of $\dot{V}$ from flow data were numerically integrated with respect to time t to obtain relative lung volume V, and the end of inhalation t_I was determined as that time when the $\dot{V}$ data crossed zero (Figure 5). The first 200 samples of the O_3 data were averaged to determine a background level, and the remainder of the O_3 data were manually inspected to determine the time t_O during inspiration when a nonzero F_{O_3} value first appeared and the time t_E during expiration when a nonzero F_{O_3} value last appeared. Final correction of the O_3 data sampled at times between t_O and t_E consisted of subtracting the background level.

MATHEMATICAL MOMENTS OF THE BOLUS RESPONSE

For each test breath, the corrected F_{O_3} data were numerically integrated to determine the first three mathematical moments (subscript j = 0, 1, or 2) of the inhaled bolus (subscript I) and the exhaled response (subscript E) according to the definitions

$$(I_j)_I = \left| \int_{t_I}^{t_O} (F_{O_3})_{corr}\, V^j\, \dot{V} dt \right| \tag{11}$$

and

$$(I_j)_E = \left| \int_{t_I}^{t_E} (F_{O_3})_{corr}\, V^j\, \dot{V} dt \right| . \tag{12}$$

As $\dot{V}dt$ is equivalent to dV, I_j could alternatively be defined in terms of volume integrals. However, time integration was more appropriate in executing numerical computations because the F_{O_3}, V, and $\dot{V}$ data sets were all equally spaced (i.e., digitized) with respect to t.

The I_j values were combined to yield physically meaningful parameters, as portrayed on the cross-plot of F_{O_3} versus V in Figure 6. Because $(I_0)_I$ and $(I_0)_E$ are equivalent to the amounts of O_3 that are inspired and expired, we defined

$$\Lambda = 1 - (I_0)_E/(I_0)_I \tag{13}$$

as the fraction of O_3 absorbed relative to the amount of O_3 in the inhaled bolus. We also defined two mean volumes relative to the end of inspiration:

$$V_P = (I_1)_I/(I_0)_I \tag{14}$$

is the penetration volume, and

$$V_B = (I_1)_E/(I_0)_E \tag{15}$$

is the breakthrough volume. Whereas V_P is equivalent to the volume of air that, on the average, follows behind the O_3 molecules while they are inhaled into the lungs, V_B is the average air volume that precedes the exhalation of O_3 out of the lungs. Finally, we defined the difference between the volume variances of the expired and inspired O_3 concentration curves as

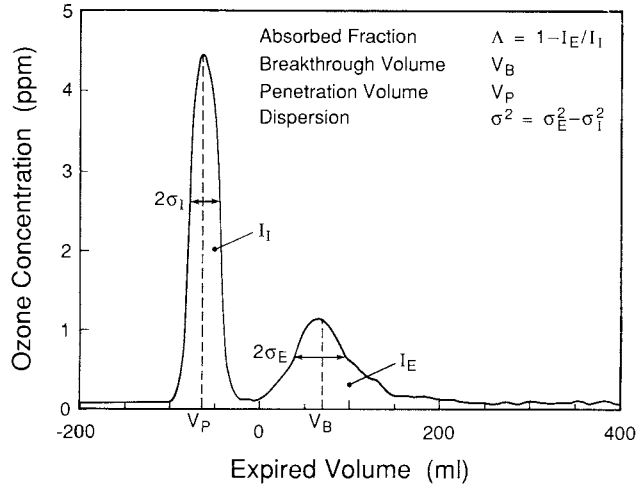

Figure 6. Graphical representation of mathematical moments generated from a bolus test breath. The origin corresponds to the end of inspiration, the curve to the left is the inhaled bolus, and the curve to the right is the exhaled response. The absorbed fraction is the amount of O_3 that is absorbed during a single respiratory cycle relative to the inhaled amount ($\Lambda = 1 - I_E/I_I$). Penetration volume is the mean airway volume that would be reached by inhaled O_3 molecules if no absorption occurred (V_P). Breakthrough volume is the mean airway volume traversed by unabsorbed O_3 molecules that reach the lips during expiration (V_B). Dispersion is a measure of the longitudinal mixing of the unabsorbed O_3 molecules ($\sigma^2 = \sigma^2_E - \sigma^2_I$).

$$\sigma^2 = [(I_2)_E/(I_0)_E - (V_B)^2] - [(I_2)_I/(I_0)_I - (V_P)^2]. \quad (16)$$

This difference may be viewed as the increment of dispersion (i.e., longitudinal mixing) of the O_3 bolus occurring during the test breath.

VARIANCE COMPONENTS ANALYSIS

The Λ, V_B, and σ^2 data obtained in the baseline, flow, oral-nasal, and concentration experiments were sorted into 10-mL increments of V_P for each subject. The data within each increment were then analyzed according to a one-way random effects model. The overall sample means of Λ, V_B, and σ^2 were estimated by the arithmetic average of the individual subject averages within each V_P increment. The standard deviation (SD) of individual measurements about a subject's mean value (i.e., the within-subject variability, SD_w) and the standard deviation of the subjects' means about the overall sample mean (i.e., the between-subject variability, SD_b), were obtained as restricted maximum likelihood estimates (S-Plus, Statistical Sciences, Inc., Seattle, WA). The standard errors (SE) of individual measurements about the overall sample means were estimated by the formula

$$SE = [SD_b^2/n_s + (SD_w^2/n_s^2)\Sigma(1/n_i)]^{1/2}, \quad (17)$$

where n_i is the number of measurements in subject i, and Σ is the summation over all subjects, n_s.

ANATOMICALLY BASED COMPARTMENTAL MODELS

As benchmarks in interpreting V_P in terms of anatomic location, we adopted 50 mL as the volume of the upper airways that are proximal to the glottis and 110 mL as the volume of the lower conducting airways that are distal to the larynx (Ultman 1985). Taking into account the 20-mL volume of the (nonabsorbing) mouthpiece assembly distal to the O_3 sampling point, the penetration region 70 mL$>V_P>$20 mL has been designated as the upper airways (UA) compartment, 180 mL$>V_P>$70 mL has been identified as the lower conducting airways (CA) compartment, and $V_P>$180 mL has been recognized as the respiratory airspace (RA) compartment.

In applying the absorption theory to Λ data, two alternative compartmental models were used. In the four-compartment model, the CA compartment was divided into equal proximal and distal compartments (CAP and CAD), and the RA compartment was bounded at its distal end by the deepest penetration from which an exhaled bolus could be recovered, namely, V_P = 250 mL. Therefore, this model consisted of the four sequential compartments, UA (50 mL), CAP (50 mL), CAD (60 mL), and RA (70 mL). In the seven-compartment model, UA, CAP, and CAD were each divided into a pair of subcompartments of equal volume (proximal and distal UA [UAP and UAD], CAP_1 and CAP_2, and CAD_1 and CAD_2). Therefore, this model consisted of the seven sequential subcompartments UAP (25 mL), UAD (25 mL), CAP_1 (25 mL), CAP_2 (25 mL), CAD_1 (30 mL), CAD_2 (30 mL), and RA (70 mL).

STATISTICAL REGRESSIONS

In the baseline, flow, and oral-nasal experiments, the longitudinal distribution of *Ka* was estimated from each subject's Λ-V_P data by using Equation 6. In particular, a linear regression of $-\log_e(1 - \Lambda)$ versus V_P was performed in a piecewise manner between the intercompartmental boundaries of either the four-compartment model or the seven-compartment model. The regression was splined such that Λ was continuous at each boundary. However, the V_P intercept in the first compartment was treated as a free parameter, so that the proximal end of the regressed Λ-V_P distribution was unconstrained.

To quantify the effect of $\dot{V}$ in the flow experiments, the *Ka* values found in each airway compartment of the spline regression were averaged over all subjects. These overall mean *Ka* values were then regressed according to Equation 9 by using a nonlinear least-square Marquart algorithm (NONLIN, SAS Institute, Cary, NC).

To quantify the effect of peak inhaled O_3 level in the concentration experiments, the data from each subject were

regressed by a linear algorithm (GLM, SAS Institute) according to the empirical polynomial model

$$\Lambda = \alpha_0 + \alpha_1 V_P + \alpha_2 V_P^2 + \beta\,(F_{O_3})_{max}, \qquad (18)$$

where $(F_{O_3})_{max}$ is the peak concentration, and α_0, α_1, α_2, and β are adjustable parameters.

RESULTS

BASELINE EXPERIMENTS

A representative test breath (from subject 15) from the baseline experiments is shown in Figure 5. These data are uncorrected for dynamic distortion or for CO_2 interference, but, because the delay times are properly accounted for, there is good alignment between the end-inspiration point, t_I, on the respired volume curve (upper panel) and the sharp dividing trough on the O_3 concentration curve (middle panel). Notice that the phase II increase in expired CO_2 concentration (lower panel) appears as the O_3 concentration is rapidly approaching zero (middle panel). In Figure 7, the O_3 concentration has been corrected for dynamic distortion and CO_2 interference and is plotted against the relative lung volume. Moving from the uppermost to lowermost panel of this plot, it is clear from the reduction in area under the expired concentration curves that the absorption of O_3 increases as V_P increases. The interrupted curves in this graph represent the bolus response of the same subject to argon, an inert insoluble gas (Larsen 1987).

To evaluate the importance of corrections to the O_3 analyzer output for CO_2 interference and for dynamic distortion, we compared the moment calculations from the corrected data of one subject (subject 4) with the corresponding calculations from uncorrected data (Table 2). At most V_P values, the correction process changed Λ, V_B, and σ^2 by 5% or less, and we conclude that CO_2 interference and dynamic distortion had a minor influence on the data. A notable exception is the 20-mL penetration volume, at which data correction decreased Λ by 97% and increased σ^2 by 98%. However, the value of Λ was only 0.023 at this low penetration volume, so the absolute effect on Λ was still small. It is not surprising that the effect of a CO_2 correction was unimportant, given that expired CO_2 usually appeared at a time when the expired O_3 concentration had already returned to a value close to zero. A relatively small effect of the correction for dynamic distortion is also reasonable, because the time constant of the O_3 analyzer was small compared with the period during which O_3 was detected in the single breath.

The longitudinal distributions of Λ, V_B, and σ^2 are graphed in Figure 8 for individual test breaths from a representative subject (subject 15). Figure 9 shows the overall sample means plus or minus standard error of these three variables, separated into 10-mL increments of V_P, for the nine subjects in the baseline experiment. In the upper panel of both Figure 8 and Figure 9, the longitudinal distribution of Λ increases in a continuous fashion once V_P exceeds 20 mL. This volume corresponds to that (nonabsorbing) portion of the mouthpiece assembly distal to the O_3 sampling port. Beyond a penetration of 180 mL, essentially all O_3 is absorbed. In the middle panel of Figures 8 and 9, values of V_B are initially greater than V_P, but at bolus penetration volumes greater than 100 mL, V_B levels out at a constant value. In the lower panels of Figures 8 and 9, values of σ^2 during the bolus response are virtually insensitive to changes in V_P.

Figure 10 compares the fit of the data to the four-compartment and seven-compartment models in one subject (subject 15). Refinement of the model beyond four com-

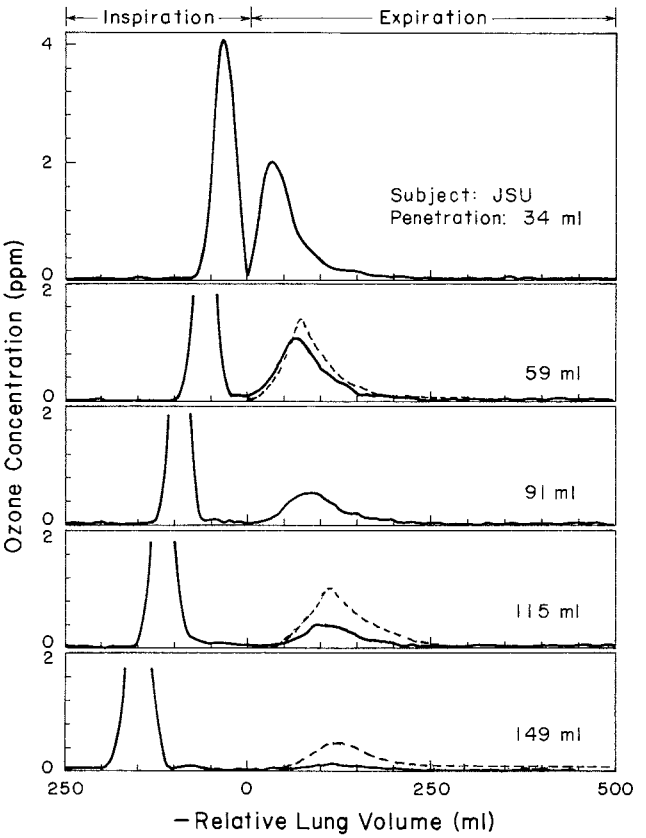

Figure 7. Representative bolus-response data from test breaths at progressively increasing bolus penetration volumes for subject 15. Voltage signals were converted to physical variables using the instrument calibrations, and time axes were translated to account for delay times. In addition, the data were corrected for CO_2 interference and for dynamic distortion and were then cross-plotted against the expired volume. The dashed-line curves are the bolus response of the same person to argon, an inert nonabsorbing gas (Larsen 1987).

Table 2. Effect of Data Correction on the Mathematical Moments for Subject 4

Penetration Volume (V_P) (mL)	Absorbed Fraction of Ozone[a] (Λ)	Change in Absorbed Fraction of Ozone[b] ($\Delta\Lambda$) (%)	Breakthrough Volume[a] (V_B) (mL)	Change in Breakthrough Volume[b] (ΔV_B) (%)	Dispersion[a] (σ^2) (mL^2)	Change in Dispersion[b] ($\Delta\sigma^2$) (%)
20	0.023	-97	37.7	6.0	1,080	98
30	0.140	-60	54.6	-13	1,290	-0.7
40	0.238	-13	63.2	-5.3	1,420	-2.8
50	0.343	4.8	70.6	2.4	1,270	-1.1
60	0.432	-2.4	78.5	3.9	1,310	8.8
70	0.458	3.8	88.4	3.1	1,770	2.7
80	0.541	5.0	93.8	3.5	1,690	-4.9
90	0.610	5.8	98.1	5.1	1,580	3.8
100	0.688	4.9	105	4.3	1,750	6.1
110	0.748	8.1	107	5.1	1,710	23
120	0.796	3.6	113	2.1	2,130	-17
130	0.847	1.0	109	6.4	1,660	33
140	0.877	0.6	117	2.5	2,160	5.5
150	0.906	1.6	116	0.3	2,050	-6.7
160	0.942	0.9	108	-1.4	1,960	-6.7
170	0.962	-0.7	109	12	1,840	16

[a] Entries for Λ, V_B and σ^2 have been corrected for both CO_2 interference and dynamic distortion.

[b] Entries for $\Delta\Lambda$, ΔV_B, and $\Delta\sigma^2$ represent the percentage of difference between the Λ, V_B, and σ^2 entries and the corresponding uncorrected data (not shown).

partments does not appear to improve the regression except in the proximal upper airways (where $V_P < 50$ mL) of subjects 2 and 15 in whom the increase in the Λ values was extraordinary. Figure 11 compares the *Ka* overall mean ± SE values that were obtained by averaging all nine subjects' *Ka* estimates from the four-compartment model (filled points) and from the seven-compartment model (unfilled points). To determine whether there was a significant difference between the *Ka*-V_P distributions obtained from the two models, a two-tailed *t* test was performed on the *Ka* difference between each of the eight adjacent pairs of filled and unfilled data points in Figure 11. For example, the difference between mean *Ka* values in the UA compartment (of the four-compartment model) at V_P = 45 mL and the UAP subcompartment (of the seven-compartment model) at V_P = 32.5 was not significantly different from zero ($p > 0.4$). In fact, for all eight of the *t* tests, the probabilities were $p > 0.4$, and we conclude that the mean *Ka* values obtained in the UA, CAP, CAD, and RA subcompartments of the four-compartment model are not significantly different from the mean *Ka* values obtained in the corresponding subcompartments of the seven-compartment model.

Values of *Ka* from both the four-compartment and seven-compartment models exhibit a high degree of uncertainty in the RA compartment, where penetrations are greater than 180 mL. This is due to two factors: for seven of the nine subjects, an expired bolus could not be resolved over background noise at such deep penetrations; and for the remaining two subjects, the Λ data leveled off at a relatively constant value.

FLOW EXPERIMENTS

To determine how accurately the targeted respiratory flows were reached in the flow experiments, the average flow was determined for each test breath beginning with the bolus injection and ending when 500 mL of air had been expired. Considering all test breaths recorded from all nine subjects, the mean respiratory flow rates ± SD were 145 ± 7, 248 ± 13, 482 ± 28, 726 ± 46, and 961 ± 59 mL/sec. The values are somewhat below the targeted values (i.e., 150, 250, 500, 750, and 1,000 mL/sec) owing to the natural deceleration of flow near the transition from inhalation to exhalation. Thus, in the data presentation and analysis that follow, we found it more convenient, yet just as logical, to use the targeted flows rather than the actual flows.

The overall sample means ± SE of Λ, V_B, and σ^2, separated into 10-mL intervals of V_P, are shown in Figure 12. The absorbed fraction increases monotonically with V_P at all flow rates, and the effect of increasing $\dot{V}$ is to shift the Λ-V_P distribution distally into the lungs. As in the baseline experiments, changes in V_B at small penetration volumes parallel changes in V_P, but at high penetration volumes, V_B levels off at a constant value. The effect of increasing $\dot{V}$ is to flatten the V_B-V_P curves and to shift them upward. While σ^2 is insensitive to V_P, it is directly related to $\dot{V}$. A linear

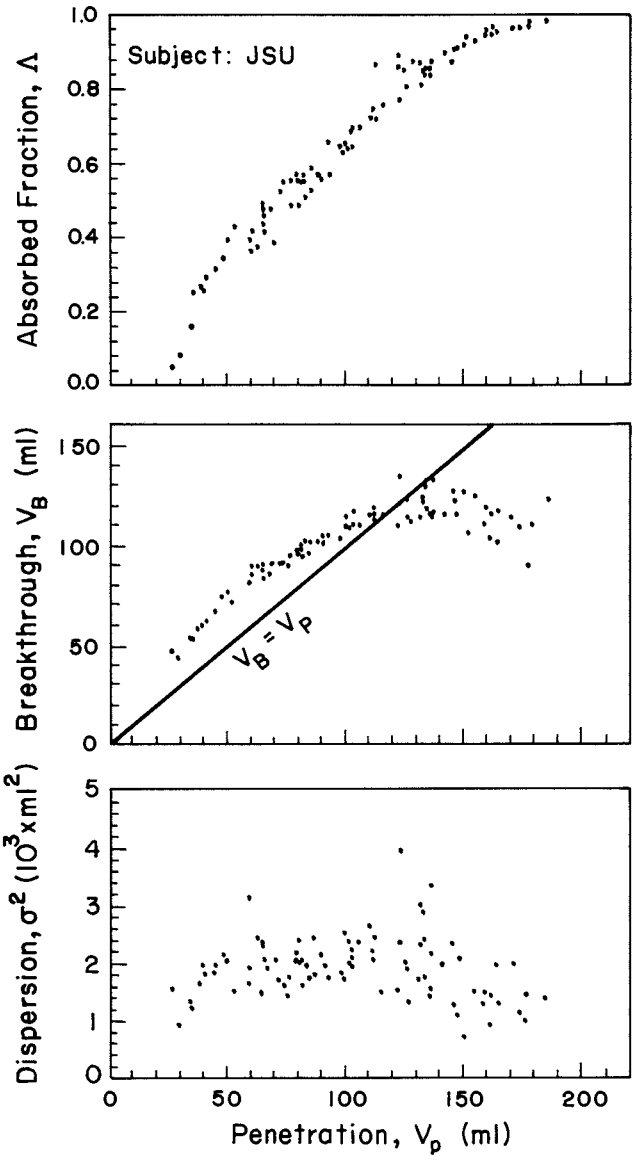

Figure 8. Mathematical moments of the bolus-response curves for subject 15.

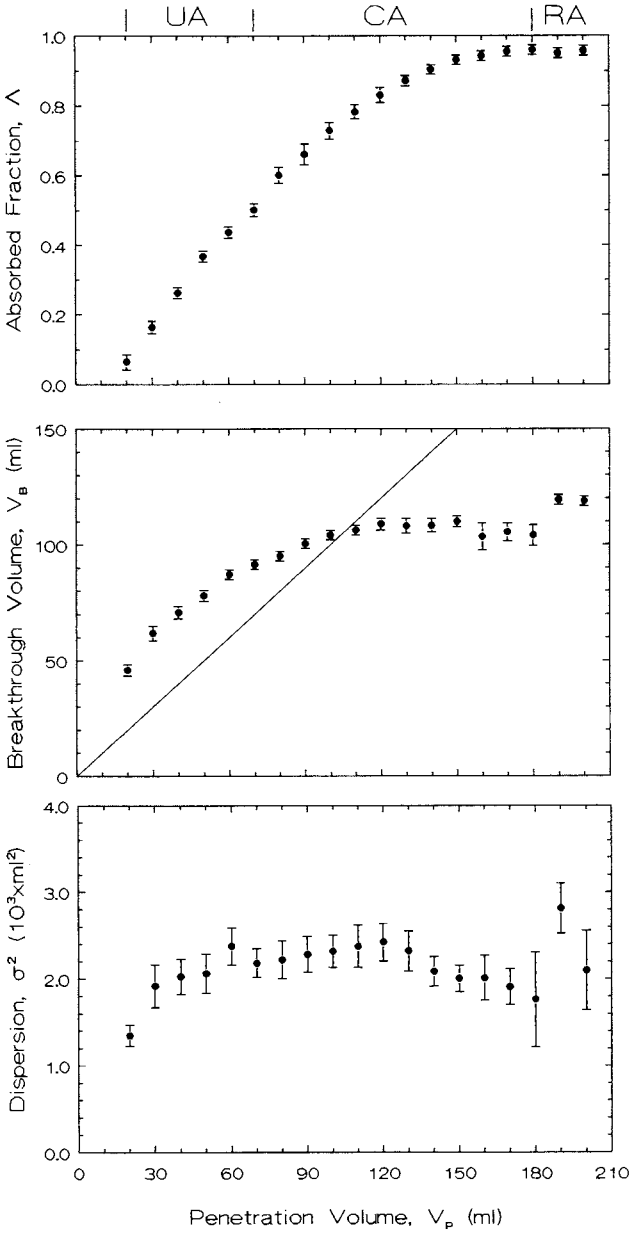

Figure 9. Mathematical moments of the bolus-response curves pooled for nine subjects in the baseline experiments (see Table 1). The overall sample means of Λ, V_B, and σ^2 within 10-mL increments of penetration volume are shown by the data points, and the standard errors of the overall means (Equation 17) are denoted by the vertical bars. The secondary abscissa indicates the approximate longitudinal position of upper airways (UA), lower conducting airways (CA), and respiratory airspaces (RA).

regression of σ^2 versus $\dot{V}$ was separately performed for each subject's data, and the nine resulting slopes and intercepts were averaged to determine the mean ± SE parameter estimates for an overall relationship:

$$\sigma^2[\text{mL}^2] = (14.4 \pm 1.3)\dot{V}[\text{mL/sec}] - (771 \pm 374). \quad (19)$$

The coefficient of determination, r^2, for the individual subjects' regressions ranged from 0.992 to 0.997, indicating a high degree of linearity of the flow dependence. Moreover, a two-tailed t test applied to the parameters of Equation 19 indicated that the mean slope was significantly different from zero ($p<0.001$), but the mean intercept was not ($p>0.07$).

Because the *Ka* distributions obtained in the baseline experiments with the four-compartment model were so similar to those obtained with the seven-compartment model, the Λ data from the flow experiments were analyzed with the simpler four-compartment model. The resulting *Ka* values are shown as data points in Figure 13. Considering that nine subjects participated in this experiment, there

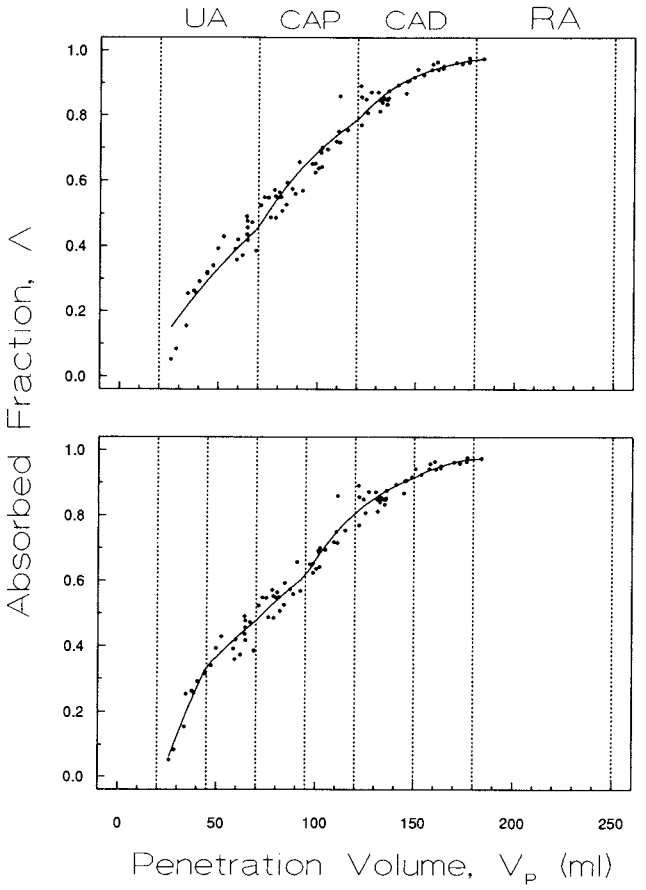

Figure 10. Regression of absorption model to the Λ-V_P data of subject 15 in the baseline experiment. The four-compartment model (top) fits the data as well as the seven-compartment model except in the proximal portion (left side) of the UA compartment. Also, data are insufficient for precise determination of *Ka* in the RA compartment using either model.

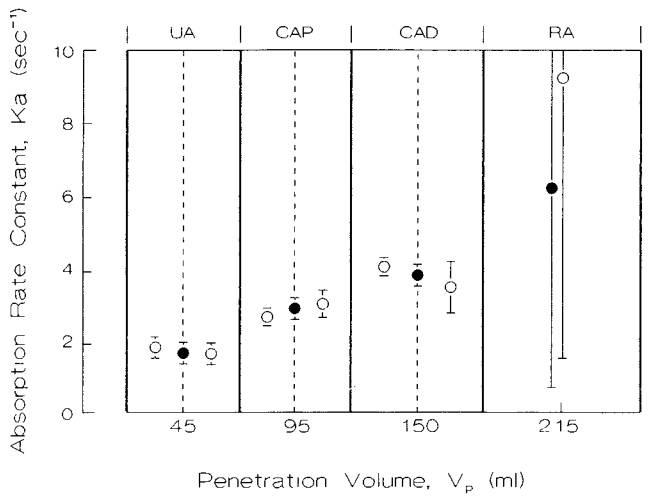

Figure 11. Comparison of the Ka-V_P distribution from the baseline experiment obtained with the four-compartment model (solid circles) and the seven-compartment model (open circles) (see Table 1). Data points and vertical bars, representing the overall mean ± SE of the *Ka* values obtained for the nine subjects, have been placed at the center of the compartment to which they apply. The *Ka* overall mean values in the RA compartment are unreliable because of the difficulty in recovering an expired bolus at such deep penetrations.

could be as many as nine different *Ka* values at each of the five respiratory flow rates within the four panels of this figure. However, at low flow rates, there were often so few values (i.e., fewer than three values) in the RA compartment that the corresponding *Ka* values were rejected, and at high flows, the same was true in the UA compartment. Table 3 lists the *Ka* overall mean ± SE values at all five flow rates and within each of the four compartments.

The data in each panel of Figure 13 were fit to Equation 9 using a nonlinear regression in which $k_\ell a$, ma, and n were all treated as adjustable parameters. The estimated values of the flow exponent, n ± SE, were close to 1 in all four compartments: 1.00 ± 0.22 (UA), 0.975 ± 0.36 (CAP), 1.01 ± 0.30 (CAD), and 1.03 ± 0.98 (RA). Whereas three of these four n values were reasonably precise, the standard errors of k_ℓ *and* ma were always much larger than the parameters themselves. Therefore, a second regression was performed in which $k_\ell a$ and ma were still treated as adjustable parameters, but n was constrained to a value of 1. The resulting estimates of $k_\ell a$ and ma were virtually the same as in the first regression, but their standard errors were reduced to more reasonable values (Table 4). The solid curves in Figure 13 represent the predicted *Ka* values obtained from the second regression.

ORAL-NASAL EXPERIMENTS

The overall sample means ± SE of Λ, V_B, and σ^2 separated into 10-mL intervals of V_P are shown in Figure 14. Relative to oral breathing, nasal breathing caused a proximal shift in the Λ-V_P distribution such that the total airway volume over which O_3 absorption occurs was compressed from 180 mL to approximately 130 mL. The relation between V_B and V_P is similar in the two modes of breathing, with the nasal values for V_B being somewhat smaller than the oral values at penetration volumes below 75 mL. Values of σ^2 for nasal breathing appear to increase with V_P, while σ^2 values for oral breathing are insensitive to V_P.

To determine whether the difference between Λ-V_P distributions during oral breathing and during nasal breathing was due to the influence of the breathing fixtures, we compared bolus data obtained when one subject (subject 10) breathed orally through the mouthpiece, through one pillow of the nasal cannula, or through the bare interconnection tube. The results indicate that the Λ-V_P distribution was the same whether or not the mouthpiece was on the interconnection tube (Figure 15). This indicates that O_3 absorption by the rubber mouthpiece was negligible. How-

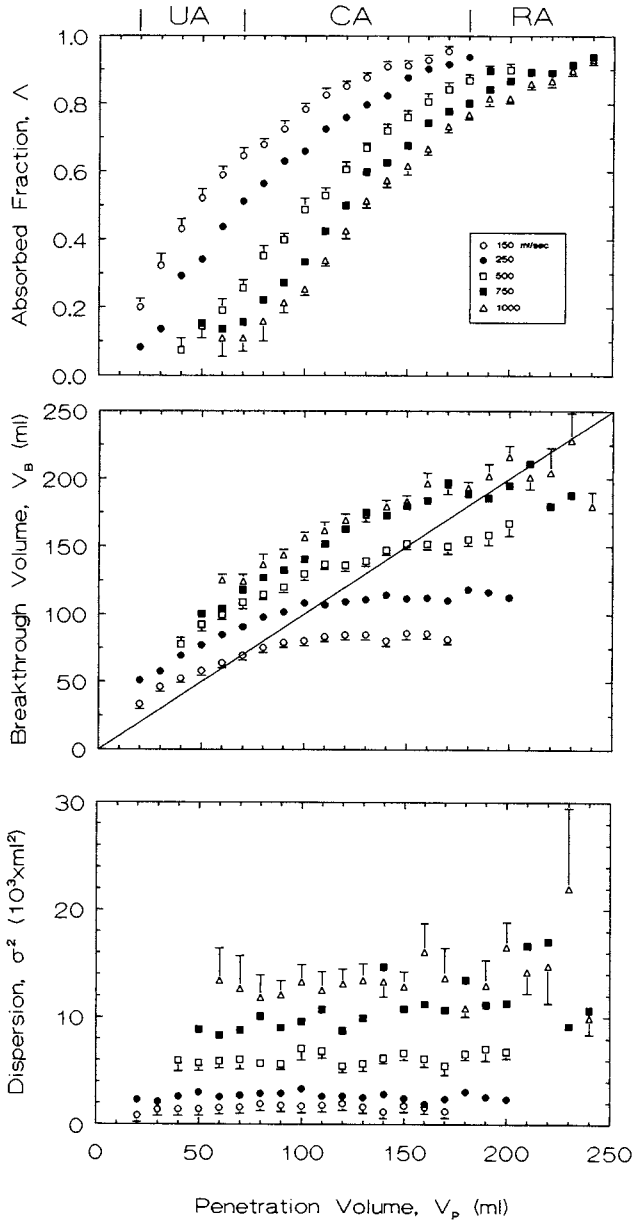

Figure 12. Mathematical moments of the bolus-response curves pooled for nine subjects in the flow experiments (see Table 1). The overall sample means of Λ, V_B, and σ^2 within 10-mL increments of penetration volume are shown by the data points, and the standard errors of the overall means (Equation 17) are denoted by the vertical bars. The secondary abscissa indicates the approximate longitudinal position of upper airways (UA), lower conducting airways (CA), and respiratory airspaces (RA). To avoid clutter, standard errors have only been indicated for the highest, lowest, and intermediate flow data. Flow rates were 150 (open circles), 250 (closed circles), 500 (open squares), 750 (closed squares), and 1,000 (open triangles) mL/sec.

ever, the addition of the cannula to the interconnection tube did result in a mean increase in Λ of 0.08. Although this increase was statistically significant, it cannot explain the large difference between the Λ-V_P distributions in Figure 14.

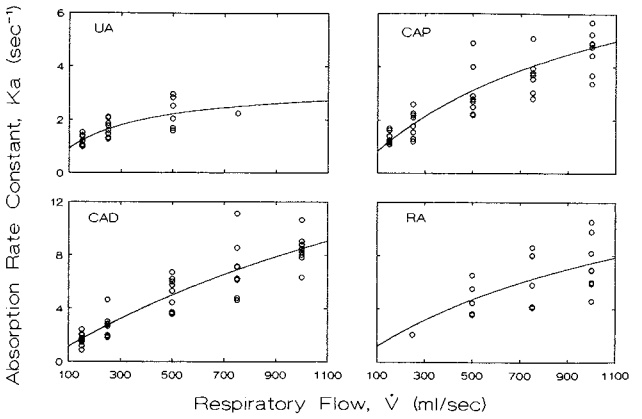

Figure 13. Flow sensitivity of Ka obtained with the four-compartment model. Data points are the individual subjects' values, and the smooth curves are the results of a nonlinear least-square regression to Equation 9.

The Λ data for nasal breathing rose more steeply than for oral breathing and, in the determination of the *Ka* distribution, it was necessary to use the seven-compartment absorption model to ensure an adequate fit. Table 5 gives a side-by-side comparison of the resulting *Ka* values from eight of the nine subjects. Subject 19 was excluded from this analysis because there were only three Λ data points within his UAP subcompartment during nasal breathing, and this resulted in a negative estimate of *Ka*. Data at $V_P > 95$ mL also were excluded for nasal breathing because the Λ had leveled out to an extent that precise values of *Ka* could not be estimated.

For nasal breathing, the *Ka* overall mean value in the UAP subcompartment was 70% larger than during oral breathing. This tendency for a larger *Ka* during nasal breathing was progressively reduced in going from the UAP to UAD to CAP_1 subcompartments. In fact, in paired two-tailed *t* tests, the difference between *Ka* during oral breathing and that during nasal breathing was highly significant in the UAP subcompartment ($p < 0.0005$) and still significant in the UAD subcompartment ($p < 0.05$), but the difference between the two modes of breathing did not have a significant effect on the *Ka* values in the CAP_1 subcompartment ($p > 0.4$).

CONCENTRATION EXPERIMENTS

The bolus-response data obtained at different peak inhaled O_3 concentrations were assigned to categories of low (0.42 ± 0.10 ppm), medium (1.10 ± 0.18 ppm), high (2.11 ± 0.23 ppm), and very high (3.48 ± 0.50 ppm). Figure 16 shows the population mean values ± SE of Λ, V_B, and σ^2 separated into 10-mL intervals of V_P. Because of the limited precision of the O_3 analyzer in the low-concentration category, only three subjects (8, 12, and 16) were tested under this condition, and it was not possible to estimate population means comparable with those in the other concentration

Table 3. Variation of the Absorption Rate Coefficient (Ka) with Respiratory Flow Rate in the Four-Compartment Model

Compartment	Nominal Flow Rate (mL/sec)	Number of Subjects[a]	Absorption Rate Coefficient[b] ($Ka \pm$ SE) (sec^{-1})
Upper airways	150	9	1.20 ± 0.07
(70 mL > V_P > 20 mL)	250	9	1.68 ± 0.11
	500	6	2.27 ± 0.24
	750	1	2.24
	1,000	0	—
Conducting airways, proximal	100	9	1.30 ± 0.07
(120 mL > V_P > 70 mL)	250	9	1.79 ± 0.17
	500	9	3.00 ± 0.30
	750	8	4.26 ± 0.62
	1,000	9	4.66 ± 0.24
Conducting airways, distal	100	8	1.65 ± 0.18
(180 mL > V_P > 120 mL)	250	9	2.71 ± 0.29
	500	9	5.04 ± 0.40
	750	8	6.96 ± 0.74
	1,000	9	8.45 ± 0.38
Respiratory airspaces	150	0	—
(250 mL > V_P > 180 mL)	250	1	2.07
	500	5	4.70 ± 0.56
	750	6	6.46 ± 0.47
	1,000	8	7.37 ± 0.71

[a] Although experiments were performed on nine subjects, absorption data were generally unavailable in the most distal compartment at low flow rates and in the more proximal compartments at high flow rates.

[b] Ka overall mean ± SE of individual subjects' Ka values.

Table 4. Individual Mass Transfer Coefficients for Ozone in Air ($k_g = m\dot{V}$) and in the Liquid-Lining Layer (k_ℓ)[a]

Compartment	$k_\ell a/\lambda \pm$ SE[b]	$ma \pm$ SE	Surface:Volume Ratio (a)	k_ℓ/λ	Flow Coefficient (m) (cm^{-2})
Upper airways (70 mL > V_P > 20 mL)	3.38 ± 0.53	0.0129 ± 0.0025	1.7[c]	2.04	7.73
Conducting airway, proximal (120 mL > V_P > 70mL)	9.87 ± 2.63	0.00913 ± 0.00165	9.3[d]	1.146	0.98
Conducting airways, distal (180 mL > V_P > 120mL)	28.0 ± 11.0	0.0122 ± 0.0017	40.9[d]	0.68	0.30
Respiratory airspaces (250 mL > V_P > 180mL)	17.8 ± 12.0	0.0128 ± 0.0052	68.8[d]	0.25	0.19

[a] k_g = air mass transfer coefficient (in cm/sec); m = flow coefficient (in cm^{-2}); $\dot{V}$ = respiratory flow (in mL/sec); k_ℓ = liquid-lining layer mass transfer coefficient (in cm/sec).

[b] λ = partition coefficient between liquid-lining layer and air.

[c] Estimated from measurements in upper airway cadaver casts (Olson et al. 1973).

[d] Average of a values obtained from models of Weibel (12.3, 50.2, 72.1), Olson (4.6, 25.7, 70.9), Hanson-Ampaya (14.3, 55.6, 56.8), and Yu-Schum (5.8, 32.0, 75.2) as presented by Yu and Diu (1982).

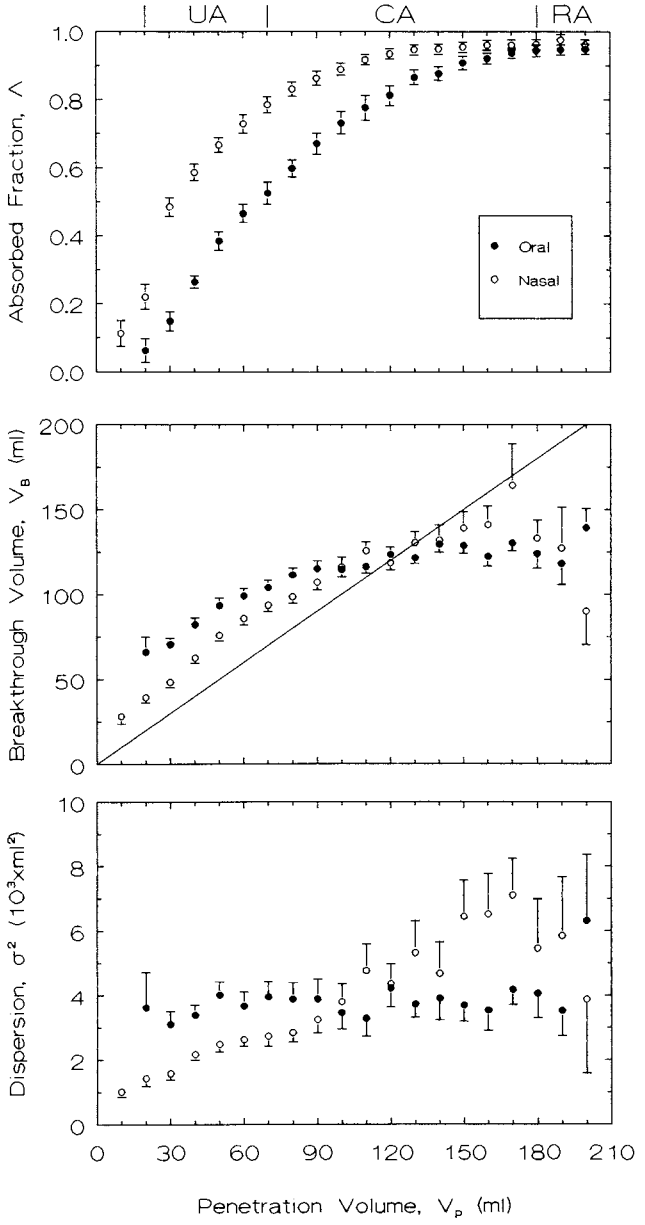

Figure 14. Mathematical moments of the bolus-response curves pooled for the nine subjects in the oral-nasal experiments (see Table 1). The overall sample means of Λ, V_B, and σ^2 within 10-mL increments of penetration volume are shown by the data points, and the standard errors of the overall means (Equation 17) are denoted by the vertical bars. The secondary abscissa indicates the approximate longitudinal position of upper airways (UA), lower conducting airways (CA), and respiratory airspaces (RA). Closed circles are data points for oral experiments, open circles for nasal experiments.

categories. Therefore, the low concentration category was not included in Figure 16. It appears from this graph that $(F_{O_3})_{max}$ does not have a systematic effect on the absorption, breakthrough, or dispersion parameters.

Table 6 contains the results for the polynomial regression

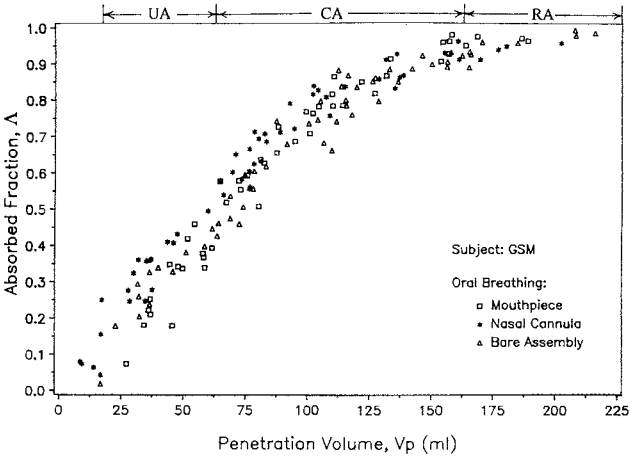

Figure 15. Effect of breathing fixture on the bolus absorption data for subject 10. The absorbed fractions are compared for mouth breathing through the rubber mouthpiece (squares), through one of the nasal pillows (asterisks), or through the bare interconnection tube of the breathing fixture in Figure 4 (triangles).

of the Λ-V_P distribution to each individual subject's data as well as the overall mean of the parameter estimates. Focusing on the β parameter, which represents the change in Λ for a 1 ppm change in $(F_{O_3})_{max}$, there is no statistically significant concentration effect for subjects 16 and 19. For the other four subjects (subjects 3, 8, 12, and 21), β is 0.03 or less and is negative in two of them and positive in the other two. In other words, the effect of $(F_{O_3})_{max}$ appears to be very small and random. As determined by a two-tailed t test, the overall mean value of β is not significant ($p>0.5$).

DISCUSSION AND CONCLUSIONS

THE ABSORBED FRACTION

The primary variable we observed was the fraction of inhaled O_3 that is absorbed into the lungs, Λ. Compared with an inert insoluble gas such as argon (Figure 7), O_3 shows a progressive loss and, therefore, a continual increase in Λ at increasing bolus penetrations. At a quiet respiratory flow rate of 250 mL/sec, Λ increases smoothly and monotonically with V_P (Figure 9). About 50% of the inhaled O_3 is absorbed in the upper airways. This is close to the 40% to 45% range for the absorbed fraction of O_3 in the upper airways measured using direct pharyngeal sampling during continuous inhalation of O_3 (Gerrity et al. 1988). Our measurements also indicate that absorption is essentially complete within the lower conducting airways during quiet breathing. However, with increasing respiratory flow, as would occur during exercise, the Λ-V_P distribution is

Table 5. Paired Comparison of Ozone Individual Absorption Rates (*Ka*) for Oral and Nasal Breathing Using the Seven-Compartment Model[a]

	Compartment and Penetration Volume Range								
	Upper Airways Proximal 20–45 mL		Upper Airways Distal 45–70 mL		Conducting Airways Proximal$_1$ 70–95 mL		Conducting Airways Proximal$_2$ 95–120 mL	Conducting Airways Distal$_1$ 120–150 mL	Conducting Airways Distal$_2$ 150–180 mL
	Oral	Nasal	Oral	Nasal	Oral	Nasal		Oral[b]	
	2.58	3.83	2.86	1.62	2.52	3.47	3.05	2.01	1.02
	2.03	4.02	2.23	2.13	3.35	2.18	3.00	4.42	4.12
	1.37	2.28	1.06	3.22	1.49	6.07	2.47	2.79	3.19
	2.57	4.42	2.17	3.66	2.72	3.57	4.43	2.51	1.45
	1.59	3.64	1.47	2.94	1.77	3.73	1.54	1.78	2.80
	2.09	4.56	1.27	1.83	2.95	1.03	2.17	3.32	4.03
	3.54	3.86	2.47	3.60	2.02	3.23	3.52	2.82	2.54
	2.50	4.61	2.54	4.81	3.64	3.20	3.19	3.18	6.27
Ka Mean ± SE	2.28 ± 0.24	3.90 ± 0.26	2.01 ± 0.23	2.98 ± 0.38	2.56 ± 0.27	3.31 ± 0.51	2.92 ± 0.31	2.85 ± 0.29	3.18 ± 0.59

[a] Data for only six compartments are shown because insufficient O_3 were obtained for $V_P > 180$ mL to allow *Ka* in the RA compartment to be determined. Values are expressed in sec^{-1}.

[b] Because of the extensive absorption in more proximal compartments, data in the CAD compartments were insufficient for estimating *Ka* during nasal breathing.

shifted distally. In other words, a smaller fraction of O_3 is absorbed in the upper airways, so more O_3 reaches the lower airways and respiratory airspaces (Figure 12).

The effect of nasal breathing was to shift the Λ-V_P distribution proximal to the distribution that was measured during oral breathing. As judged from Figure 14, this would occur if the fraction of O_3 absorbed by the nose is 0.3 (60%) more than the fraction absorbed by the mouth. But, this would also occur if the dead space of the nasal flow path from the O_3 sampling site to the pharynx is 50 mL smaller than the volume of the oral flow path. The mouthpiece and nasal cannula had similar volumes of 25 and 29 mL, respectively, and breathing orally through them resulted in almost identical Λ-V_P distributions (Figure 15). Moreover, the subject's mouth was only partially open when it grasped the rubber mouthpiece, so it is improbable that the dead space of the mouth was much greater than the dead space of the nose. We conclude that the highly efficient absorption of the nose accounts for the proximal shift in the Λ-V_P distribution. Thus, during quiet breathing or light exercise, when nasal breathing predominates over oral breathing, the lower airways are better protected from O_3 than during heavier exercise, when oral breathing is important.

This conclusion differs from the conclusions of Gerrity and associates (1988) and Weister and colleagues (1991), who observed little difference between O_3 absorption in human lungs during oral and during nasal breathing. We believe that the experiments of Weister and colleagues lacked sensitivity to differences between nasal and oral breathing, because they only measured O_3 absorption by the entire respiratory system. To demonstrate this, we integrated our absorbed fraction curves and determined that the equivalent volume of inspired air that is stripped of all its O_3 is 26 mL larger during nasal breathing than during oral breathing. Thus, for a 600-mL tidal volume of continuously inhaled O_3, the absorption efficiency of the respiratory system is only 4% (26/600) greater during nasal breathing than during oral breathing. It is doubtful that the precision of the experiments by Weister and colleagues was adequate to resolve this small difference. Although it is difficult to identify a single factor that explains why Gerrity and associates did not observe oral-nasal differences in O_3 absorption, two possible factors are readily seen. The most obvious limitation of their measurements was the pharyngeal sampling tube they used. The tube became partially obstructed with condensed water vapor and secretions, and the presence of the tube modified the velocity patterns in the upper airways. The second limitation was the O_3 analyzer they used with a step-response time of 700 msec, which distorted the concentration measurements.

The Λ-V_P distribution was not influenced by changes in peak inspired O_3 concentration from 0.3 to 4.0 ppm (Figure 16), implying that the diffusion and chemical reaction responsible for absorption into mucus are both linear processes. The linearity of O_3 diffusion rate is an expected consequence of Fick's law (Treybal 1980). The linearity of the reaction rate with respect to O_3 concentration implies that the rate-controlling step is the interaction of one molecule of O_3 with one or more molecules of substrate. Most probably, the reaction rate also depends on the concentration of substrate. However, in bolus-response experiments, the time that an O_3 bolus is in contact with the mucosal

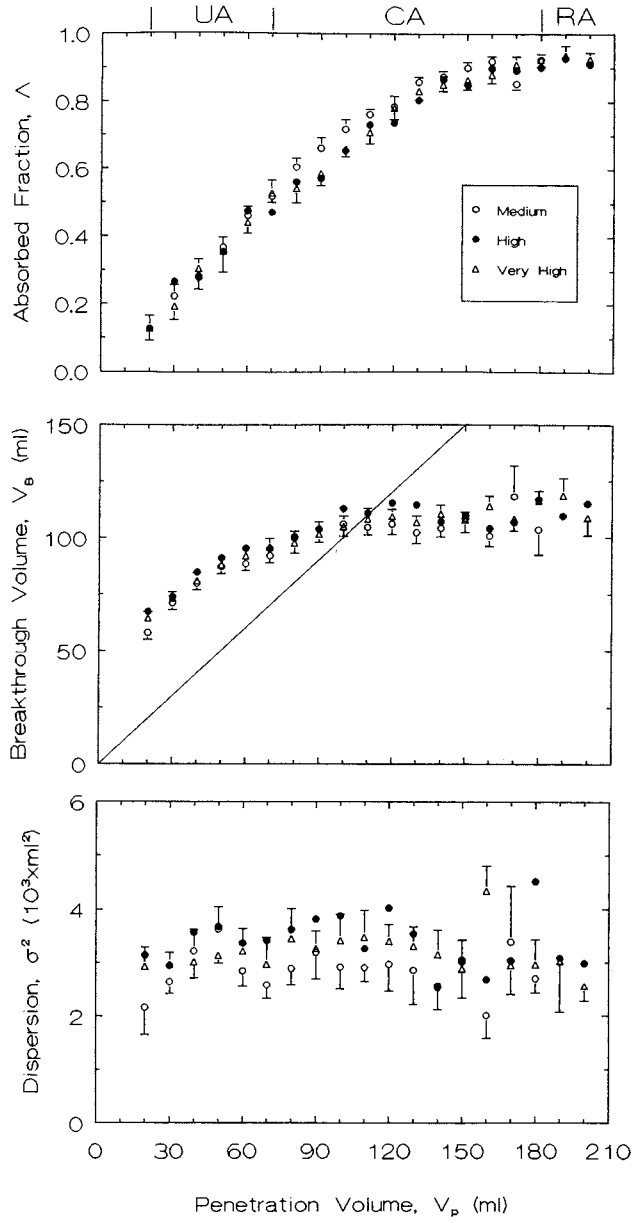

Figure 16. Mathematical moments of the bolus-response curves pooled for six subjects in the concentration experiments (see Table 1). The overall sample means of Λ, V_B, and σ^2 within 10-mL increments of penetration volume are shown by the data points, and the standard errors of the overall means (Equation 17) are denoted by the vertical bars. The secondary abscissa indicates the approximate longitudinal position of upper airways (UA), lower conducting airways (CA), and respiratory airspaces (RA). To avoid clutter, standard error bars have been indicated only for the very high and medium inhaled peak concentration data. The data at low concentrations have not been included because they were obtained for only three subjects.

surface is so short that the substrate concentration is essentially unchanged by the chemical reaction. On the other hand, if subjects were preexposed to a constant level of inhaled O_3 for several hours before the bolus-response measurements were made, substrates might be significantly depleted. This would reduce the reaction rate of O_3 in mucus, and as a result, the Λ-V_P distribution would be shifted distally to that obtained in individuals who are not preexposed to O_3.

MASS TRANSFER COEFFICIENTS

Whereas Λ represents cumulative absorption from the airway opening to a particular V_P, often the local rate of absorption is of interest. A suitable quantity for characterizing local absorption is Ka (sec^{-1}), representing the uptake rate in a particular region normalized by the local O_3 gas concentration and by the region volume. This parameter is the product of an overall mass transfer coefficient, K (cm/sec), reflecting the contribution of diffusion and chemical reaction, and a local surface:volume ratio, a (cm^{-1}), accounting for lung anatomy. Airway branches are somewhat cylindrical, so a is inversely proportional to their inner radius. In human lungs, in which airway radius generally decreases with longitudinal distance from the mouth (Weibel 1963), a is an increasing function of cumulative airway volume.

The computed Ka values indicate that the nose is a more effective absorber of O_3 than the mouth (Table 5). Most dramatic is the proximal subcompartment of the nose, where Ka is 70% larger than the corresponding mouth compartment. The value of Ka in the CAP_1 subcompartment was essentially the same during oral and nasal breathing, implying that differences in absorption due to the mode of respiration are confined to the upper airways. This would not be the case if the proximal shift of the Λ-V_P distribution observed during nasal breathing were due to a uniform translation of the V_P axis, as would occur if the nasolaryngeal air route had a smaller dead space than the orolaryngeal route.

The CAP_1 subcompartment included the trachea as the major airway, and Ka values in this compartment were about 1.7 sec^{-1} during quiet oral breathing (Figure 11). This is about twice the value we previously obtained in excised pig and sheep tracheas (Ben-Jebria et al. 1991). Moreover, Ka values in the excised preparations were insensitive to gas flow, unlike the Ka values in intact lungs that were positively correlated with respiratory flow.

In particular, the flow-dependent portion of Ka had a flow coefficient, n, of 1 throughout the upper and lower conducting airways. This implies that the gas-phase absorption rate constant is directly proportional to flow according to the formulas (Table 4):

$$k_g a\ [\text{sec}^{-1}] = 0.0129\ \dot{V}\ [\text{mL/sec}] \quad \text{UA} \quad (20)$$

$$k_g a = 0.0091\ \dot{V} \quad \text{CAP} \quad (21)$$

Table 6. Regression of Absorbed Fraction Data to the Polynomial Model[a]: Effect of Peak Inspired Ozone Concentration

	Peak O_3 (ppm) ± SD				Parameter Estimates ± SE[b]			
Subject	Low[c]	Medium	High	Very High	α_0	α_1 (10^{-3}/mL)	α_2 (10^{-5}/mL^2)	β (ppm^{-1})
3	–	1.32 ± 0.13	2.25 ± 0.21	4.06 ± 0.31	0.0489 ± 0.0178	9.03 ± 0.31	−2.08 ± 0.14	−0.0272 ± 0.0033
8	0.43 ± 0.10	1.03 ± 0.11	2.15 ± 0.23	2.97 ± 0.24	−0.1899 ± 0.0282	12.25 ± 0.57	−3.45 ± 0.28	0.0131 ± 0.0065
12	0.26 ± 0.05	1.03 ± 0.16	2.16 ± 0.21	3.03 ± 0.41	0.0285[d] ± 0.0178	8.95 ± 0.53	−2.20 ± 0.25	0.0157 ± 0.0068
16	0.45 ± 0.05	1.21 ± 0.12	2.09 ± 0.21	3.29 ± 0.26	−0.0251[c] ± 0.0214	11.39 ± 0.43	−3.21 ± 0.22	−0.0021[f] ± 0.0044
19	–	1.01 ± 0.15	2.09 ± 0.21	3.41 ± 0.24	−0.0700 ± 0.0178	8.91 ± 0.49	−1.94 ± 0.21	−0.0039[g] ± 0.0051
21	–	1.01 ± 0.13	1.99 ± 0.21	3.41 ± 0.43	−0.2053 ± 0.0336	12.15 ± 0.51	−3.07 ± 0.29	−0.0219 ± 0.0057
Mean ± SE	0.38 ± 0.06	1.10 ± 0.05	2.12 ± 0.03	3.36 ± 0.16	−0.0688 ± 0.0442	10.44 ± 0.67	−2.05 ± 0.26	−0.0044 ± 0.0072

[a] The model is: ($\Lambda = \alpha_0 + \alpha_1 V_P + \alpha_2 V_P^2 = \beta F_{O_3 max}$). See the Statistical Regressions section under Data Analysis and Statistical Methods for more information.

[b] All parameter estimates are significantly different from zero ($p < 0.05$) except in the four footnoted cases.

[c] Because the O_3 analyzer has limited precision at low concentrations, only three subjects were tested in this range.

[d] $p > 0.3$

[e] $p > 0.2$

[f] $p > 0.6$

[g] $p > 0.4$

$$k_g a = 0.0122\ \dot{V} \qquad \text{CAD} \qquad (22)$$

Making measurements during steady unidirectional flow in a hollow airway model, Nuckols (cited in Hannah et al. 1989) found n values in upper airways of 0.80 and 1.3 and n values in the lower conducting airways of 0.73 and 0.75 during inspiratory-directed and expiratory-directed flows, respectively. Considering that the standard errors of our n estimates ranged from 0.22 to 0.36, we conclude that the flow coefficients measured on intact lungs are consistent with those measured in Nuckol's physical model.

The strong dependence of Ka on respiratory flow indicates that the diffusion resistance of the gas boundary layer can be an important determinant of O_3 absorption. For example, at a quiet respiratory flow rate of 250 mL/sec, these equations predict that $k_g a$ is equal to 3.2, 2.3, and 3.1 sec^{-1} in the three compartments, while the corresponding values of Ka are 1.7, 1.8, and 2.7 sec^{-1} (Table 3). Thus, the gas boundary layer contributes 53% (1.7/3.2) of the overall diffusion resistance in the UA compartment, 78% (1.8/2.3) in the CAP compartment, and 87% (2.7/3.1) in the CAD compartment. This increasing importance of the gas diffusion resistance with distal penetration into the airways is consistent with the fact that gas velocity progressively decreases as the airways subdivide.

To isolate the values of individual mass transfer coefficients k_g and k_ℓ/λ from the "lumped parameters" $k_g a$ and $k_\ell a/\lambda$ found in the flow experiments, it was necessary to estimate a in the four model compartments: along the orolaryngeal path (UA), as well as within cumulative airway volumes of 0 to 50 mL (CAP), 50 to 110 mL (CAD), and 110 to 180 mL (RA) within the tracheobronchial tree. This was accomplished by using measurements from cadaver upper airway casts (Olson et al. 1973) and dimensions from a combination of the lower airway models of Weibel, Olson, Hanson-Ampaya, and Yu-Shum (Yu and Diu 1982). The resulting values for k_ℓ/λ progressively decrease with longitudinal distance into the lung (Table 4).

To examine the implication of this result, we assume that as O_3 diffuses through the liquid-lining layer, it undergoes a first-order homogeneous chemical reaction with biochemical substrates. In that case, there is a conventional diffusion-reaction theory for formulating k_ℓ (Hobler 1966):

$$k_\ell/\lambda = (k_r D_\ell)^{1/2} \coth[t(k_r/D_\ell)^{1/2}]/\lambda, \qquad (23)$$

where coth is the hyperbolic cotangent function, k_r is the reaction rate constant, D_ℓ is the diffusion constant, and t is the thickness of the liquid-lining layer. Assuming that D_ℓ is relatively constant throughout the liquid-lining layer, Equation 23 predicts that k_ℓ increases as t decreases or as k_r increases. However, according to Table 4, k_ℓ/λ progressively decreases as the bolus penetration increases and, consequently, as the liquid-lining layer decreases in thickness. We conclude that the reactivity of the liquid-lining layer must decrease between the mouth and the peripheral airways.

To quantify this trend, the values of k_r in the mucous layer were computed with the k_ℓ/λ values given in Table 4, by approximating $\lambda = 0.69$ and $D_\ell = 2.7 \times 10^{-5}$ cm/sec by their aqueous values (Miller et al. 1985), and by making the reasonable assumption that $t > 0.2$ μm in all conducting air-

ways. Fortuitously, this constraint on t allows the reaction rate constant to be computed from Equation 23 by using a limiting case that is independent of the actual thickness of the liquid-lining layer (i.e., $k_r = [\lambda(k_\ell/\lambda)]^2/D_\ell$). The results are that k_r is equal to 7.3×10^6, 2.3×10^6, and 8.2×10^5 sec^{-1} in the mucous lining of the UA, CAP, and CAD compartments, respectively.

BREAKTHROUGH AND DISPERSION

The relationship between V_B and V_P (Figure 9) provides a means of evaluating the reversibility of gas transport processes during a respiratory cycle. Whereas V_P is the mean airway volume to which a bolus of gas would penetrate during inspiration if there were no absorption, V_B is the mean airway volume from which the expired molecules originate. For an insoluble gas flowing in a straight tube, there is no absorption, and these two volumes would be equal.

But the bronchial tree is not a straight tube. Rather, it has an expanding cross-section that can create a mouthward diffusion velocity (Reisfeld and Ultman 1988) causing V_B to be smaller than V_P. The higher Ka value of O_3 in the distal airways as compared with the proximal airways is another factor that tends to reduce V_B in relation to V_P. Both of these effects can contribute to the leveling off of V_B values observed at large penetration volumes. At low penetration volumes, changes in breakthrough tend to parallel changes in penetration, but V_B is systematically larger than V_P. This implies that there is a dead zone within the proximal airways that slows, but does not eliminate, the expiration of O_3 molecules.

The dispersion parameter characterizes the cumulative longitudinal mixing of a test gas bolus with surrounding air. Therefore, σ^2 should continually increase with V_P. This expectation was previously confirmed for inert insoluble gases, helium and sulfur hexafluoride, for which σ^2 rose from 0 to 6,000 mL^2 over the first 200 mL of bolus penetration volume (Ultman et al. 1978). In contrast, our data obtained with O_3 indicate that σ^2 is generally independent of V_P (Figure 9). This difference in behavior can be explained as follows. Inert insoluble gases accumulate in distal airspaces and reach a residual concentration that appears as a long "tail" on the expired concentration curve. The deeper the penetration, the more pronounced is the tail (Figure 7), and the larger is the computed value of σ^2. On the other hand, O_3 rapidly and completely absorbs into distal airways, so the tail of the expired O_3 curve is short at all penetrations, and this imposes a constant limit on the value of σ^2.

We previously reported that sulfur hexafluoride boluses inhaled to a V_P of 160 mL produced σ^2 values that were virtually independent of the inspiratory flow rates but were linearly related to the expiratory flow rate, with an average slope of 4.8 mL-sec for the three subjects tested (Ultman and Thomas 1979). From this linear behavior, we concluded that mixing in conducting airways was due to Taylor dispersion. In the current study, we found that σ^2 for O_3 boluses was linearly related to respiratory flow, in this case with a slope of 14.4 mL•sec (Equation 14). For flow through straight tubes, Taylor dispersion theory indicates that the slope of the σ^2-$\dot{V}$ line for a strongly absorbing gas is 11 times greater than the slope for an insoluble gas, and for both types of gases, the slope is inversely proportional to the diffusion coefficient (Dayan and Levenspiel 1969). Because the diffusion coefficient of O_3 is about 2.5 times larger than that of sulfur hexafluoride, the expected ratio of the σ^2-$\dot{V}$ slopes for these two gases is 4.4 (11/2.5), which is reasonably close to the ratio of 3.0 (14.4/4.8) that was measured in conducting airways.

VARIABILITY OF DATA

The variance components analysis performed for the baseline experiments indicated that for Λ, V_B, and σ^2 alike, the within-subject variability (SD_w) was about the same as the between-subject variability (SD_b) (Table 7). Moreover, SD_w and SD_b did not change in a systematic manner between V_P increments. Because SD_w was similar to SD_b, it was equally important to replicate measurements on individual subjects and to include a sufficient number of subjects in the study.

As was the case in the baseline experiments, the SD_w and SD_b values were always similar to each other in the flow, oral-nasal, and concentration experiments (data not shown). The variability of Λ, as characterized by either SD_w or SD_b, was comparable under all experimental conditions. On the other hand, the SD_w and SD_b associated with V_B and σ^2 tended to increase with increasing $\dot{V}$; the specific increases in variability were directly proportional to the increases in V_B and σ^2 that also occurred as $\dot{V}$ was elevated. A decline in the peak inhaled O_3 concentration also increased the SD_w and SD_b associated with V_B and σ^2, but a switch from oral to nasal breathing did not affect the variability of the data.

To better understand the source of SD_b, the possibility that O_3 absorption is influenced by differences between the lung geometries of those people being tested was explored. In particular, the FVC that was available from the spirometric screening tests was viewed as a surrogate for total lung volume, and the anatomic dead space (V_D), computed by Fowler's method (Fowler 1948) from the expired CO_2 data, was used as an estimate of the conducting airway volume.

Table 7. Components of Variance for Baseline Experiments

V_P (mL)	Number of Subjects	Number of Tests	Absorbed Fraction					Breakthrough Volume					Dispersion				
			Λ[a]	SE[b]	SD_b	SD_w	SD_b/SD_w	V_B[a] (mL)	SE[b] (mL)	SD_b (mL)	SD_w (mL)	SD_b/SD_w	σ^2[a] (mL^2)	SE[b] (mL^2)	SD_b (mL^2)	SD_w (mL^2)	SD_b/SD_w
20	5	11	0.064	0.022	0.038	0.041	0.9	45	2	4	4	0.8	1,340	120	000	380	0.0
30	9	38	0.163	0.018	0.036	0.071	0.5	61	3	8	5	1.5	1,910	240	700	360	1.9
40	9	42	0.262	0.015	0.039	0.046	0.8	70	2	7	4	1.8	2,020	200	570	370	1.5
50	9	42	0.367	0.015	0.037	0.054	0.6	78	2	6	5	1.2	2,060	220	630	440	1.4
60	9	53	0.435	0.015	0.041	0.047	0.8	87	2	5	4	1.3	2,370	210	590	490	1.1
70	9	54	0.500	0.018	0.051	0.054	0.9	91	1	3	4	0.7	2,180	160	450	430	1.0
80	9	65	0.599	0.023	0.067	0.043	1.5	94	1	3	4	0.7	2,210	210	600	570	1.0
90	9	51	0.659	0.030	0.087	0.058	1.5	100	1	3	5	0.5	2,280	200	550	590	0.9
100	9	55	0.728	0.024	0.071	0.038	1.8	104	1	5	5	1.0	2,310	180	520	410	1.2
110	9	51	0.728	0.020	0.056	0.043	1.2	106	2	5	5	1.0	2,370	240	650	660	0.9
120	9	54	0.831	0.021	0.061	0.035	1.7	108	2	6	7	0.8	2,420	210	560	790	0.7
130	9	58	0.872	0.014	0.041	0.033	1.2	108	3	9	7	1.1	2,310	220	580	790	0.7
140	9	51	0.904	0.013	0.039	0.023	1.6	108	2	7	10	0.7	2,080	170	440	600	0.7
150	9	35	0.931	0.008	0.020	0.028	0.7	109	2	4	9	0.5	2,000	150	230	720	0.3
160	8	30	0.943	0.009	0.024	0.012	2.0	103	5	15	9	1.5	2,000	250	610	670	0.9
170	8	22	0.955	0.009	0.019	0.024	0.7	105	3	7	11	0.7	1,900	200	250	770	0.3
180	4	16	0.959	0.013	0.023	0.018	1.2	103	4	4	12	0.3	1,760	540	1,010	620	1.6
190	2	4	0.950	0.004	0.000	0.007	0.0	119	1	1	2	0.6	2,810	280	240	400	0.5
200	2	3	0.958	0.011	0.000	0.018	0.0	118	1	0	2	0.0	2,090	450	610	240	2.4

[a] Overall sample mean.

[b] Standard error of individual measurements about the overall sample mean.

Moreover, the value of V_P required to achieve $\Lambda = 0.8$ during oral breathing at a respiratory flow rate of 250 mL/sec was defined as a characteristic absorption volume, $(V_P)_{80\%}$.

Performing a linear least-square regression of $(V_P)_{80\%}$ against V_D and against FVC led us to the conclusion that O_3 absorption is positively correlated with conducting airway volume but is uncorrelated with total lung volume (Figure 17). The coefficient of determination of $r^2 = 0.69$ for the V_D regression suggests that 69% of the variation in absorption between subjects may be due to differences in their conducting airway volumes. In fact, considering that CO_2 measurements by the slower-responding capnometer probably overestimates the dead space relative to the faster-responding mass spectrometer, it is possible that the dependence of O_3 absorption on dead space is even stronger than portrayed by these data.

Our explanation of these results is that men with large conducting airways have a small local surface:volume ratio and therefore a small cumulative surface at a particular penetration volume within the anatomic dead space. Because O_3 uptake is proportional to cumulative surface, men with a large conducting airway volume require a greater penetration volume to absorb a specified fraction of inhaled O_3 relative to men with a small conducting airway volume. The same argument cannot be made for vital capacity. That is, it is possible to observe large differences in vital capacity due to variations in respiratory airspace anatomy. This would have little influence on $(V_P)_{80\%}$, however, as these airspaces lie distal to the region where O_3 absorption occurs.

SAFETY CONSIDERATIONS

Because of limitations in the resolution of the chemiluminescent analyzer, we implemented the bolus measurement with peak inhaled O_3 concentrations of about 3 ppm. As this is much higher than the National Ambient Air Quality Standard (NAAQS) of 0.1 ppm for a one-hour exposure, it is important to compare the O_3 doses acquired by lung tissue during bolus inhalation and during continuous inhalation. In the absence of actual measurements, we developed a mathematical simulation to serve this purpose (see Appendix A).

The simulation incorporates both longitudinal and lateral diffusion of O_3 as it flows through a symmetrically branched model of the airways and airspaces. The chemical reactivity of mucus and of surfactant lining layers is taken into account when computing the O_3 delivery to underlying epithelial cells. Two alternative exposure scenarios, both at a respiratory flow rate of 250 mL/sec and at a tidal volume of 600 mL, were considered: continuous inhalation at a constant concentration of O_3, and inhalation of O_3 with a concentration pattern typical of that produced by our O_3 bolus generator. In Table 8, the results of the simulations are lumped into five sequential tissue regions: the upper airways, trachea, and primary and secondary bronchi (region

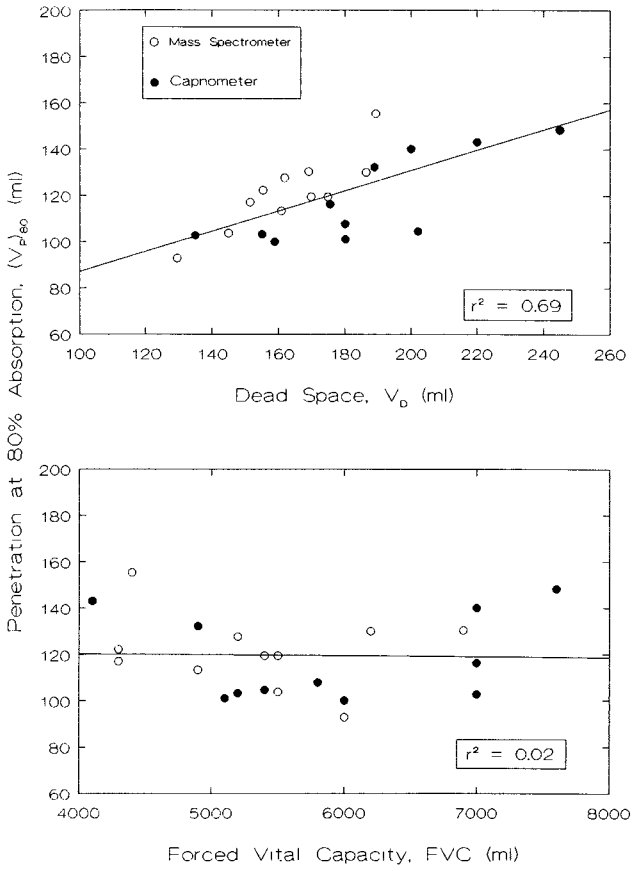

Figure 17. Influence of differences in dead space (top) and vital capacity (bottom) on the characteristic volume of O_3 absorption in different men. Each data point represents a different subject. Data points were obtained with CO_2 measurement by a mass spectrometer using the mouthpiece assembly with a gradually tapering constriction as in Figure 3 (open circles), or were obtained with CO_2 measurement by an in-line capnometer using the mouthpiece assembly with an abrupt constriction as in Figure 4 (solid circles). The r^2 value was obtained by applying a linear regression to all the data points.

1); bronchial generations 3 through 9 (region 2) ; bronchial generations 10 through 16 (region 3); the transitional airways (region 4); and the respiratory zone (region 5).

The "equivalent constant exposure" is that concentration of continually inhaled O_3 required to produce the same epithelial O_3 dose as is produced by the inhalation of a 3-ppm bolus. The simulations indicate that in the penetration volume range of 0 to 200 mL relevant to our studies, the equivalent exposure is always 0.2 ppm or below. This attenuation in the potency of O_3 peak concentration is due to the short contact time between a bolus and any particular point on the gas-liquid surface as well as to the protection afforded to underlying epithelium by the scavenging action of the mucous layer. Although 0.2 ppm is above the NAAQS, this O_3 level causes only modest and reversible changes in pulmonary function (McDonnell et al. 1983). Moreover, our protocol requires that a subject take several cleansing breaths of room air after each bolus test breath, and this substantially reduces the time-averaged O_3 dose. In testing a total of 23 healthy subjects with the bolus method (Table 1), we did not observe any respiratory symptoms associated with the O_3 bolus exposure.

SUMMARY AND CONCLUSIONS

It is becoming increasingly apparent that to extrapolate O_3 exposure-response data from animals to humans, from high concentrations to low concentrations, and from nonsusceptible to susceptible populations requires a better understanding and improved quantification of the inhaled dose that is delivered to target tissues. In this study, a bolus-response method of noninvasively determining the longitudinal distribution of O_3 absorption in intact, previously unexposed human lungs was developed, and measure-

Table 8. Simulations of Ozone Dose to Tissue After Inhalation of a 3-ppm Ozone Bolus

	Region 1[a]	Region 2[b]	Region 3[c]	Region 4[d]	Region 5[e]
Generations of Bronchi	0–2	3–9	10–16	17–19	20–23
Region volume (mL)	95	14	56	158	2,360
Penetration volume (mL)	Equivalent Constant Exposure (ppm)				
50	0.12	0.00	0.00	0.00	0.01
100	0.23	0.15	0.02	0.00	0.01
200	0.16	0.19	0.21	0.20	0.18
300	0.14	0.17	0.20	0.22	0.23
400	0.14	0.17	0.20	0.22	0.23

[a] Upper airways, trachea, and primary and secondary bronchi.

[b] Bronchial generations 3 through 9.

[c] Bronchial generations 10 through 16.

[d] The transitional airways.

[e] The respiratory zone.

ments were carried out on healthy male subjects at alternative respiratory flow rates ranging from 150 to 1,000 mL/sec, at peak inhaled O_3 concentrations ranging from 0.5 to 4.0 ppm, and during oral as well as nasal breathing.

We conclude from these studies that the large majority of inhaled O_3 does not reach the respiratory zone during quiet breathing. However, an elevated respiratory flow concomitant with exercise does deliver O_3 to the alveolar region. Moreover, because the nose is more efficient at O_3 uptake than the mouth, oral breathing results in a deeper penetration of O_3 than nasal breathing. During diffusion through the mucous blanket, while en route to underlying epithelium, O_3 undergoes a chemical reaction with biochemical substrates; the rate constant of this reaction is on the order of one million reciprocal seconds. Because of this very rapid rate, the diffusion resistance through mucus is relatively low, and the larger diffusion resistance through the respired gas boundary layer is an important determinant of O_3 absorption rate. Finally, we conclude that the intersubject variation of O_3 absorption in the conducting airways is due in part to corresponding variations of the anatomic dead space.

ACKNOWLEDGMENTS

Dr. Joseph Kabel played a major role in conducting the oral-nasal and concentration experiments. Mr. Thomas F. Ruscitti and Professor Steven F. Arnold designed and carried out most of the statistical analyses presented in this report.

REFERENCES

Barry BE, Miller FJ, Crapo JD. 1985. Effects of inhalation of 0.12 and 0.25 parts per million ozone on the proximal alveolar region of juvenile and adult rats. Lab Invest 53:692–704.

Ben-Jebria A, Hu S-C, Kitzmiller EL, Ultman JS. 1991. Ozone absorption into excised sheep trachea by a bolus-response method. Environ Res 56:144–157.

Ben-Jebria A, Walton C, Mench B, Hatzfeld C. 1981. Injecteurs d'emboles de gaz inerte et marqué. Bull Eur Physiopathol Respir 17:261–267.

Brain JD. 1970. The uptake of inhaled gases by the nose. Ann Otol Rhinol Laryngol 79:529–539.

Colucci AV. 1983. Pulmonary dose/effect relationships in ozone exposure. In: Advances in Modern Environmental Toxicology, Vol. V (Lee SD, Mustafa MG, Mehlman MS, eds.). Princeton Scientific Publishers, Princeton, NJ.

Dayan J, Levenspiel O. 1969. Dispersion in smooth pipes with adsorbing walls. Ind Eng Fund 8:840–842.

Fowler WS. 1948. Lung function studies: II. The respiratory dead space. Am J Physiol 154:405–416.

Fredberg JJ, Wohl ME, Glass GM, Dorkin HL. 1980. Airway area by acoustic reflections measured at the mouth. J Appl Physiol 48:749–758.

Gerrity TR, Weaver RA, Berntsen J, House DE, O'Neil JJ. 1988. Extrathoracic and intrathoracic removal of ozone in tidal breathing humans. J Appl Physiol 65:393–400.

Hannah LM, Frank R, Scherer PW. 1989. Absorption of soluble gases and vapors in the respiratory system. In: Respiratory Physiology—An Analytical Approach (Chang HK, Paiva M, eds.). Marcel Dekker, New York, NY.

Hobler T. 1966. Chapter 5, Mass Transfer in Absorbers. Pergamon Press, New York, NY.

Hu S-C, Ben-Jebria A, Ultman JS. 1992. Simulation of ozone uptake distribution in the human airways by orthogonal collocation on finite elements. Comp Biomed Res 25:264–278.

Knudsen RJ, Slatin RC, Lebowitz MD, Burrows B. 1976. The maximal expiratory flow-volume curve. Am Rev Respir Dis 113:587–600.

Koren HS, Devlin RB, Graham DE, Mann R, McGee MP, Horstman DH, Kozumbo WJ, Becker S, House DE, McDonnell WF, Bromberg PA. 1989. Ozone-induced inflammation in the lower airways of human subjects. Am Rev Respir Dis 139:407–415.

Larsen R. 1987. Longitudinal Mixing Coefficients in Human Pulmonary Airways by Parameter Estimation with the One-Dimensional Diffusion Equation. Doctoral dissertation. Pennsylvania State University, University Park, PA.

McDonnell WF, Horstman DH, Abdul-Salaam S, House DE. 1985. Reproducibility of individual responses to ozone exposure. Am Rev Respir Dis 131:36–40.

McDonnell WF, Horstman DH, Hazucha MJ, Seal E, Haak ED, Salaam SA, House DE. 1983. Pulmonary effects of ozone exposure during exercise: Dose-response characteristics. J Appl Physiol 54:1345–1352.

McJilton CE, Thielke J, Frank R. 1972. A model to predict the uptake of ozone and other pollutant gases by the respira-

tory system. Presented at the American Industrial Hygiene Association, San Francisco, CA, May 14–19. (Unpublished manuscript courtesy of R. Frank.)

Mellick PW, Dungworth DL, Schwartz LW, Tyler WS. 1977. Short term morphologic effects of high ambient levels of ozone on lungs of rhesus monkeys. Lab Invest 36:82–90.

Miller FJ, Graham JA, Overton JH, Jaskot RH, Menzel DB. 1985. A model of the regional uptake of gaseous pollutants in the lung: I. The sensitivity of the uptake of ozone in the human lung to lower respiratory tract secretions and to exercise. J Toxicol Environ Health 79:11–27.

Miller FJ, McNeal CA, Kirtz JM, Gardner DE, Coffin DL, Menzel DB. 1979. Nasopharyngeal removal of ozone in rabbits and guinea pigs. Toxicology 14:273–281.

Miller FJ, Menzel DB, Coffin DL. 1978. Similarity between man and laboratory animals in regional pulmonary deposition of ozone. Environ Res 17:84–101.

Niinimaa V, Cole P, Mintz S, Sheppard RJ. 1980. The switching point from nasal to oronasal breathing. Respir Physiol 42:61–71.

Olson DE, Sudlow MF, Horsfield K, Filley GF. 1973. Convective patterns of flow during inspiration. Arch Intern Med 131:51–57.

Pryor WA. 1992. How far does ozone penetrate into the pulmonary air/tissue boundary before it reacts? Free Radic Biol Med 12:83–88.

Reisfeld B, Ultman JS. 1988. Longitudinal mixing in dog lungs during high-frequency forced flow oscillation. Respir Physiol 71:269–286.

Treybal RE. 1980. Mass Transfer Operations, 3rd ed. McGraw-Hill, New York, NY.

Ultman JS. 1985. Gas transport in the conducting airways. In: Gas Mixing and Distribution in the Lung (Engel LA, Paiva M, eds.). Marcel Dekker, New York, NY.

Ultman JS. 1988. Transport and uptake of inhaled gases. In: Air Pollution, the Automobile, and Public Health (Watson AY, Bates RR, Kennedy D, eds.). National Academy Press, Washington, DC.

Ultman JS, Ben-Jebria A. 1990. Noninvasive Determination of Respiratory Ozone Absorption: Development of a Fast-Responding Ozone Analyzer. Research Report Number 39. Health Effects Institute, Cambridge, MA.

Ultman JS, Doll BE, Spiegel R, Thomas MW. 1978. Longitudinal mixing in pulmonary airways—normal subjects respiring at a constant flow. J Appl Physiol 44:297–303.

Ultman JS, Thomas MW. 1979. Longitudinal mixing in pulmonary airways—comparison of inspiration and expiration. J Appl Physiol 46:799–805.

Vaughan TR, Jennelle LF, Lewis TR. 1969. Long-term exposure to low levels of air pollutants: Effects on pulmonary function in the beagle. Arch Environ Health 19:45–50.

Weibel E. 1963. Chapter 11, Morphometry of the Human Lung. Academic Press, Orlando, FL.

Weister MJ, Stevens MA, McDonnell WF, Gerrity TR, McKee JL. 1991. Efficiency of ozone (O_3) uptake in human lungs during quiet breathing. Am Rev Respir Dis 143:A707.

Yokoyama E, Frank R. 1972. Respiratory uptake of ozone in dogs. Arch Environ Health 25:132–138.

Yu CP, Diu CK. 1982. A comparative study of aerosol deposition in different lung models. Am Ind Hyg Assoc J 43:54–65.

APPENDIX A. Mathematical Simulation

To develop a computer simulation of the bolus measurement, the lung is viewed as a symmetrically branching structure in which the longitudinal distributions of ozone concentration and absorption are the same along all possible airway paths from the airway opening to the alveolar sacs. Moreover, it is assumed that O_3 reacts so rapidly in mucus and tissue that its absorption rate is proportional to the local gas phase concentration of O_3. The transport of O_3 can then be described by the gas-phase species conservation equation (Ultman 1988).

$$\frac{\partial F_{O_3}}{\partial t} + \frac{\dot{V}}{A}\frac{\partial F_{O_3}}{\partial y} = \frac{1}{A}\frac{\partial}{\partial y}\left(D_{\text{eff}} A \frac{\partial F_{O_3}}{\partial y}\right) - KaF_{O_3}, \tag{A.1}$$

where $F_{O_3}(y,t)$ is the mole fraction of O_3, which is a function of time, t, and longitudinal distance from the airway opening, y; $\dot{V}(t)$ is respiratory flow; $A(y)$ is the cross-section available for flow; D_{eff} is the longitudinal dispersion coefficient; K is the overall mass transfer coefficient for absorption between the gas and mucous or surfactant liquid-lining layers; and a is the local surface:volume ratio of the interface between gas and liquid layers.

Such a mathematical model was used previously for the lower respiratory tract (McJilton et al. 1972; Miller et al. 1978) and was extended to include absorption in the nasal

passages (Hannah et al. 1989). Without exception, the purpose of this previous work was to simulate the dose distribution resulting from continuous inhalation of O_3. Our intention, on the other hand, was to develop a computer simulation that can be applied to the bolus inhalation method. In our mathematical model, the lower airways are represented by Weibel's anatomic model "A" (Weibel 1963) scaled to a total volume of 2.65 L, and the upper airways are represented by an equivalent cylinder whose length, mean cross-section, and mean hydraulic diameter are matched to the actual oropharyngeal path (Fredberg et al. 1980).

To solve Equation A.1, an initial condition as well as conditions at two boundaries are required. At the start of a test breath, we assumed that no O_3 was present within the lungs. At the lips, a specific O_3 concentration pattern was prescribed during inspiration, and the gradient of O_3 concentration was assumed to be zero during expiration. At the distal end of the lung, the diffusional flux of O_3 was equated to a local value of KaF_{O_3}.

Simulations were implemented with a numerical technique, orthogonal collocation on finite elements, that is fully described elsewhere (Hu et al. 1992). This technique is not subject to the computational instabilities inherent in the finite difference techniques that were previously used to integrate Equation A.1. Also, the technique self-selects optimal grid positions, and this decreases the computer time necessary to complete a simulation. In specifying input parameters, the longitudinal distribution of a was calculated from the anatomic data described above, literature values of mucous- and surfactant-layer thicknesses were used (Miller et al. 1985), and D_{eff} was equated to the molecular diffusion coefficient of O_3 in air. Values of K were estimated using the equations formulated by Miller and associates (1985).

ABOUT THE AUTHORS

James S. Ultman is Professor of Chemical Engineering at the Pennsylvania State University, where he has been a faculty member since 1970. He received his Ph.D. in chemical engineering at the University of Delaware in 1969, and then served as a National Institutes of Health Postdoctoral Fellow at the University of Minnesota. In 1978, Professor Ultman was a Fulbright Lecturer at the Technion (Israel Institute of Technology), and a visiting researcher at the Silverberg Medical School (Haifa, Israel). In 1989, he was a Visiting Research Professor in the Department of Medicine of Duke University Medical School. Dr. Ultman is interested in the application of the physical principles of fluid flow, diffusion, and chemical reaction to problems in pulmonary physiology, pathology, and toxicology.

Abdellaziz Ben-Jebria is a Researcher at the Institut National de la Santé et de la Recherche Médicale (INSERM, France), working in the Respiratory Pathophysiology Research Unit in Paris from 1980 to 1984, and thereafter in the Physiology Laboratory at the University of Bordeaux-II. Dr. Ben-Jebria earned a Ph.D. in biophysics in 1979 and a State Doctorate degree in natural science in 1984, both at the University of Pierre and Marie Curie in Paris. From 1987 to 1990, he was a Visiting Associate Professor in the Department of Chemical Engineering at the Pennsylvania State University where he is now an Associate Professor. His major research interests are pulmonary gas transport and uptake processes as well as airway reactivity in toxicology.

Shu-Chieh Hu is a Postdoctoral Research Assistant at the Center for Environmental Medicine at the University of North Carolina at Chapel Hill. He earned his Ph.D. at the Pennsylvania State University, where he was a Graduate Research Assistant in the Department of Chemical Engineering. His major research interests are in the transport of gases and aerosols in the respiratory tract.

PUBLICATIONS RESULTING FROM THIS RESEARCH

Ben-Jebria A, Ultman JS. 1989. Fast-responding chemiluminescent ozone analyzer for respiratory applications. Rev Sci Instrum 60:3004–3011.

Ben-Jebria A, Hu S-H, Ultman JS. 1990. Improvements in a chemiluminescent analyzer for respiratory applications. Rev Sci Instrum 61:3435–3439.

Ben-Jebria A, Hu S-H, Kitzmiller EL, Ultman JS. 1991. Ozone absorption into excised sheep trachea by a bolus-response method. Environ Res 56:269–286.

Hu SC, Ben-Jebria A, Ultman JS. 1992. Longitudinal distribution of ozone absorption in the lung: Quiet respiration in healthy subjects. J Appl Physiol 73:1655–1661.

Hu S-C, Ben-Jebria A, Ultman JS. 1992. Simulation of ozone uptake distribution in the human airways by orthogonal collocation on finite elements. Comp Biomed Res 25:264–278.

Ultman JS, Hu S-C, Ben-Jebria A. 1992. Ozone distribution in human lungs—effect of respiratory air flow. Am Rev Respir Dis 145:A802.

Hu SC, Ultman JS, Ben-Jebria A. 1993. Single-breath bolus exposure for noninvasive determination of ozone dose distribution. In: Advances in Controlled Clinical Inhalation

Studies (Mohr U, Bates DV, Fabel H, Utell MJ, eds.) pp. 309–316. Springer-Verlag, New York, NY.

Hu SC, Ben-Jebria A, Ultman JS. 1994. Longitudinal distribution of ozone absorption in the lung: Effect of respiratory flow. J Appl Physiol (in press).

Kabel JR, Ben-Jebria A, Ultman JS. 1994. Longitudinal distribution of ozone absorption in the lung: Comparison of nasal and oral quiet breathing. J Appl Physiol (in press).

ABBREVIATIONS

a	surface:volume ratio
CA	lower conducting airways
CAD	lower conducting airways, distal
CAP	lower conducting airways, proximal
CO_2	carbon dioxide
FEF_{25-75}	forced expiratory flow from 25% to 75% of the vital capacity
FEV_1	forced expired volume in one second
F_{CO_2}	CO_2 volume fraction
F_{O_3}	O_3 volume fraction
FRC	functional residual capacity
FVC	forced vital capacity
K	overall mass transfer coefficient
$1/K$	overall mass transfer resistance
Ka	mass transfer coefficient representing the absorption rate normalized by the concentration driving force and the volume of the gas-filled conduit
$1/k_g$	individual mass transfer resistance of gas-boundary layer
Λ	O_3 absorbed fraction, or amount of O_3 absorbed during a single breath relative to the amount in the inhaled bolus
λ	equilibrium partition coefficient
λ/k_ℓ	individual mass transfer resistance of liquid-lining layer
NAAQS	National Ambient Air Quality Standard
O_2	oxygen
O_3	ozone
ppm	parts per million
r^2	coefficient of determination
RA	respiratory airspaces
SD_b	standard deviation between subjects
SD_w	standard deviation within subjects
t_O	time during inspiration when a nonzero value for F_{O_3} first appears
t_E	time during inspiration when a nonzero value for F_{O_3} last appears
UA	upper airways
UAD	upper airways, distal
UAP	upper airways, proximal
$\dot{V}$	volumetric gas flow
V_B	breakthrough volume
V_D	dead space volume
V_P	penetration volume, or the airway volume to which an inspired bolus would penetrate if there were no absorption

INTRODUCTION

The Health Effects Institute (HEI) has had a long-standing interest in supporting the improvement of methods to measure the amount of ozone absorbed by target sites within the respiratory tract. One aspect of HEI's activity in this area has been the support of basic research to develop biological markers of ozone exposure. Another was a focused research program to develop personal ozone samplers (Hackney et al. 1994; Koutrakis et al. 1994; Yanagisawa 1994) and noninvasive procedures for measuring ventilation (McCool and Paek 1993; Samet et al. 1993). A related project was proposed by Dr. James Ultman and colleagues of Pennsylvania State University in 1987 when they submitted a preliminary application to HEI with two objectives: (1) to develop an apparatus and methodology to obtain single-breath measurements of ozone concentration, and (2) to measure regional uptake and distribution of ozone in the lungs of human volunteers. The HEI Health Research Committee approved a pilot study in 1988 to address the first objective, the results of which were published in HEI Research Report Number 39. The study was extended in 1990 to address the second objective. The two-year project began in July 1990, and total expenditures were $256,646. The Investigators' Report was received in September 1992, and was accepted for publication by the Health Review Committee in October 1993.

During the review of the Investigators' Report, the Review Committee and the principal investigator had the opportunity to exchange comments and to clarify issues in the Investigators' Report and in the Review Committee's Commentary. This commentary is intended to highlight the strengths and limitations of the research findings and to place the Investigators' Report in perspective as an aid to the sponsors of the HEI and to the public.

REGULATORY BACKGROUND

The U.S. Environmental Protection Agency (EPA) sets standards for criteria pollutants under Section 202 of the Clean Air Act, as amended in 1990. Section 202(a)(1) directs the Administrator to "prescribe (and from time to time revise) . . . standards applicable to the emission of any air pollutant from any class or classes of new motor vehicles or new motor vehicle engines, which in his judgment cause, or contribute to, air pollution which may reasonably be anticipated to endanger public health or welfare." Sections 202(a), (b)(1), (g), and (h), and Sections 207(c)(4), (5), and (6) impose specific requirements for reducing motor vehicle emissions of certain oxidants (and other pollutants) and, in some cases, provide the EPA with limited discretion to modify those requirements.

As further outlined in Section 202(a) of the Clean Air Act Amendments, the EPA Administrator shall determine whether emissions of any unregulated pollutant present an unreasonable risk to the public health, welfare, or safety. One approach used by the EPA to estimate the likelihood that pollutants will produce adverse health effects is risk assessment. This mathematical approach characterizes and quantifies potential detrimental effects that may result from exposures to harmful agents in the environment. One phase of the risk assessment process is exposure assessment, which estimates the magnitude, frequency, duration, and route of exposure to a pollutant. Exposure assessment is critical for appropriately interpreting an association between an individual's exposure to a pollutant and the amount of the pollutant potentially reaching its target site in the body and producing a biological effect. Studies that lead to improvements in exposure assessment methodology, such as the one discussed in this report, can improve assessments of the potential adverse health effects of exposure to ozone.

SCIENTIFIC BACKGROUND

Ozone is a ubiquitous pollutant in the form of an irritant gas that reacts with biomolecules, and thus can be toxic to humans, animals, and vegetation. It is a major constituent of photochemical smog, which is produced from oxides of nitrogen and volatile organic compounds emitted by mobile and stationary combustion sources, and by natural sources (Finlayson-Pitts and Pitts 1993). The National Ambient Air Quality Standard (NAAQS)* for ozone, which is designed to protect sensitive individuals, is a one-hour maximum concentration of 0.12 parts per million (ppm), to be exceeded only one day per year. Global ozone concentrations are commonly 0.03 to 0.05 ppm, and appear to be rising. However during the summer in heavily populated areas such as southern California, the Northeast corridor, and other metropolitan areas worldwide, ozone concentrations can often exceed 0.12 ppm. Furthermore, a person living in these regions can readily be exposed to high ozone concentrations for several hours (Rombout et al. 1986).

These elevated levels are of concern because several controlled human exposure studies (reviewed by Lippmann

* A list of abbreviations appears at the end of the Investigators' Report.

1989, 1993) have shown that, in subjects who are exercising, short-term exposure to ozone causes dose-dependent decreases in lung function (decreased forced expiratory flow and increased airway resistance), increases in airway reactivity in response to inhaled nonspecific agents, and increases in markers of inflammation in bronchoalveolar lavage fluid (elevated levels of proteins, mediators, inflammatory cells, and enzymes released from lung tissues) (McDonnell et al. 1983, 1991; Folinsbee et al. 1988; Koren et al. 1989; Devlin et al. 1991). In fact, significant changes in both lung function and lung fluid content were found at 0.08 and 0.10 ppm, which are below the NAAQS (Devlin et al. 1991; McDonnell et al. 1991).

Although the changes in lung function may be viewed as transient and reversible, the biochemical and cellular changes are consistent with a picture of ozone-induced inflammation in the lower lung. This is of concern because they are not readily reversible and could lead to permanent changes in lung tissue. Experiments in laboratory animals indicate that ozone can injure several types of cells in many regions of the lungs. Because of its low solubility in water, ozone can penetrate to the deep lung. As a result of chronic exposure, a characteristic focal lesion develops in the region of the lung where the airways covered with mucus meet the gas-exchange tissues, which are covered with surfactant (Stephens et al. 1974; Schwartz et al. 1976; Mellick et al. 1977; Plopper et al. 1978; Castleman et al. 1980; Barry et al. 1985; Chang et al. 1992).

EXPOSURE, DOSE, AND RESPONSE RELATIONS

To establish from a rigorous toxicological perspective the health hazard that ozone poses to humans, regulators need to determine the relations among ozone exposure, dose to the tissues of the respiratory tract, and the subsequent biologic responses. First, one would analyze ozone exposure in terms of ozone concentration, breathing parameters, and duration. On the basis of these parameters one would calculate the amount of ozone that entered the respiratory tract. Second, one would want to know the actual dose to the respiratory tissues. By knowing the percentage of inhaled ozone absorbed by the respiratory tract (known as the absorption efficiency or, simply, absorption), one could then multiply this percentage by the amount of ozone entering the respiratory tract to calculate the mass of ozone that reacted with the mucus, fluids, and cells that line the airways and pulmonary gas-exchange regions. Dose could be expressed in various ways: the total mass of ozone absorbed by the total respiratory tract or specific regions within the respiratory tract, or the amount of ozone absorbed per unit of lung surface area, volume, or target cell. Dose also can be usefully calculated in terms of an absorption rate, which is related to the diffusion rate of ozone to the respiratory tract surface and the chemical reaction rate between ozone and the constituents of the surface. Third, one would define the health effects for each level of ozone exposure and dose. Such an analysis would identify the initial cellular, biochemical, and neurological responses; the damage to the tissues; and then the more global impairments on lung function and airway reactivity. One would also explore the possibility that the exposure, dose, and response relations are modified by the subject's characteristics such as age, gender, activity patterns, and health status.

DOSE: CALCULATED DOSES

Although some data relate ozone exposure to biologic response, the critical relations between exposure and dose, and dose and response are less well defined. This is primarily because it has been problematic to quantify ozone dose accurately. One approach has been to calculate dose based solely upon exposure parameters, neglecting ozone absorption by the respiratory tract. One such calculated parameter is the cumulative dose, which is useful for animal studies because it is based upon the product of ozone concentration and exposure time (Gelzleichter et al. 1992). Another parameter is the effective dose, which is more accurate because it accounts for breathing pattern. Effective dose is expressed either as the product of ozone concentration in the air being breathed, volume of air inhaled in one minute of ventilation (minute ventilation), and exposure time (Silverman et al. 1976), or as a mathematical function that gives these factors different weights (Folinsbee et al. 1978; Adams et al. 1981). Minute ventilation is included in these calculations because, given the same ozone concentration, greater health effects have been demonstrated in human subjects who are exposed to ozone while exercising than in subjects at rest (Bates et al. 1972; DeLucia and Adams 1977; Folinsbee et al. 1978). Presumably, the larger inhaled volumes and faster breathing frequencies associated with exercise increase the dose of ozone to the lower lungs, and also replace ozone reaction products at a faster rate (DeLucia and Adams 1977; Miller et al. 1985; Grotberg et al. 1990). Of the three factors (concentration, ventilation, and time), ozone concentration appears to be more related to decreased lung function than minute ventilation, which, in turn, is more related than time (Silverman et al. 1976; Folinsbee et al. 1978; Adams et al. 1981; Hazucha 1987). Two notable limitations of both cumulative and effective dose are that (1) they cannot account for intersubject differences in response to ozone (Adams et al. 1981), and (2) they ignore the absorption of ozone in the respiratory tract. Thus, these dose estimates cannot address differences in ozone uptake either among individuals or among different regions of the respi-

ratory tract. For example the nose and mouth remove substantial amounts of inhaled ozone and thus reduce the concentration of ozone entering the lungs (Gerrity et al. 1988).

Kleinman (1991) calculated an internal thoracic dose of ozone to analyze the relations between ozone dose and changes in lung function. The internal thoracic dose extends the concept of effective dose to include the amount of inhaled ozone that reaches and is absorbed by the airways and the gas-exchange regions of the lung on the basis of body weight; it also addresses whether breathing is oral, nasal, or combined oronasal. He found that internal thoracic dose increases with exercise, and is greater on a per-body-weight basis for children under six years of age than for older children and adults. Upon applying estimates of internal thoracic dose to data from several controlled ozone exposure studies with humans, Kleinman concluded that internal thoracic dose is linearly related to decreased forced expiratory flow rates.

DOSE: MATHEMATICAL DOSIMETRY MODELS

In comparison with calculated estimates of dose, mathematical dosimetry models offer a more comprehensive approach to defining ozone dose to the respiratory tract tissues. These models generally have two components. The first is to determine the regional distribution of the inhaled ozone in the respiratory tract. Mathematical expressions or equations are used to describe the transport of ozone by convection (bulk transport), or by longitudinal and radial diffusion. With these equations it is possible to analyze how ozone is transported within the respiratory tracts of humans and animals, and how its transport is altered by changing breathing patterns. The second component is to determine how much ozone is absorbed by the mucus in the airways and the surfactant in the alveoli, and how much then moves by convection and diffusion through these fluid layers to react with the underlying respiratory tissues. This final quantity is the tissue dose of ozone and is the most useful value for exposure-dose-response relations.

The dosimetric models of Miller and coworkers (1985), Grotberg and coworkers (1990), and Hu and coworkers (1992) used different approaches to describe ozone transport and absorption in an idealized human lung; Hu and coworkers were the only ones to include the oral passages. The idealized model (Weibel 1963) portrays the lung as a symmetrically branching network with 24 "generations" of airways. Each generation consists of only one type of airway that are all located at the same volumetric depth in the lungs. For example, the trachea is generation 0 and the terminal bronchioles are at generation 16. Despite their theoretical differences, all the models predict that for resting breathing, the tissue dose increases gradually from the trachea to a maximum value at generation 17, which corresponds with the respiratory bronchioles where the mucus-covered conducting airways lead into the surfactant-covered gas-exchange tissues in the acinus (i.e., respiratory bronchioles, alveolar ducts, alveolar sacs, and alveoli). At deeper generations within the acinus, tissue dose decreases markedly. At the acinar entrance, the liquid-lining layer is thin and the cross-sectional surface area of the lung starts to expand to promote gas transport to the lung surface. Both of these factors work to increase the dose of ozone to the local tissues. Even though the conducting airways absorb a large fraction of ozone fairly evenly over their length, the relatively thick mucous layer provides protection to the underlying airway epithelium. Therefore, the tissue dose increases appreciably only where the covering layer becomes thinner in the terminal portions of the conducting airways. It is significant that the highest tissue dose predicted by the models is at the acinar entrance because this region corresponds to the primary site of tissue damage found in animals exposed to ozone (Stephens et al. 1974; Mellick et al. 1977). The three mathematical dosimetry models predicted different patterns and magnitudes of tissue dose in humans. Miller and colleagues (1985) and Hu and colleagues (1992) predicted that a broad region of high tissue dose extends from generation 11 (terminal bronchi) to generation 18 or 19 (respiratory bronchioles). In contrast, Grotberg and coworkers (1990) predicted a sharp peak of tissue dose from generation 17 (maximum) to 19, with the maximum dose at generation 17 being almost one order of magnitude greater than that predicted by Miller and coworkers (1985).

Overton and Graham (1989) modified the model of Miller and colleagues (1985) to examine the influence of age on tissue dose and ozone absorption. They used different data to describe lung dimensions and different thicknesses for the fluid thickness. They also included the airways in the head, but assumed they were nonabsorbing. Like Grotberg and coworkers (1990) they found that tissue dose peaks sharply in the respiratory bronchioles leading into the acini. However, in contrast to Grotberg and coworkers, who attributed their tissue dose peak to increased transport of ozone from the air to the acinar surface, Overton and Graham attributed their tissue dose peak to a sudden transition in the lining fluid thickness between the mucus (1.75 μm) and the surfactant (0.125 μm). For resting breathing, Overton and Graham found that total and regional ozone uptake and tissue dose are generally independent of age. The ozone absorption of the total lung (omitting the extrathoracic airways) is about 85%. About 30% of the inhaled ozone is removed in the conducting airways, with 23% reacting with the mucus and 7% managing to reach the airway epithelium; about 55% of the inhaled ozone is removed in the acinus, with 54% going

to the acinar tissues and 1% being trapped in the surfactant and blood.

When tidal volume and breathing frequency are increased to represent exercise, the models predict that tissue dose increases dramatically in the respiratory bronchioles at the acinar entrance and in the distal acinar generations, but that dose to the airway epithelium is either the same as resting breathing (Miller et al. 1985; Grotberg et al. 1990) or only modestly increased despite a lower absorption per breath because of the greater number of breaths taken per unit of time (Overton and Graham 1989). Overton and Graham (1989) predicted that, during maximal exercise, ozone absorption for the total lung increases with age ranging from 87% for 2-year-old children to 93% for adults; the respective values for acinar absorption are 78% for 2-year-olds and 90% for adults.

Because ozone is highly reactive, it is important to consider the chemical reaction kinetics between ozone and biomolecules within the mucus and surfactant in order to assess tissue dose accurately. For ozone, it may be misleading to consider only the portion of the absorbed ozone that may escape reacting with substrates and penetrates through the mucus and surfactant, as was done in the dosimetric models described above. It is possible that ozone reacts partially or completely with glycoproteins, unsaturated lipids, proteins, and other constituents at the surface of the mucous and surfactant layers to form products, such as aldehydes and hydrogen peroxide, that are themselves reactive. These reaction products may, in turn, initiate a cascade of chemical reactions that produce other reactive products that ultimately come in contact with and damage tissues (Pryor 1992). Ozone and its reactive products can react with the lipid membranes of cells, causing lipid peroxidation and the production of free radicals, which then go on to cause further damage. Protection of the tissues from ozone also depends upon variations in the thickness and completeness of the fluid layers: the mucus may be 20 μm thick in the upper airways and decrease to about 0.1 μm in the small airways; surfactant may be only 0.1 μm in the alveoli (Miller et al. 1985). Where the layers are thin, especially in the terminal bronchioles, areas of tissue may be incompletely covered by mucus or surfactant. Pryor (1992), using conservative assumptions of ozone reaction rates, estimated that in regions of the lower lung where the fluid thickness is only 0.1 μm, all adsorbed ozone would react with substrates in the fluid, such as glutathione and unsaturated lipids, and thus would not reach the underlying tissues. Pryor concluded that in areas completely covered by mucus or surfactant, it was the reaction products of ozone that could be damaging to the underlying tissues. However, in areas with a very thin or incomplete fluid covering, such as in the terminal bronchioles, ozone may lead directly to tissue damage.

DOSE: MEASUREMENTS UNDER EXPERIMENTAL CONDITIONS

The most direct way to assess ozone dose to the respiratory tract is to measure the amount of ozone absorbed by the airways and acini. Such a study is technically challenging because of the need for a fast-responding ozone analyzer that measures the ozone concentration in each breath. Gerrity and coworkers (1988) used a modified chemiluminescent ozone analyzer with a 90% response time of 700 msec to measure regional ozone uptake in 18 healthy young men. The men breathed known ozone concentrations while in a controlled exposure chamber. A sampling tube to the ozone analyzer was placed into the posterior pharynx to measure how much of the inhaled ozone remained after it had passed through the extrathoracic airways (nose, mouth, and pharynx) and the intrathoracic airways (larynx, trachea, bronchi, conducting airways, and gas-exchange tissues). By knowing the amount of ozone entering and leaving the extrathoracic and intrathoracic airways, the cumulative absorption (also referred to as absorption efficiency) could be computed for each region. Breathing was oral, nasal, and oronasal. The only breathing parameter that varied was the respiratory rate, which was 12 and 24 breaths/min. The tested ozone concentrations were 0.1, 0.2, and 0.4 ppm.

These investigators found that the overall mean absorption for the extrathoracic region was about 40% and for the intrathoracic region was 91%. The total absorption of ozone in the entire respiratory tract was about 95%. In general, the effects of breathing mode, breathing frequency, and ozone concentration upon ozone uptake in each region were small, changing the measurement of ozone uptake by less than 5%. The nose was less effective at removing inhaled ozone than the mouth: The absorption was 36% for nose breathing, 40% for oral breathing, and 43% for oronasal breathing. Increasing the breathing frequency had little effect on uptake: At 12 breaths/min extrathoracic ozone uptake was 41%, whereas at 24 breaths/min it was 38%. For intrathoracic uptake at the two breathing rates, the respective values were 93% and 89%. The greater absorption at the slower frequency was probably due to the longer time available for ozone absorption to occur. The authors acknowledged that due to systematic errors the absorption values were accurate only to within 5% to 10%.

Direct measurements of ozone uptake also have been made in several animal species. To measure uptake in the nasopharynx, many studies recorded flow only on inhalation with a sampling tube inserted into the pharynx via a

tracheostomy. All studies were done with slow-responding ozone analyzers. In rabbits and guinea pigs, Miller and colleagues (1979) found about 50% of inhaled ozone (0.1 to 2 ppm) was removed in the nasopharynx. In dogs, Yokoyama and Frank (1972) found the nasopharynx removed from 27% to 72% of inhaled ozone (0.3 to 0.8 ppm), with a greater percentage being removed at the lower flow rate (approximately 5 versus 40 L/min) and lower concentration (0.3 versus 0.8 ppm). When the ozone was inhaled orally, ozone uptake was only about 40% of that for the nose. To measure absorption in the lungs, the ozone was inhaled and exhaled through a tracheostomy tube, and was found to be about 82%; ozone concentration and flow rate had little influence on absorption. The absorption for the entire dog lung while breathing quietly was at least 90%, which compares well with measurements in spontaneously breathing dogs (Moorman et al. 1973). However in rats breathing spontaneously through the nose, ozone uptake in the entire respiratory tract was only 40% (Wiester et al. 1987).

Another newer experimental approach that has the potential to measure absorbed ozone dose is to perform inhalation exposures with ozone labeled with the stable isotope ^{18}O (Hatch et al. 1989). After exposure, the ^{18}O-labeled ozone can be recovered by lavage in humans and then analyzed; in animal studies, the labeled ozone can be recovered by homogenizing the lungs after necropsy.

In terms of relating ozone exposure to subsequent health effects, it has been well documented that people having the same exposure can have different responses. For example, McDonnell and coworkers (1983) exposed healthy young subjects to 0.40 ppm ozone for 2.5 hours and found decreases in forced expiratory flow rate ranging from 3% to 48%, and cough severity from "none" to "severe." Those at increased risk are individuals who exercise or engage in moderate to strenuous work; the increased breathing involved with these activities increases the risk of adverse effects (Lippmann 1989).

One could think that intersubject variations in ozone absorption would explain some intersubject variation in decreased lung function; however current data indicate only about 6% of the variation can be explained on the basis of ozone uptake (Gerrity and McDonnell 1989; McDonnell 1991). Thus, it may be that intersubject differences in the intrinsic properties of the lung tissues may account for the observed variation in responses to ozone. This idea is supported by the large variations in the susceptibility of different strains of mice and rats to ozone toxicity (Kleeberger et al. 1990; Henderson et al. 1993). Some of these differences may be due to variations in the ozone uptake of the upper airways (Kleeberger et al. 1993), or the biochemical profile of the liquid-lining layers or the target tissues (Paquette et al. 1993).

Another interesting factor in assessing response to dose is the possibility of adaption. People tend to have very reproducible responses when ozone exposures are separated by weeks (McDonnell et al. 1985). When the exposures are on successive days, lung function decreases on the first and second days of exposure; however, on the following days, lung function recovers. This indicates that people can adapt to ozone exposure, at least in terms of lung function changes stimulated by acute exposure (Hackney et al. 1977; Folinsbee et al. 1980).

IMPORTANCE OF KNOWING DOSE REVISITED

In summary, there are at least three features of ozone toxicity that emphasize the importance of knowing the dose of ozone to the target tissues within the respiratory tract in order to predict adequately the health hazards associated with breathing a given concentration of ozone. First, studies using controlled human exposures show that the alterations in lung function, airway reactivity, and inflammation are related to dose. Second, animal studies show that a major site of injury is the bronchiole entrance to the acinus. Other regions of the lung are exposed to ozone, but there appear to be unique characteristics of the acinar-entrance region that increase its susceptibility. Dosimetric models suggest that a large transfer of ozone to the tissues occurs in this region and that the protective layer of mucus is insufficient to withstand injury. Third, the intersubject variation in response to ozone indicates that either some people receive higher doses of ozone delivered to sensitive tissues than other people, or that the tissues differ in susceptibility among people.

The dose of ozone to the target tissues in the respiratory tract is dependent on several factors: (1) the ambient ozone concentration; (2) the amount of ozone inspired into the respiratory tract during exposure; (3) the amount of ozone absorbed in the mouth, nose, and in airways upstream of the target tissues; (4) the amount of ozone absorbed in the lower airways and acini; (5) the amount of ozone that reacts with the mucus and surfactant overlying the target tissues; and (6) the amount of ozone and reactive products that ultimately reach and react with the target cells. The first two factors currently can be quantified with reasonable accuracy. The challenge has been to accurately quantify the latter four factors. Among these, accurate measurements of the regional distribution of ozone absorption within the respiratory tract has remained a challenging but critical step in determining the dose of ozone and any of its reaction

products to the vulnerable tissues of the airway epithelium and acinus.

RATIONALE FOR THE STUDY

Better methods are needed to provide quantitative data on human exposures to automotive emissions and their constituents. In his original application to HEI, Dr. Ultman and coworkers proposed to develop a fast-responding ozone analyzer that would continuously monitor ozone concentrations in air inspired and expired by human subjects who inhaled a bolus of ozone of varying concentrations. The ozone analyzers available at the time of the investigator's original proposal were limited in their application to human studies because of their slow response time and their requirement for relatively large samples of gas for analysis. In the pilot study, Dr. Ultman and his collaborators (1990) designed and constructed two instruments essential for noninvasively measuring respiratory absorption of ozone in human subjects: (1) a fast-responding ozone analyzer capable of continuously monitoring ozone concentrations during the four-second period of a normal breath, and (2) a small-scale ozone bolus generator suitable for producing boluses of specified volume and concentration. The logical next step was to test the application of the instruments in human subjects under conditions of varying ozone exposure concentrations and levels of exercise.

OBJECTIVES AND STUDY DESIGN

The goal of this study was to make noninvasive measurements of ozone absorption (also called the efficiency of ozone absorption) among different regions of the human respiratory tract for various breathing conditions and ozone concentrations. These particular variables were chosen to mimic a range of potential human exposures so that dose-response relations could be established. Pertinent dose-response measurements would include the doses that cause damage to respiratory epithelial cells, inflammation, and alterations in lung function and airway reactivity. To this end, Dr. Ultman and colleagues previously developed and validated an ozone analyzer with a response time that was fast enough (90% step-response time of 110 msec) to sample the inhaled and exhaled ozone concentrations of single breaths (Ben-Jebria and Ultman 1989; Ben-Jebria et al. 1990; Ultman and Ben-Jebria 1990), and an associated ozone-bolus generator (Ultman and Ben-Jebria 1990; Ben-Jebria et al. 1991). Dr. Ultman and colleagues also have developed a bolus-response method to measure the regional distribution of inhaled gases (Ultman et al. 1978; Ben Jebria et al. 1981). While a subject breathes a 500-mL tidal volume from functional residual capacity, a 10-mL bolus of gas such as ozone is introduced into the inhaled air at a predetermined volume. The penetration volume (V_P) refers to the volume of air that follows the mean of the ozone bolus into the respiratory tract, and thus allows absorption to be described longitudinally. To probe the upper airways (20 mL$<V_P<$70 mL), the bolus is introduced later in the breath; to probe the lower airways and gas-exchange region ($V_P>$70 mL), the bolus is introduced earlier in the breath. The absorption of ozone at a given V_P is calculated from the integral of expired to inspired ozone concentration. Thus, the term "absorption" represents the cumulative uptake efficiency of the airways through which the bolus passes as it is inhaled to and exhaled from a certain V_P.

The specific aims of the proposal were:

1. To incorporate the previously developed ozone bolus generator and analyzer into a computer-controlled bolus inhalation system;
2. To measure the longitudinal distribution of ozone absorption in the respiratory tract during quiet breathing at a flow of 250 mL/sec (baseline measurements);
3. To evaluate how changing the respiratory flow rate from 150 to 1,000 mL/sec affects the longitudinal ozone absorption (flow experiments);
4. To evaluate how inhaling ozone either through the mouth or the nose affects longitudinal ozone absorption (oral-nasal experiments); and
5. To evaluate how altering the peak inspired ozone concentration from 0.5 to 4 ppm affects longitudinal ozone absorption (concentration experiments).

In specific aim 1, the computer-controlled bolus system was to be assembled for human inhalation studies. This system had to be capable of (1) delivering a well-defined ozone bolus to a human subject breathing via either the mouth or the nose, (2) measuring respired flow rate and volume, (3) providing feedback to the subjects so they could follow a prescribed breathing pattern, (4) measuring rapidly changing inspired and expired ozone concentrations, (5) measuring expired carbon dioxide concentrations, and (6) acquiring all input signals and matching them with respect to time. The ozone analyzer had to be calibrated and characterized in terms of its sensitivity, step-response times, and its susceptibility to interference from exhaled carbon dioxide and water. (These factors were part of the initial project to develop the ozone analyzer [Ultman and Ben-Jebria 1990].) The carbon dioxide analyzer had to be calibrated and characterized in a similar manner. Because the signals from each analyzer had to be matched with respect to time, it was also necessary to characterize and correct for the delay times of each analyzer.

In specific aims 2 through 5, the ozone bolus inhalation system was to be used to measure the distribution and absorption of an inhaled 10-mL ozone bolus as a function of the V_P in the respiratory tract of 23 healthy adult men. The subjects had a mean age of 29 ± 5 years, had normal lung function as assessed by spirometry, were current nonsmokers, and had no history of allergies or asthma. Subjects participated in only some of the experiments: different combinations of nine subjects took part in the baseline measurements, flow experiments, and oral-nasal experiments. Six subjects took part in the concentration experiments. For each measurement, a single bolus was introduced into the inspiration at a predetermined point in order to reach a desired V_P in the respiratory tract. For each experimental condition, boluses were delivered to levels of V_P between 20 and 200 mL in 10-mL increments, so that a total of 19 levels of V_P were tested. In an attempt to relate the V_P of the inhaled bolus to the actual anatomic region of the respiratory tract that the bolus reached, the investigators created an anatomically based lung compartment model. The upper airway compartment, which encompassed the volume between the mouth or nose to the larynx, was designated as V_P between 20 and 70 mL, the lower conducting airway compartment was at a V_P between 70 and 180 mL, and the respiratory airspace compartment was at a V_P greater than 180 mL.

In specific aim 2, the bolus inhalation system was to be used at an inhaled and exhaled flow rate of 250 mL/sec. The data from specific aim 2 were to provide baseline data from which the investigators could then study how longitudinal ozone distribution and absorption were affected by flow rates from 150 to 1,000 mL/sec (specific aim 3), oral versus nasal breathing (specific aim 4), and ozone concentrations from 0.5 to 4 ppm (specific aim 5). In specific aims 3 and 5, the flow rates were to be fixed at 250 mL/sec and the breathing was oral. To characterize the longitudinal distribution of the bolus in aims 2, 3, 4, and 5, the investigators were to use a "mathematical moment analysis" similar to their previously developed bolus-response analysis design (Ultman et al. 1978).

An additional feature of the study was the development of a mathematical model of the kinetics of ozone absorption in various compartments of the respiratory tract, which could then be used to formulate regional dose-response relations. The measured absorption reflects the cumulative efficiency of ozone uptake and thus by itself relates little about regional or local dose. However by assigning each V_P to an anatomical compartment, and within each compartment computing the rate of change of absorption with V_P (the plot of the slope of the absorption versus V_P), the investigators could obtain a local absorption rate of ozone in each compartment. The local absorption rate of ozone was characterized by a combined parameter Ka (sec^{-1}), where K is the mass transfer coefficient (i.e., absorption rate normalized by local ozone concentration and tissue surface area), and a is the local surface-to-volume ratio that accounts for differences in regional geometry. The investigators assumed that the value of K depended upon the diffusional transport of ozone through the gas boundary layer, and the diffusional transport and chemical reactions within the liquid-lining mucous and surfactant layers. Once at the cell surface, the ozone would react rapidly and completely with cell surfaces so that there would be no further ozone transport. The investigators thought this latter assumption was justified based upon estimated reaction rates between ozone and biomolecules in the respiratory tract (Pryor 1992). By determining the sensitivity of absorption to flow rate, the investigators could gauge how absorption was affected by transport of ozone molecules in the gas-exchange region (dependent on rate of flow) and in the liquid-lining layers (independent from rate of flow).

TECHNICAL EVALUATION

ATTAINMENT OF STUDY OBJECTIVES

This was an excellent bioengineering study. The objectives were clear, the measurements were carefully and systematically performed, and the report was of high quality. The bolus inhalation system was able to deliver reproducible boluses to human subjects using different breathing patterns. The dynamic characteristics and delay times among the ozone analyzer, carbon dioxide analyzer, and pneumotachograph were successfully corrected so that the transport of ozone and carbon dioxide could be directly related to respired volume. Furthermore, the ozone analyzer signal was reliably corrected for interference from exhaled carbon dioxide. As it turned out, both the effects of dynamic distortion and carbon dioxide interference were small. With this system, the investigators have met their overall objective to make noninvasive measurements of the distribution and absorption of ozone among different regions of the human respiratory tract for various ozone concentrations and breathing conditions representative of subjects at rest to subjects engaged in light activity.

Among the few limitations of the study was that the ozone absorption at breathing levels simulating moderate and strenuous levels of exercise could not be mimicked because the dynamic response of the ozone analyzer was too slow to provide reliable data at flow rates above 1,000 mL/sec. It had been one of the original objectives of this study to have the dynamic response of the ozone analyzer be fast enough to provide data at 2,000 mL/sec, but this goal

could not be met. Similarly the ozone analyzer had limited precision to detect the exhaled boluses for the lowest inhaled concentration of ozone tested (0.4 ppm). The current bolus-response system was thus limited to using ozone concentrations considerably higher than those found in the ambient air.

METHODS AND STUDY DESIGN

The investigators did an excellent job of attaining their goals and describing the data upon which they based their conclusions. By studying a range of flow rates and the results of breathing, they mimicked the ozone exposure of people at rest and engaged in light activity. As mentioned above, the investigators originally sought to make measurements at flow rates of 2,000 mL/sec, which would have mimicked heavy exercise. Exercise is known to heighten the physiologic responses caused by ozone exposure and to stimulate these responses at lower ozone levels. Unfortunately, limitations in the performance of the ozone analyzer prevented a thorough study of ozone absorption during exercise.

Because the investigators were primarily focused on developing the bolus-response methodology to measure ozone absorption in humans, they wanted to eliminate any confounding sources of variation from the study population. Therefore they limited the study population to a standard group of 23 healthy male adults of varying ethnic background (Caucasian, Asian, and Indian) and broad age range. Thus, the results may not be applicable to women, children, the elderly, or persons with lung disease. In the future, the investigators plan to measure ozone absorption in women, and may include people of varying ages.

To characterize the longitudinal distribution of the bolus in aims 2, 3, 4, and 5, the investigators were to use the bolus-response analysis methods they had developed previously (Ultman et al. 1978). To appreciate the considerations that go into the bolus-response analysis, it is helpful to understand the phenomenology of bolus transport in the respiratory tract. As the ozone bolus is inhaled, it predominately travels by convective flow (bulk transport) in the airways, and then predominately by diffusion in the gas-exchange regions (Ultman 1985). Furthermore at the first airway bifurcation (the carina) the bolus divides into two, and then continues to divide at each successive bifurcation so that at the end of inspiration the initial single bolus has divided into thousands of tiny ozone packets (Heyder et al. 1988). Upon exhalation, these tiny packets then reassemble at each bifurcation to form the exhaled bolus. If the transport of the ozone molecules within the respiratory tract were perfectly reversible and there were no absorption, then the exhaled bolus would have the exact same shape and size as the inhaled bolus. However, this situation is not the case. As the ozone molecules pass through the air passages, they undergo irreversible mixing via convection and diffusion with air molecules from adjacent ozone-free air. Ozone molecules are also absorbed into the respiratory tract surface and not exhaled. As a result of mixing and absorption, the exhaled ozone bolus has a much different shape and size than the inhaled bolus.

In comparison to the inhaled bolus, typical characteristics of the exhaled bolus are that (1) it is spread or dispersed over a greater volume of air, which reflects longitudinal mixing, (2) it has a smaller area under the curve due to absorption in the respiratory tract, and (3) the mean volumetric position of the exhaled bolus may or may not have shifted with respect to the V_P. If the mean exhaled volumetric position always equalled V_P, then the lung would be ventilating homogeneously in a first-in, last-out manner. This matching could be expected for nonabsorbing gases, but not necessarily for ozone (see Figure 7 in the Investigator's Report). A shift in the mean position of the exhaled bolus toward the mouth may reflect greater ozone absorption in the portions of the ozone bolus that travel deeper in the lungs in comparison to the portions that only travel to shallow depths. In essence the deeper portions are "eroded" away so that the bulk of the ozone bolus remaining airborne is located at a shallower depth. Shifts in the mean exhaled position could also be due to diffusion of the ozone gas towards the mouth (Reisfeld and Ultman 1988).

The objective of the bolus-response analysis was to measure the inhaled and exhaled bolus in terms of area, mean volumetric position, and dispersion. These parameters were calculated from the first three mathematical moments of the inhaled and exhaled ozone concentration versus time/volume data (Ultman et al. 1978). The difference between the areas under the curves (zero moments) of the inspired and expired boluses was used to compute absorption, Λ. The mean position (first moment) of the inspired bolus was the penetration volume, V_P; and the mean position of the expired bolus was the breakthrough volume, V_B. The difference in the variances (second moments) of the inspired and expired curves was a measure of longitudinal bolus mixing, which is referred to as dispersion, σ^2. This type of analytical plan was entirely appropriate for this study and provided the pertinent data to understand ozone bolus transport and absorption in the respiratory tract. Furthermore, the absorption data was doubly valuable in that it could be used to calculate the rate of ozone absorption within specified respiratory tract compartments.

One disadvantage of expressing the distribution of bolus absorption as a function of V_P is that the true anatomic regions that absorb the ozone remained unknown. Because the bolus divides at each bifurcation, it is possible that the bolus may distribute itself asymmetrically, especially if it divides unevenly at any of the major bifurcations due to in-

stantaneous differences in the ventilation in the downstream regions. Another example is comparing oral to nasal breathing. The volumes of the nose and mouth may differ so that the V_P to a given lung region would be different in these two instances. Considering the problems associated with verifying the regional distribution of the bolus with an alternative strategy, such as boluses of radioactive gas, the use of an anatomically based compartmental model is certainly justified and appropriate for this study.

Another consideration is that the bolus-response method is for single breaths. Because the ozone reacts with lung fluids, it is possible that continual breaths of ozone would lead to saturation of more proximal lung fluids and thus cause the distribution of absorption to eventually shift distally.

Each experiment consisted of two sets of analyses. The first was to make the experimental bolus-response measurements and to test for significant effects of flow rate, mode of breathing, and ozone concentration on the bolus-response parameters. The second analysis used the experimental ozone absorption data to compute the dose rate of ozone to each respiratory tract compartment. For this analysis, the data for ozone absorption at a given V_P were converted into data for absorption within a given respiratory tract compartment using the anatomical compartment model. Then the investigators employed the ozone absorption model to estimate the local rate of ozone absorption *Ka* within each compartment. The investigators tested both four- and seven-compartment models.

STATISTICAL METHODS

The statistical analyses were appropriate and highly satisfactory. These analyses tested hypotheses that flow rate, mode of breathing, and ozone concentration significantly alter the relations of V_P to ozone bolus absorption, breakthrough volume, and dispersion. Data on absorption, breakthrough volume, and dispersion were averaged at each V_P. When subjects' responses had been measured for multiple parameters at a given V_P, the analysis incorporated measurement-to-measurement variation for each subject and subject-to-subject variations. From these variations, the standard errors of the mean values for absorption, breakthrough volume, and dispersion were calculated at each V_P. The overall sample mean and standard error values at each V_P then were used to test each hypothesis (see Tables 5 and 6 in the Investigators' Report).

RESULTS AND INTERPRETATION

Ozone Absorption

The investigators found that ozone absorption increased with increasing V_P. With quiet oral breathing (250 mL/sec), about 50% of the ozone was absorbed in the upper airways and the remainder was absorbed by a V_P of 180 mL. When the flow rate increased from 150 to 1,000 mL/sec, the absorption-V_P relation shifted distally; less ozone was absorbed in the upper airways, and more reached and was absorbed by the distal conducting airways and the acini. Thus, although the investigators were unable to make measurements for flow rates corresponding to moderate or heavy exercise, the range of flow rates that were tested was sufficient to reveal that exercise leads to increased acinar dose, which means that these results agree with those predicted by dosimetric models. With quiet nasal breathing, the absorption-V_P relation shifted proximally from its position with quiet oral breathing. About 50% of the inhaled ozone was absorbed by a V_P of 30 mL, and 80% was absorbed by the end of the upper airways. Thus the nose, due it its greater surface-to-volume ratio and its creation of tortuous airflows, protects the deeper regions of the lung. The investigators examined the possibility that if these oral-nasal differences were in some way attributable to artifacts introduced by different breathing fixtures used to deliver the ozone to the nose versus the mouth. They convincingly showed that the breathing accessories were not involved.

Increases in ozone concentration, within the range tested, caused no change in the absorption-V_P relations. This means that the efficiency of ozone absorption is independent of ozone concentration, and that the chemical reactions and diffusional processes underlying ozone absorption are linear. However, these results can be applied only to ozone concentrations between 1 and 3.5 ppm. Evaluation of lower concentrations was hampered because at 0.42 ppm ozone, the exhaled bolus was at a concentration too low to be detected accurately by the ozone analyzer.

Local Rate of Absorption

To evaluate how local absorption rates within defined respiratory tract compartments could be expressed best, the investigators had to determine how many compartments to use. For oral breathing they found it was adequate to use a four-compartment respiratory tract model, which consisted of the upper airways ($20 < V_P < 70$ mL), proximal conducting airways ($70 < V_P < 120$ mL), distal conducting airways ($120 < V_P < 180$ mL), and respiratory airspaces ($180 < V_P < 250$ mL). Unfortunately, the *Ka* values calculated for the respiratory airspaces were uncertain because, in most situations, the concentration of ozone exhaled from this depth was below the detection limit of the ozone analyzer.

The oral-nasal studies revealed that, during quiet breathing, the nose is a more effective absorber of inhaled ozone than the mouth. With nasal breathing, the local ozone absorption increased so rapidly with V_P that absorption was

complete by a V_P of 130 mL, compared with 180 mL when breathing was oral. For nasal breathing, the investigators found the seven-compartment model, which subdivided the first three airway compartments into six, provided significantly more resolution about the local distribution of ozone absorption than the four-compartment model. In the seven-compartmental model, the value for *Ka* for the most proximal upper airway region ($20 < V_P < 45$ mL), which included the nose, was 70% greater than the *Ka* for comparable mouth compartment. The important implication here is that the lungs are better protected from ozone when breathing through the nose. In contrast to the findings here, Gerrity and coworkers (1988) found that absorption in the nose was slightly less than in the mouth. The investigators have addressed possible reasons for this discrepancy, one of which could be the slower-responding ozone analyzer used by Gerrity and coworkers.

With increasing flow rates during oral breathing, a clearly associated increase in *Ka* was noted in all compartments (see Table 3 in the Investigators' Report), and a trend for *Ka* to increase with V_P. These data show that even modest exercise, which entails both oral breathing and flow rates of 1,000 mL/sec, increases the absorption rate to the entire respiratory tract and, in particular, increases the rate of absorption in the lower airways and gas-exchange tissues by more than a factor of 3. With more strenuous exercise, it is likely that the absorption rate to the lower lung regions would be even greater (see Figure 13 in the Investigators' Report).

One strength of using the mass transfer coefficient K is that it can reveal the mechanisms at the air-lung interface that affect ozone transport from the inhaled air to the target tissue surface. To be absorbed and then reach the epithelial tissues, ozone molecules must first diffuse through the layer of air between the bolus and the respiratory tract surface, and then through the layer of mucus or surfactant on the respiratory tract surface. By calculating *Ka* for various flow rates, the investigators could discern the relative resistance that the two layers offered to ozone transport. The resistance of the gas-boundary layer would be dependent on flow rate, and the resistance of the liquid-lining layer would be independent of flow rate. They found that *Ka* was highly dependent upon flow rate, indicating that the major impediment to ozone absorption was the ability of an airborne molecule of ozone to cross the gas-boundary layer to the respiratory tract surface. Further modeling analysis revealed that the mucous layers closest to the mouth undergo the most reaction with absorbed ozone, and that those in the deeper lung are less reactive.

Breakthrough Volume and Dispersion

Breakthrough volume (V_B) and dispersion were analyzed to understand the transport of an absorbing gas in the respiratory tract. An interesting finding was that V_B did not equal V_P, as would have been expected for a nondiffusing gas. At intermediate V_P, V_B was less than V_P, which the investigators attributed to the bolus diffusing appreciably mouthward because of the expanding cross-section of the bronchial tree. In addition, the greater *Ka* of the distal lung could "erode" the distal bolus and cause a proximal shift in the V_B of the remaining bolus. At deeper V_P, both of these factors could contribute to the observed leveling of the V_B - V_P relations. The extent of erosion was made very apparent by comparing the exhaled boluses of ozone with those of argon, a nonabsorbing gas. Another interesting finding was that the bolus dispersion was generally independent of V_P. Conversely, with boluses of insoluble gases or aerosol particles, dispersion increases with V_P (Ultman et al. 1978). The investigators attributed this finding to the "eroding" of the distal tail of the ozone bolus.

Intersubject Variability

Differences in ozone absorption were noted among subjects. In an attempt to account for these differences, the investigators tested the possibility that the extent of absorption was related to intersubject differences in vital capacity which is closely related to total lung volume, or to differences only in the volume of the conducting airways (anatomic dead space volume), which they could measure from the profile of exhaled carbon dioxide. They found that the V_P needed to absorb 80% of the inhaled bolus was greater in subjects with larger airway volumes. To explain this, they reasoned that larger airway volumes are associated with smaller local surface-to-volume ratios; therefore, relatively less surface would be available to absorb ozone at a given V_P in people with larger airway volumes than in people with smaller airway volumes.

IMPLICATIONS FOR FUTURE RESEARCH

This successful application of the bolus-response method to ozone absorption and transport in the respiratory tract opens many exciting possibilities for future study. Some of these can be addressed with the current system, others would require further modification of the ozone analyzer. This study necessarily focussed on a rather homogeneous male population. Future studies should involve a wider range of subjects involving females and people of different ages, races, and health status. Such studies are planned. It would be of particular interest to examine subjects, such as the elderly and people who smoke, who are reported to have blunted lung function changes in response to ozone inhalation. Such studies would determine if the blunted re-

sponses are due to alterations in absorption or to the intrinsic properties of the lungs. Conversely, people with heightened responses to ozone could be studied, such as individuals with asthma. With a faster-responding ozone analyzer, it would be valuable to revisit the issue (first addressed by Gerrity and McDonnell 1989) of whether intersubject differences in response to ozone exposure (e.g., decreased lung function and increased airway reactivity) are related to ozone absorption. Furthermore, extended exposures to ozone are known to cause some degree of lung adaptation. Bolus-response measurements could be done before and after extended exposures to assess if adaptation is related to changes in ozone absorption. People often breath oronasally, so measurements during oronasal breathing should also be done. Two of the primary applications of the ozone absorption data are to validate and further refine dosimetric models and to validate dose extrapolations from animals to humans. The present system is readily adaptable for bolus-response measurements in large animals such as dogs. Similar measurements in smaller animals, such as rats, would require appreciable miniaturization of the system. Furthermore, adapting the system for animal studies would make it possible to study other toxic gases and possible interactions among gases.

By modifying the ozone analyzer to have a faster response time and lower limit of detection, human studies could be done that cover a wider range of activity levels, from rest to heavy exercise, as was the original intent of the study. Such studies would require that the ozone analyzer be capable of providing reliable data at flow rates up to 2,000 mL/sec. A lower limit of detection would provide ozone concentration data at environmentally relevant concentrations.

To examine if the sensitivity to ozone is greater in different regions of the respiratory tract, several boluses of ozone could be successively delivered to one volumetric depth. This would concentrate the dose to a known volumetric region of the respiratory tract, and the biologic responses of interest could be measured. By altering the depth, different respiratory regions could be tested.

CONCLUSIONS

The investigators developed a fast-responding ozone analyzer and incorporated this instrument into a computer-controlled bolus generation system to measure inhalation parameters. Using an analytical method previously developed to analyze bolus-response data, they met the objectives of this project by noninvasively measuring the regional distribution of ozone absorption in the respiratory tract of healthy adult males. To mimic different exposure scenarios, the subjects breathed ozone at different flow rates and by mouth or nose. Ozone concentration also was varied. To estimate local dose to different regions of the respiratory tract, they used the measured absorption-V_P relations to compute the ozone absorption rate within different respiratory compartments.

The investigators found that, with quiet mouth breathing, ozone absorption is essentially complete within the conducting airways. With modest increases in flow rate, the absorption-V_P relation shifts distally so that the distal airways and acini receive a larger ozone dose per breath. Both of these results are in agreement with the results of theoretical dosimetric models. With nasal breathing, the absorption-V_P relation shifts proximally, indicating that the nose protects the lung from ozone exposure. The theoretical absorption rate of ozone is 70% greater for the proximal part of the nose than for the comparable region of the mouth. The data also show that, with only modest exercise, which entails both oral breathing and flow rates of 1,000 mL/sec, the absorption rate to the lower airways and gas-exchange tissues was more than three-fold that for rest. Even higher absorption rates could be expected with more strenuous exercise. Ozone absorption was independent of ozone concentration, showing that the mass of ozone absorbed increases in proportion to ozone concentration. Drs. Ultman, Ben-Jebria, and Hu suggested that differences in ozone absorption among subjects was related to intersubject variations in the surface-to-volume ratio of the conducting airways, such that persons with larger airway volumes have less ozone absorption at a given V_P.

Due to limitations of the ozone analyzer, studies could not be done at flow rates in excess of 1,000 mL/sec, so the effects of moderate to heavy exercise on ozone absorption were not evaluated. In addition, the relatively high limit of detection meant that only relatively high peak ozone concentrations (greater than 0.5 ppm) could be studied.

Overall, the investigators made substantial advances in the methodology to measure noninvasively the distribution of ozone absorption in the respiratory tract. Their efforts provide a valuable research tool for ozone dosimetry studies, and their results advance our understanding of ozone uptake by the respiratory tract of humans. These studies have important applications for future studies that relate the dose to target tissues for ozone as well as other inhaled pollutants.

ACKNOWLEDGMENTS

The Health Review Committee wishes to thank the ad hoc reviewers for their help in evaluating the scientific merit of the Investigators' Report, and Drs. James Blanchard and Kathleen Nauss for assisting the Committee in preparing its Commentary. The Committee also acknowledges Virgi

Hepner and Valerie Carr for overseeing the publication of this report and Diane Foster for her editorial and administrative support.

REFERENCES

Adams WC, Savin WM, Christo AE. 1981. Detection of ozone toxicity during continuous exercise via the effective dose concept. J Appl Physiol 51:415–422.

Barry BE, Miller FJ, Crapo JD. 1985. Effects of inhalation of 0.12 and 0.25 parts per million ozone on the proximal alveolar region of juvenile and adult rats. Lab Invest 53:692–704.

Bates DV, Bell GM, Burham CD, Hazucha M, Mantha J, Pengelley LD, Silverman F. 1972. Short-term effects of ozone on the lungs. J Appl Physiol 32:175–181.

Ben-Jebria A, Ultman JS. 1989. Fast-responding chemiluminescent ozone analyzer for respiratory applications. Rev Sci Instrum 60:3004–3011.

Ben-Jebria A, Hu S-H, Ultman JS. 1990. Improvements in a chemiluminescent analyzer for respiratory applications. Rev Sci Instrum 61:3435–3439.

Ben-Jebria A, Hu S-H, Kitzmiller EL, Ultman JS. 1991. Ozone absorption into excised sheep trachea by a bolus-response method. Environ Res 56:144–157.

Castleman WL, Dungworth DL, Schwartz LW, Tyler WS. 1980. Acute respiratory bronchiolitis: An ultrastructural and autoradiographic study of epithelial cell injury and renewal in rhesus monkeys exposed to ozone. Am J Pathol 98:811–840.

Chang L-Y, Huang Y, Stockstill BL, Graham JA, Grose EC, Menache MG, Miller FJ, Costa DL, Crapo JD. 1992. Epithelial injury and interstitial fibrosis in the proximal alveolar regions of rats chronically exposed to a simulated pattern of urban ambient ozone. Toxicol Appl Pharmacol 115:241–252.

DeLucia AJ, Adams WC. 1977. Effects of O_3 inhalation during exercise on pulmonary function and blood chemistry. J Appl Physiol 43:75–81.

Devlin RB, McDonnell WF, Mann R, Becker R, House DE, Schreinemachers D, Koren HS. 1991. Exposure of humans to ambient levels of ozone for 6.6 hours causes cellular and biochemical changes in the lung. Am J Respir Cell Mol Biol 4:72–81.

Finlayson-Pitts BJ, Pitts, JN Jr. 1993. Atmospheric chemistry of tropospheric ozone formation: Scientific and regulatory implications. J Air Waste Manage Assoc 43:1091–1100.

Folinsbee LJ, Drinkwater BL, Bedi JF, Horvath SM. 1978. The influence of exercise on the pulmonary function changes due to exposure to low concentrations of ozone. In: Environmental Stress: Individual Human Adaptations (Folinsbee LJ, Wagner JA, Borgia JF, Drinkwater BL, Gliner JA, Bedi JF, eds.) pp. 125–145. Academic Press, New York, NY.

Folinsbee LJ, Bedi JF, Horvath SM. 1980. Respiratory responses in humans repeatedly exposed to low concentrations of ozone. Am Rev Respir Dis 121:431–439.

Folinsbee LJ, McDonnell WF, Horstman DH. 1988. Pulmonary function and symptom responses after 6.6-hour exposure to 0.12 ppm ozone with moderate exercise. J Air Pollut Control Assoc 38:28–35.

Gelzleichter TR, Witschi H, Last JA. 1992. Concentration-response relationships of rats to exposure to oxidant air pollutants: A critical test of Haber's Law for ozone and nitrogen dioxide. Toxicol Appl Pharmacol 112:73–80.

Gerrity TR, Weaver RA, Berntsen J, House DE, O'Neil JJ. 1988. Extrathoracic and intrathoracic removal of O_3 in tidal-breathing humans. J Appl Physiol 65:393–400.

Gerrity TR, McDonnell WF. 1989. Do functional changes in humans correlate with the airway removal efficiency of ozone? In: Atmospheric Ozone Research and Its Policy Implications (Schneider T, Lee DS, Wolters GJR, Grant LD, eds.) pp. 398–400. Elsevier Science Publishing Co., New York, NY.

Grotberg JB, Sheth BV, Mockros LF. 1990. An analysis of pollutant gas transport and absorption in pulmonary airways. J Biomech Eng 112:168–176.

Hackney JD, Avol EL, Linn WS, Anderson K. 1994. Active and passive ozone samplers based on a reaction with a binary reagent. In: Development of Samplers for Measuring Human Exposures to Ozone. Research Report Number 63. Health Effects Institute, Cambridge, MA.

Hackney JD, Linn WS, Mohler JG, Collier CR. 1977. Adaption to short-term respiratory effects of ozone in men exposed repeatedly. J Appl Physiol 43:82–85.

Hatch GE, Koren H, Aissa M. 1989. A method for comparison of animal and human alveolar dose and toxic effect of inhaled ozone. Health Phys 57(Suppl 1):37–40.

Hazucha M. 1987. Relationship between ozone exposure and pulmonary function changes. J Appl Physiol 62:1671–1680.

Henderson RF, Harkema JR, Hotchkiss JA, Burt DG, Hobbs CH. 1993. Rat strain and substrain differences in response to ozone. Am Rev Respir Dis 147:A483.

Heyder J, Blanchard JD, Feldman HA, Brain JD. 1988. Convective mixing in the human respiratory tract: Estimates with aerosol boli. J Appl Physiol 64:1273–1278.

Hu S-C, Ben-Jebria A, Ultman JS. 1992. Simulation of ozone uptake distribution in the human airways by orthogonal collocation on finite elements. Comput Biomed Res 25: 279–291.

Kleeberger SR, Bassett DJP, Jakab GJ, Levitt RC. 1990. A genetic model for evaluation of susceptibility to ozone-induced inflammation. Am J Physiol (Cell Mol Physiol) 2:L313-L320.

Kleeberger SR, Zhang L-Y, Wierenga C, Harkema JR. 1993. Regional differences in airway susceptibility to sub-acute ozone (O_3) exposure in inbred mice. Am Rev Respir Dis 147:A484.

Kleinman MT. 1991. Effect of ozone on pulmonary function: The relationship of response to dose. J Exposure Anal Environ Epidemiol 1:309–325.

Koren HS, Devlin RB, Graham DE, Mann R, McGee MP, Horstman DH, Kozumbo WJ, Becker S, House DE, McDonnell WF, Bromberg PA. 1989. Ozone-induced inflammation in the lower airways of human subjects. Am Rev Respir Dis 139:407–415.

Koutrakis P, Wolfson JM, Bunyaviroch A, Froelich S. 1994. A passive ozone sampler based on a reaction with nitrite. In: Development of Samplers for Measuring Human Exposures to Ozone. Research Report Number 63. Health Effects Institute, Cambridge, MA.

Lippmann M. 1989. Health effects of ozone: A critical review. J Air Pollut Control Assoc 39:672–695.

Lippmann M. 1993. Health effects of tropospheric ozone: Review of recent research findings and their implications to ambient air quality standards. J Exposure Anal Environ Epidemiol 3:103–129.

McCool FD, Paek D. 1993. Measurements of ventilation in freely ranging subjects. In: Noninvasive Methods for Measuring Ventilation in Mobile Subjects. Research Report Number 59. Health Effects Institute, Cambridge, MA.

McDonnell WF, Horstman DH, Hazucha MJ, Seal E, Haak ED, Salaam S, House DE. 1983. Pulmonary effects of ozone exposure during exercise: Dose-response characteristics. J Appl Physiol 54:1345–1352.

McDonnell WF, Horstman DH, Abdul-Salaam S, House DE. 1985. Reproducibility of individual responses to ozone exposure. Am Rev Respir Dis 131:36–40.

McDonnell WF. 1991. Intersubject variability in acute ozone responsiveness. Pharmacogenetics 1:110–113.

McDonnell WF, Kehrl HR, Abdul-Salamm S, Ives, PJ, Folinsbee LJ, Devlin RB, O'Neil JJ, Horstman DH. 1991. Respiratory response of humans exposed to low levels of ozone for 6.6 hours. Arch Environ Health 46:145–150.

Mellick PW, Dungworth DL, Schwartz LW, Tyler WS. 1977. Short term morphologic effects of high ambient levels of ozone on the lungs of rhesus monkeys. Lab Invest 36:82–90.

Miller FJ, McNeal CA, Kirtz JM, Gardner DE, Coffin DL, Menzel DB. 1979. Nasopharyngeal removal of ozone in rabbits and guinea pigs. Toxicology 14:273–281.

Miller FJ, Overton JH Jr, Jaskot RH, Menzel DB. 1985. A model of the regional uptake of gaseous pollutants in the lungs: I. The sensitivity of the uptake of ozone in the human to lower respiratory tract secretions and exercise. Toxicol Appl Pharmacol 79:11–27.

Moorman WJ, Chmiel JJ, Stara JF, Lewis TR. 1973. Comparative decomposition of ozone in the nasopharynx of beagles. Arch Environ Health 26:153–155.

Overton JH, Graham RC. 1989. Predictions of ozone absorption in humans from newborn to adult. Health Phys 57(Suppl 1):29–36.

Paquette NC, Zhang L-Y, Ellis W, Kleeberger SR. 1993. Ozone-induced changes in tissue tocopherol, retinol, and retinyl palmitate in differentially susceptible inbred mice (Abstract). Am Rev Respir Dis 147:A484.

Plopper CG, Chow CK, Dungworth DL, Brummer M, Nemeth TJ. 1978. Effect of low levels of ozone on rats: II. Morphological responses during recovery and re-exposure. Exp Molecul Pathol 39:400–411.

Pryor WA. 1992. How far does ozone penetrate into the pulmonary air/tissue boundary before it reacts? Free Radical Biol Med 12:83–88.

Reisfeld B, Ultman JS. 1988. Longitudinal mixing in dogs during high-frequency forced flow oscillation. Respir Physiol 71:269–286.

Rombout PJA, Lioy PJ, Goldstein BD. 1986. Rationale for an eight-hour ozone standard. J Air Pollut Control Assoc 36:913–917.

Samet JM, Lambert WE, James DS, Mermier CM, Chick TW.

1993. Assessment of heart rate as a predictor of ventilation. In: Noninvasive Methods for Measuring Ventilation in Mobile Subjects. Research Report Number 59. Health Effects Institute, Cambridge, MA.

Schwartz LW, Dungworth DL, Mustafa MG, Tarkington BK, Tyler WS. 1976. Pulmonary responses of rats to ambient levels of ozone: Effects of 7-day intermittent or continuous exposure. Lab Invest 34:565–578.

Silverman F, Folinsbee LJ, Barnard J, Shepard RJ. 1976. Pulmonary function changes in ozone: Interaction of concentration and ventilation. J Appl Physiol 41:859–864.

Stephens RJ, Sloan MF, Evans MJ, Freeman G. 1974. Early response to low levels of ozone. Am J Pathol 74:31–58.

Ultman JS. 1985. Gas transport in conducting airways. In: Gas Mixing and Distribution in the Lung (Engel LA, Paiva M, eds.) pp. 63–136. Marcel Dekker, New York.

Ultman JS, Ben-Jebria A. 1990. Noninvasive Determination of Respiratory Ozone Absorption: Development of a Fast-Responding Ozone Analyzer. Research Report Number 39. Health Effects Institute, Cambridge, MA.

Ultman JS, Doll BE, Spiegel R, Thomas MW. 1978. Longitudinal mixing in pulmonary airways–normal subjects respiring at a constant flow. J Appl Physiol 44:297–303.

Weibel ER. 1963. Morphometry of the Human Lung. Springer-Verlag, New York

Wiester MJ, Williams TB, King ME, Menache MG, Miller FJ. 1987. Ozone uptake in awake Sprague-Dawley rats. Toxicol Appl Pharmacol 89:429–437.

Yanagisawa Y. 1994. A passive ozone sampler based on a reaction with iodide. In: Development of Samplers for Measuring Human Exposures to Ozone. Research Report Number 63. Health Effects Institute, Cambridge, MA.

Yokoyama E, Frank R. 1972. Respiratory uptake of ozone in dogs. Arch Environ Health 25:132–138.

RELATED HEI PUBLICATIONS: OZONE AND DOSIMETRY

Report No.	Title	Principal Investigator	Publication Date
Ozone			
Research Reports			
1	Estimation of Risk of Glucose 6-Phosphate Dehydrogenase-Deficient Red Cells to Ozone and Nitrogen Dioxide	M. Amoruso	1985
3	Transport of Macromolecules and Particles at Target Sites for Deposition of Air Pollutants	T. Crocker	1986
6	Effect of Nitrogen Dioxide, Ozone, and Peroxyacetyl Nitrate on Metabolic and Pulmonary Function	D.M. Drechsler-Parks	1987
11	Effects of Ozone and Nitrogen Dioxide on Human Lung Proteinase Inhibitors	D.A. Johnson	1987
14	The Effects of Ozone and Nitrogen Dioxide on Lung Function in Healthy and Asthmatic Adolescents	J.Q. Koenig	1988
22	Detection of Paracrine Factors in Oxidant Lung Injury	A.K. Tanswell	1989
37	Oxidant Effects on Rat and Human Lung Proteinase Inhibitors	D.A. Johnson	1990
38	Synergistic Effects of Air Pollutants: Ozone Plus a Respirable Aerosol	J.A. Last	1991
44	Leukocyte-Mediated Epithelial Injury in Ozone-Exposed Rat Lung	K. Donaldson (J.M.G. Davis)	1991
48	Effects of Ozone on Airway Epithelial Permeability and Ion Transport	P.A. Bromberg	1991
50	The Role of Ozone in Tracheal Cell Transformation	D.G. Thomassen	1992
60	Failure of Ozone and Nitrogen Dioxide to Enhance Lung Tumor Development in Hamsters	H. Witschi	1993
65	Consequences of Prolonged Inhalation of Ozone on F344/N Rats: Collaborative Studies		
	Part I: Content and Cross-Linking of Collagen	J.A. Last	1994
	Part II: Mechanical Properties, Responses to Bronchoactive Stimuli, and Eicosanoid Release in Isolated Large and Small Airways	J.L. Szarek	1994
HEI Communications			
1	New Methods in Ozone Toxicology: Abstracts of Six Pilot Studies	L-Y.L. Chang R.A. Floyd W.C. Parks K.E. Pinkerton D.A. Uchida R. Vincent	1992
Air Pollutant Dosimetry			
Research Reports			
10	Predictive Models for Deposition of Inhaled Diesel Exhaust Particles in Humans and Laboratory Species	C.P. Yu	1987
28	Nitrogen Dioxide and Respiratory Infection: Pilot Investigations	J.M. Samet	1989
39	Noninvasive Determination of Respiratory Ozone Absorption: Development of a Fast-Responding Ozone Analyzer	J.S. Ultman	1991
40	Retention Modeling of Diesel Exhaust Particles in Rats and Humans	C.P. Yu	1991

(continued on next page)

RELATED HEI PUBLICATIONS: OZONE AND DOSIMETRY (*continued*)

45	The Effects of Exercise on Dose and Dose Distribution of Inhaled Automotive Pollutants	M.T. Kleinman	1991
58	Nitrogen Dioxide and Respiratory Illness in Infants	J.M. Samet W.E. Lambert	1993
59	Noninvasive Methods for Measuring Ventilation in Mobile Subjects	F.D. McCool J.M. Samet	1993
63	Development of Samplers for Measuring Human Exposures to Ozone		1994
	Active and Passive Ozone Samplers Based on a Reaction with a Binary Reagent	J.D. Hackney	
	A Passive Ozone Sampler Based on a Reaction with Nitrate	P. Koutrakis	
	A Passive Ozone Sampler Based on a Reaction with Iodide	Y. Yanagisawa	

Copies of these reports can be obtained by writing or calling the Health Effects Institute, 141 Portland Street, Suite 7300, Cambridge, MA 02139. Phone 617 621-0266. FAX 617 621-0267. Request a Publications and Documents booklet for a complete listing of publications resulting from HEI-sponsored research.

HEI

The Board of Directors

Archibald Cox *Chairman*
Carl M. Loeb University Professor (Emeritus), Harvard Law School

William O. Baker
Chairman (Emeritus), Bell Laboratories

Douglas Costle
Chairman of the Board and Distinguished Senior Fellow, Institute for Sustainable Communities

Donald Kennedy
President (Emeritus) and Bing Professor of Biological Science, Stanford University

Walter A. Rosenblith
Institute Professor (Emeritus), Massachusetts Institute of Technology

Health Research Committee

Bernard Goldstein *Chairman*
Director, Environmental and Occupational Health Sciences Institute

Joseph D. Brain
Chairman, Department of Environmental Health, and Cecil K. and Philip Drinker Professor of Environmental Physiology, Harvard University School of Public Health

Glen R. Cass
Professor of Environmental Engineering and Mechanical Engineering, California Institute of Technology

Seymour J. Garte
Professor and Deputy Director, Department of Environmental Medicine, New York University Medical Center

Leon Gordis
Professor and Chairman, Department of Epidemiology, Johns Hopkins University, School of Hygiene and Public Health

Stephen S. Hecht
Director of Research, American Health Foundation

Meryl H. Karol
Professor of Environmental and Occupational Health, University of Pittsburgh, Graduate School of Public Health

Robert F. Sawyer
Class of 1935 Professor of Energy (Emeritus), University of California at Berkeley

Gerald van Belle
Chairman, Department of Environmental Health, School of Public Health and Community Medicine, University of Washington

Health Review Committee

Arthur Upton *Chairman*
Clinical Professor of Pathology, University of New Mexico School of Medicine

A. Sonia Buist
Professor of Medicine and Physiology, Oregon Health Sciences University

Gareth M. Green
Associate Dean for Education, Harvard School of Public Health

Donald J. Reed
Professor and Director, Environmental Health Sciences Center, Oregon State University

David J. Riley
Professor of Medicine, University of Medicine and Dentistry of New Jersey—Robert Wood Johnson Medical School

Herbert Rosenkranz
Chairman, Department of Environmental and Occupational Health, Graduate School of Public Health, University of Pittsburgh

Robert M. Senior
Dorothy R. and Hubert C. Moog Professor of Pulmonary Diseases in Medicine, Washington University School of Medicine at The Jewish Hospital

James H. Ware
Dean of Academic Affairs and Professor of Biostatistics, Harvard School of Public Health

Frederick A. Beland *Special Consultant to the Committee*
Director for the Division of Biochemical Toxicology, National Center for Toxicological Research

Henry A. Feldman *Special Consultant to the Committee*
Senior Research Scientist, New England Research Institute

Edo D. Pellizzari *Special Consultant to the Committee*
Vice President for Analytical and Chemical Sciences, Research Triangle Institute

Officers and Staff

Daniel S. Greenbaum *President*
Richard M. Cooper *Corporate Secretary*
Kathleen M. Nauss *Director for Scientific Review and Evaluation*
Elizabeth J. Story *Director of Finance and Administration*
Jane Warren *Director of Research*
Maria G. Costantini *Senior Staff Scientist*
Chester A. Bisbee *Staff Scientist*
Aaron J. Cohen *Staff Scientist*
Bernard Jacobson *Staff Scientist*
Debra A. Kaden *Staff Scientist*
Martha E. Richmond *Staff Scientist*

Gail V. Allosso *Senior Administrative Assistant*
Valerie Anne Carr *Publications Production Coordinator*
Diane C. Foster *Editorial Assistant*
L. Virgi Hepner *Managing Editor*
Debra N. Johnson *Controller*
Teresina McGuire *Accounting Assistant*
Jean C. Murphy *Research Associate*
Mary L. Stilwell *Administrative Assistant*
Stacy Synan *Administrative Assistant*
Susan J. Walsh *Receptionist*

HEI HEALTH EFFECTS INSTITUTE 141 Portland Street, Cambridge, MA 02139 (617) 621-0266

Research Report Number 69 August 1994